THE DEVELOPMENT OF A DISCHARGE HEATED PENNING ION SOURCE FOR MULTIPLY-CHARGED IONS IN A K=500 SUPERCONDUCTING CYCLOTRON

BY

Timothy Allen Antaya

A DISSERTATION

Submitted to
Michigan State University
in partial fulfillment of the requirements
for the degree of

DOCTOR OF PHILOSOPHY

Department of Physics

1984

ABSTRACT

THE DEVELOPMENT OF A DISCHARGE HEATED
PENNING ION SOURCE FOR MULTIPLY-CHARGED
IONS IN A K=500 SUPERCONDUCTING CYCLOTRON

By

Timothy Allen Antaya

We present the studies made during the design, testing, operation and development of a PIG ion source for the production of multiply-charged ions in the K500 Cyclotron. In Chapter 1 the fundamental properties of Penning (PIG) ion sources and the design of the K500 cyclotron ion source are presented.

Pulsed operation of the source, including the power supply operation and modification, the ion source operating characteristics, and the effects on the production of Ne^{5+} and Ar^{6+} ions, is discussed in Chapter 2. At low duty factors (< 30%) the source output of these ions increases five to ten times over dc operation. The instantaneous arc current and voltage are both several times their dc levels, resulting in a large instantaneous arc power that drives the increased ion production.

The use of hafnium as a cathode material is discussed in Chapter 3, where analyses of lifetime and output effects are made. Replacement of the normal tantalum cathodes with hafnium resulted in a factor of four increase in source

lifetime for nitrogen discharges, due to the formation of a HfN layer having a lower sputtering rate. For dc operation, the ion output is reduced due to a large vapor pressure of Hf inside the source, thereby increasing the loss of ions by charge exchange.

An ion source activation hazard, due to the stripping of accelerating ions, is discussed in Chapter 4. We review the model for this process and then show how the addition of tantalum cover plates to the ion source reduces the activation of its copper surfaces.

In Chapter 5, the modifications made to the source to produce ions from solids via the back-bombardment sputtering process developed at the Oak Ridge National Laboratory, as well as the successful testing with lithium and boron ions, are reviewed.

In Chapter 6, the results of a measurement of the effect of varying the ion source cathode separation on ion production are shown. Outputs of N^{4+} and N^{5+} ions decrease as the cathode separation increases, and this is best explained as a shift in the arc alignment due to magnetic field curvature off the axis of the cyclotron.

ACKNOWLEDGMENTS

The development of the ion sources required the assistance of individuals spanning nearly all of the areas of expertise at the National Superconducting Cyclotron Laboratory. My thanks go out to the laboratory as a whole with special acknowledgments to the following individuals.

I would like to thank Dr. M. L. Mallory for an introduction to ion source physics, which led directly to my involvement in the development of the K500 ion sources. Futhermore, Merrit's drive and enthusiasm has made our collaborations truly memorable.

To Dr. H. G. Blosser, director of the National Superconducting Cyclotron Laboratory and responsible for the exciting projects that we have had to work on, I would like to thank for his advice and direction as we tackled them.

A special thanks to Dr. M. M. Gordon, who was my chief academic advisor, for his constructive suggestions as to the presentation of this work, and for his assistance in the writing of this dissertation.

I would like to acknowledge Drs. E. Kashy and S. M. Austin, who served as the cyclotron research directors

during the first and second operating periods respectively, for their support for the inclusion of ion source measurements in the operating schedule of the K500 cyclotron. Dr. Kashy was also the prime motivator for the choice of topics included in this dissertation.

In addition to Dr. Mallory, I had other collaborators for the work contained in this dissertation. Mr. J. Riedel was responsible for the power supply modifications that enabled us to run the ion sources pulsed, as well as giving us advice on many other electronics hardware issues. Dr. P. S. Miller and his cyclotron operations group: D. Poe, M. Garbicz, G. Horner, G. Humenik, N. Friedman and L. Wilkinson, were intimately involved in the operation of the ion sources, and their discussions and insights have helped shape this work. Dr. Felix Marti's advice on cyclotron tuning and other matters was always valued. I would like to thank Gary Horner and Bruce Milton for the use of the data in Figures 2.7-2.9.

A substantial mechanical design and fabrication effort was required in the development of the sources. Mr. J. A. Kuchar was the chief mechanical designer, contributing both to the initial source design, and also at each step in the development process, often supervising directly the fabrication and installation. It is a real pleasure to work with him. I would like to thank Mr. J. Kitsmiller and the rest of the machine shop crew who

worked diligently to supply us with ion sources parts that we so quickly wore out!

Good friends make all of this worthwhile, and I have some of the best: Charles and Judith Filice, Donald and Suzzanne May, Edward and Dianne Rister, Kenneth and Linda Steibel.

My parents, John and Patricia Antaya, through early encouragement of my interest in science, did start me out well on the path that led to this degree, and so this is their degree too. In the same way I do greatly value all the help and encouragement given by Douglas and Joyce Martyn. I have a very special grandmother, Agnes Kennedy, who has always been a strong supporter.

One acknowledgment is difficult to express in words, because nothing I would say could convey completely the importance that Ann Louise Martyn, my wife, has been to my studies, and so it is to her that I dedicate this dissertation. Thank you Ann, for giving me the support, encouragement and love that was necessary to complete this work.

TABLE OF CONTENTS

LIST OF TABLES

LIST OF FIGURES

CHAPTER 1

INTRODUCTION

The K500 cyclotron is the first of a new generation of high-field superconducting cyclotrons that can accelerate heavy-ions to energies well above the coulomb barrier. For first harmonic acceleration, where the ion orbital frequency equals the dee voltage frequency, and the three dees are phased 120° apart, the cyclotron operating diagram is as shown in Figure 1.1. Light ions in general and heavy ions with Q/A approaching 0.5 have a final energy limited by the focusing strength of the magnet, while heavy ions with low Q/A have a maximum energy limited by the bending strength of the magnet. Quite a large range of Q/A and energy values for accelerated ions is evidently feasible. Moreover, this does not include RF operation on higher harmonics which will be available in the future.

The ion source, residing at the center of the

cyclotron, must be able to produce ions over a broad range of masses and charge states to fully exploit the capabilities of the K500 cyclotron. Furthermore, the charge state dependence of the final energy is

$$E_f = KQ^2/A \qquad (1.1)$$

where K is the cyclotron K-factor, which for this cyclotron has a maximum of K=500, and where it is assumed that the cyclotron focusing limit is not exceeded. It is obvious that the final beam energy for a species with mass A can be raised, often significantly, by increasing the charge state Q, since the final energy goes as Q^2.

When work on this dissertation began, the K500 cyclotron was nearing completion, and we were about to start building the first ion source. At that time the Penning Ion Gauge (PIG) ion source was considered the best type of source for heavy-ion cyclotrons. It uses the existing axial magnetic field of the cyclotron to guide hot electrons ($\approx 10^2$eV) coming from an arc discharge through a chamber called the arc chamber (or chimney) that contains a low pressure gas ($\approx 10^{-2} - 10^{-3}$Torr). Collisions of the electrons with gas atoms in this chamber result in successive ionizations to higher and higher Q values.

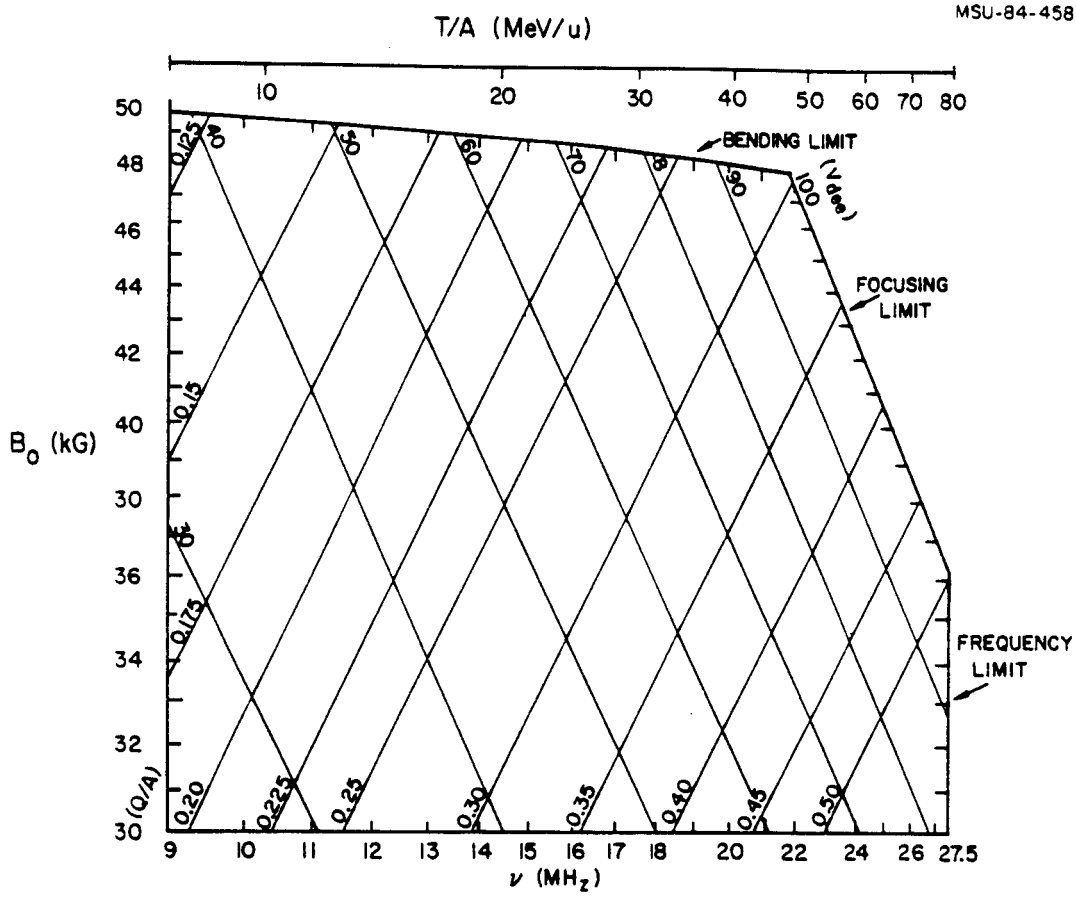

Figure 1.1. The first harmonic operating diagram of the K500 cyclotron is shown. The central magnetic field is plotted as a function of the cyclotron resonance frequency, with constant dee voltage and Q/A lines indicated. The final beam energy in MeV/n is also given.

By putting an aperture in this arc chamber the rf voltage on one of the dees can be used to extract positive ions for acceleration. Such an ion source was designed for the K500 cyclotron.

This dissertation is concerned with the development of such ion sources in the K500 cyclotron for the production of heavy ions. Chapters 2-6 present the properties of these PIG sources and the studies that were made to understand them. Since these chapters are generally concerned with different properties of these ion sources, they have been written to stand independently and new concepts are introduced where appropriate. The remainder of this introductory chapter describes the properties of PIG sources, and then discusses the actual design of the K500 sources.

1.1 Fundamental Properties of the Penning Ion Source

1.1.1 The Arc Discharge Mode

The basic PIG ion source geometry is shown in Figure 1.2. The steady state operation of the source will be described first, and later we will consider how this operating mode was achieved.

The source is operated in a vacuum chamber. The hot cathodes produce thermionically emitted electrons that travel along axial magnetic field lines through a hollow grounded anode. The magnetic field may come from coils that are part of the source design or, as in our case, from the existing field of the cyclotron. A small gas flow to the anode raises the pressure to a few millitorr and ionization of the atoms there results in the formation of a plasma. Electrons that suffer no collisions are decelerated at the opposite cathode. Electrons that do suffer a collision are effectively trapped within the anode and can make many passes through the plasma before their energy is completely dissipated. For this reason the effective path length of the electrons through the plasma can be many times the actual length of the anode, and this raises the probability that an electron will make an ionizing collision with an ion or a neutral gas atom. As a result, cold positive ions with several electrons removed can be produced in the plasma. Some of these ions bombard the cathodes and in designs such as ours this is the source of cathode heating. Unfortunately this also means that a source operated in this way has a finite lifetime set by the sputtering rate of the cathodes. Although there is a confining electric field at the ends of the anode acting on the electrons, this same field is of course anti-confining for the positive ions. In addition, the ions are highly collisional at the operating

Figure 1.2. The PIG ion source arc discharge mode is shown in schematic form.

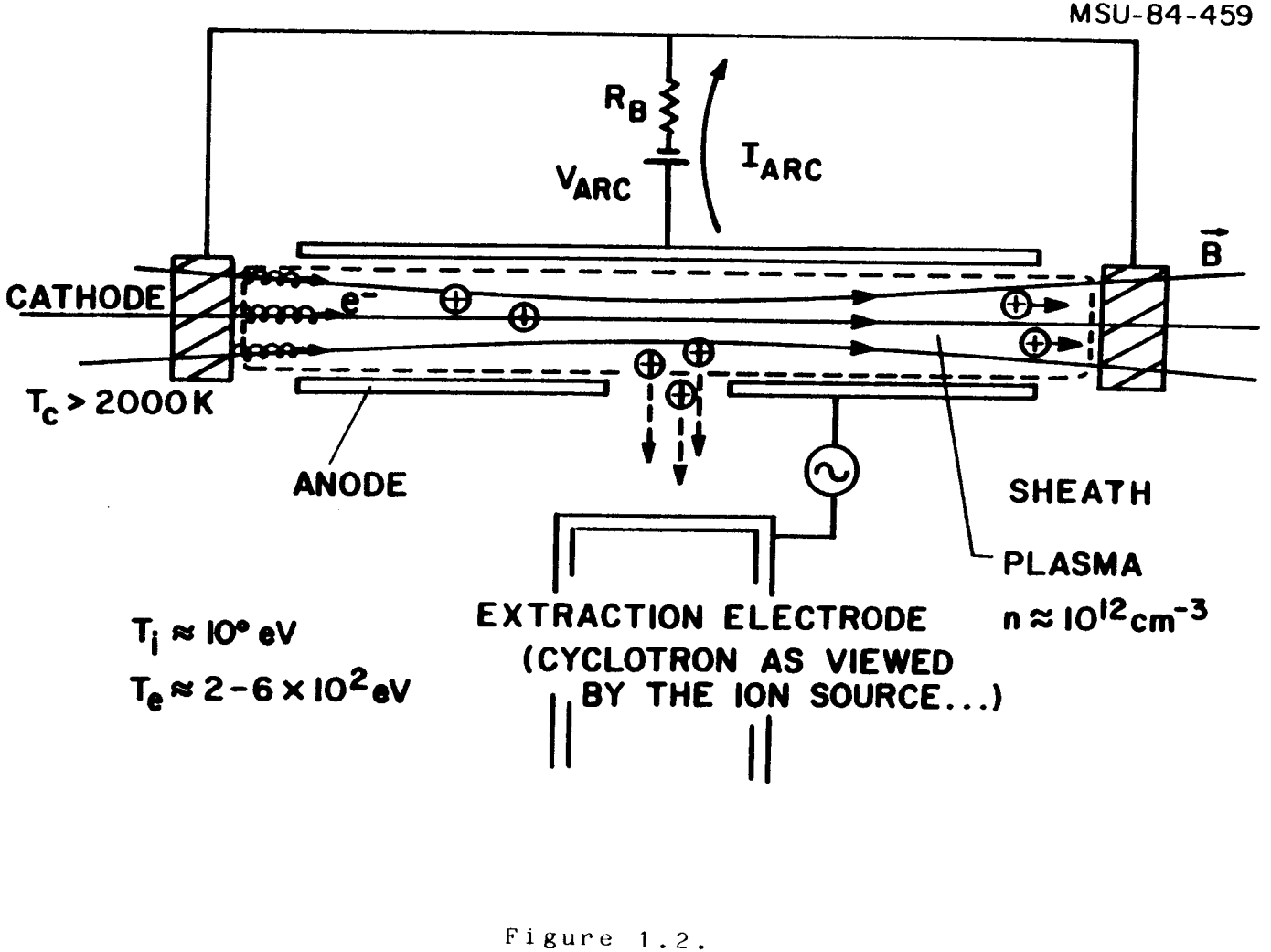
MSU-84-459
R_B
V_{ARC}
I_{ARC}
$\vec{B}$
CATHODE
e^-
$T_c > 2000K$
ANODE
SHEATH
PLASMA
$n \approx 10^{12} cm^{-3}$
$T_i \approx 10^0 eV$
$T_e \approx 2-6 \times 10^2 eV$
EXTRACTION ELECTRODE
(CYCLOTRON AS VIEWED
BY THE ION SOURCE...)

Figure 1.2.

pressure within the source so that a radial drift across the magnetic field becomes possible. We will show later that this lack of ion confinement sets an upper limit on the average charge state made in the plasma.

The discharge that we have been discussing is in fact just one type of arc discharge that can be produced in a magnetic field at low pressure. Many other modes are possible, but only two turn out to be important for the production of positive ions, and both are encountered in the normal operation of a PIG source. Externally the discharge is characterized by the arc voltage and arc current (both indicated in Figure 1.2). Note that the arc current has contributions coming from electron emission in one direction and ion bombardment in the other. The operating diagram for this discharge is shown in Figure 1.3. The arc voltage is plotted as a function of the arc current and two modes can be distinguished. In the first, a very large arc voltage is observed at very low arc current. This is the pure Penning discharge from which the ion source gets its name [Pe 37]. In this mode the cathodes are cold and their electron emission is secondary emission from ion bombardment, and the output current is primarily composed of singly-charged ions. As the arc current increases the arc voltage rises corresponding to a positive impedance (and also confirming that the source is operating in this mode), and in addition,

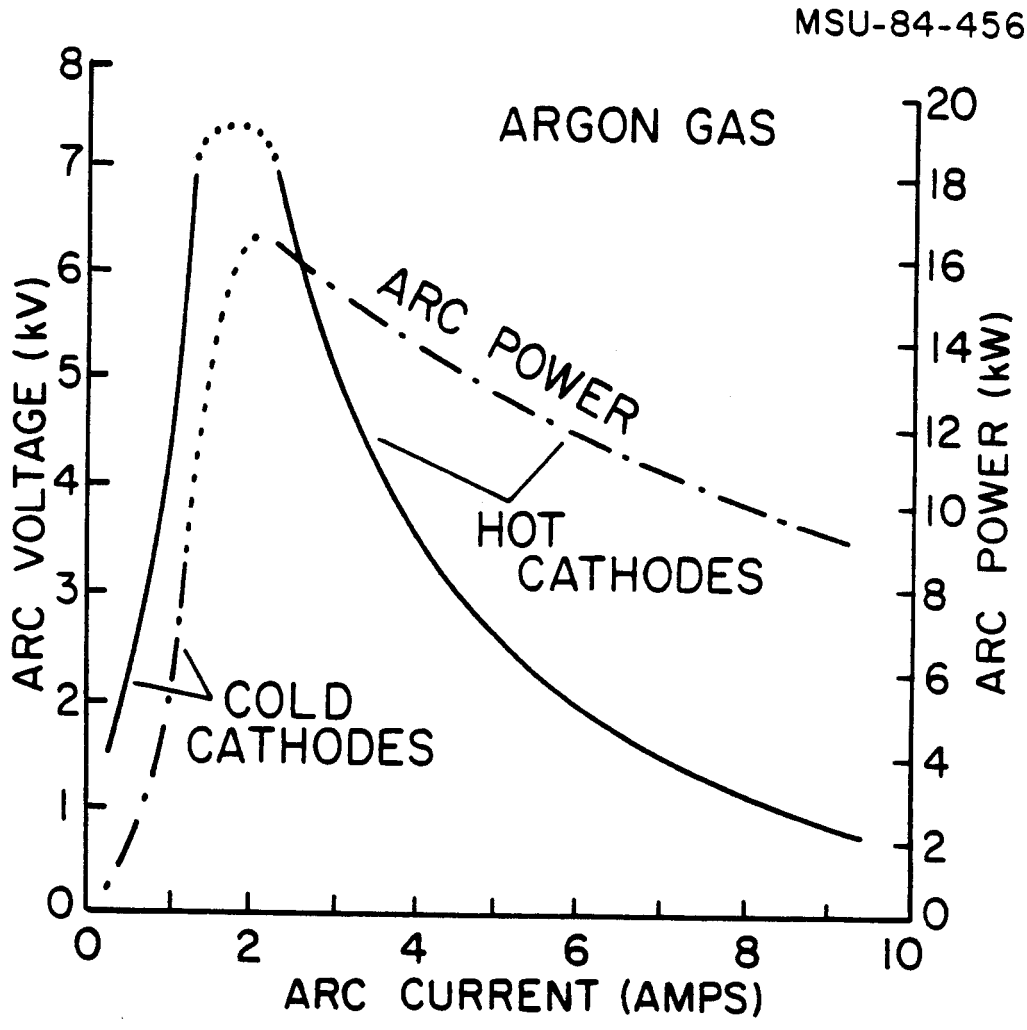

Figure 1.3. The operating diagram for the PIG ion source is shown for operation on argon gas, from reference [Be 72].

the cathode temperature slowly rises. At some point thermionic emission of electrons from the cathodes becomes greater than the secondary emission. The ion production accelerates and the flux of ions striking the cathodes then also rises, driving the source into a second mode. In this second mode, the cathodes run hot and therefore we call this the hot cathode mode, the discharge heated cathode mode, or the arc discharge mode. The pure Penning discharge can also be driven into an arc discharge by increasing the gas flow of a source already at high voltage; this is referred to as "striking the arc", and is generally the main way in which the arc discharge is initiated. The fact that the source must be able to support both a high voltage initially and later a high current, complicates the design. A comparison of the range of operating parameters for these two discharges is made in Table 1.1. One final observation is in order. The charge state distribution shifts to a higher average charge state in the arc discharge mode, where the large electron current going into the plasma significantly raises the ionization rate over the cold cathode mode, and therefore makes the arc discharge mode the one that is utilized for the production of multiply-charged ions for acceleration in the cyclotron.

Table 1.1. A comparison of the two useful operating modes of the Penning Ion Source.

PROPERTY	PENNING DISCHARGE	ARC DISCHARGE
CATHODE TEMP.	<< 2000°K	2000°K
ARC VOLTAGE	> 1 kV	≲ 1 kV
ARC CURRENT	≲ 0.1 A	> 1 A
GAS FLOW	< 1 SCCM	2-4 SCCM
SOURCE LIFETIME	> 20 hours	≈few hours
CATHODE SPUTTERING RATE	low	high
ELECTRON EMISSION MECHANISM	secondary	thermionic

1.1.2 Production of Multiply-charged Ions

The production of multiply-charged ions in a PIG source is a complex balance of ion formation and ion loss processes. Since the primary mechanism is electron impact ionization, the rate of ion formation will depend on the electron density (supplied by the arc discharge) and the magnitude of the cross-sections for electron impact ionization (there are several ionization paths). At the same time the ions in an arc discharge are subject to extensive losses -- principally due either to recombination via charge exchange with neutrals or leakage to the walls of the arc chamber via Bohm diffusion.

It is unfortunately true that after more than 20 years of operation of this kind of positive ion source, many key features of this balance are still known only in a general way. This is in part due to a strong coupling of operating parameters. An obvious example is the ion source arc voltage, of importance since it establishes the initial electron energy. The arc voltage is only indirectly adjustable through changes in the arc current and/or the gas flow rate, but changes in these parameters will alter the characteristics of the arc. The lack of knowledge of fundamental processes can also be ascribed to a lack of good measurements of fundamental parameters. The list of unknowns is long and includes the electron velocity distribution, the ion confinement times, the neutral pressure in the arc, and the cross-sections for the ionization to very high charge states. With this caveat, we will briefly review what <u>is known</u> about the production of positive ions in PIG sources.

The general consensus is that in the arc discharge mode of operation, positive ions are produced through successive collisions with electrons, such that the ionization process proceeds stepwise to higher and higher charge states from lower charge states [Fu 72]. Here we review some of the basic data supporting that consensus.

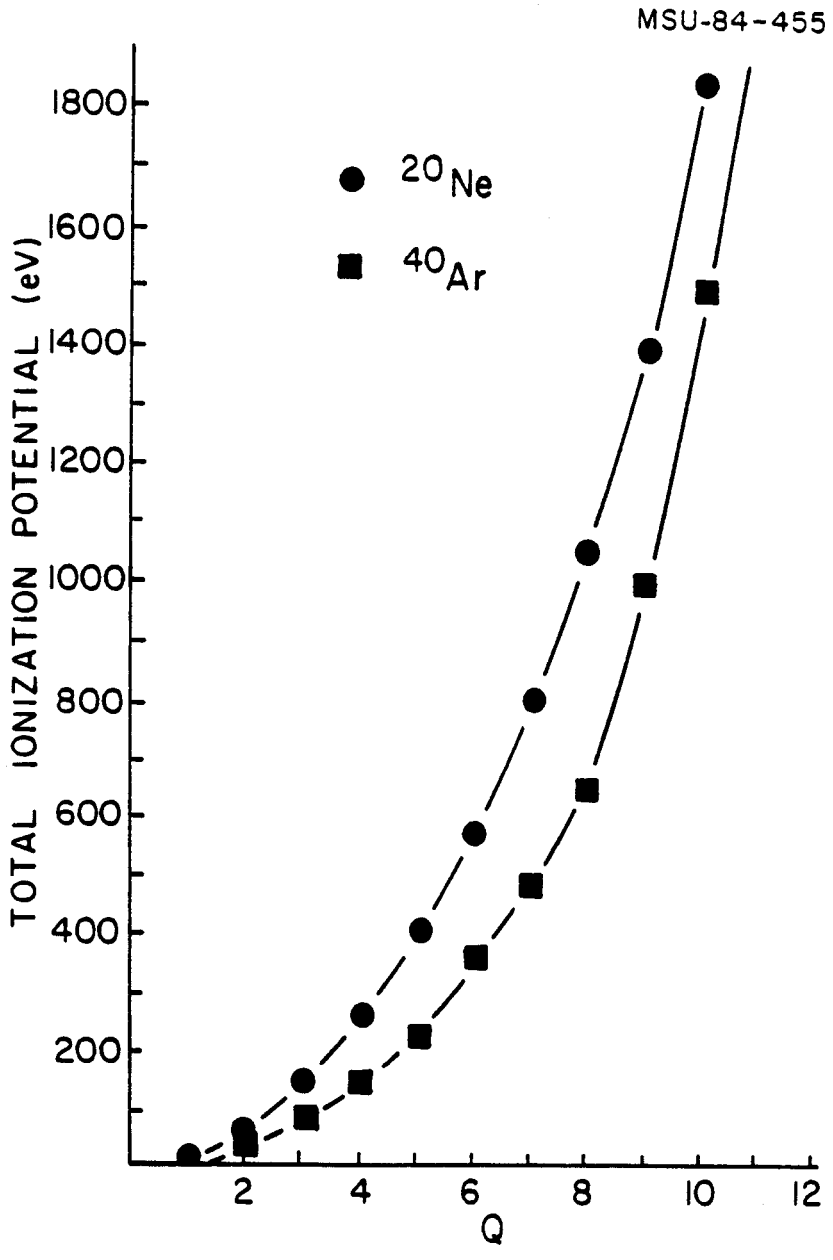

Figure 1.4. The total ionization potentials from neon and argon are plotted as a function of the number of electrons (Q) removed for the atom, according to reference [Ca 70].

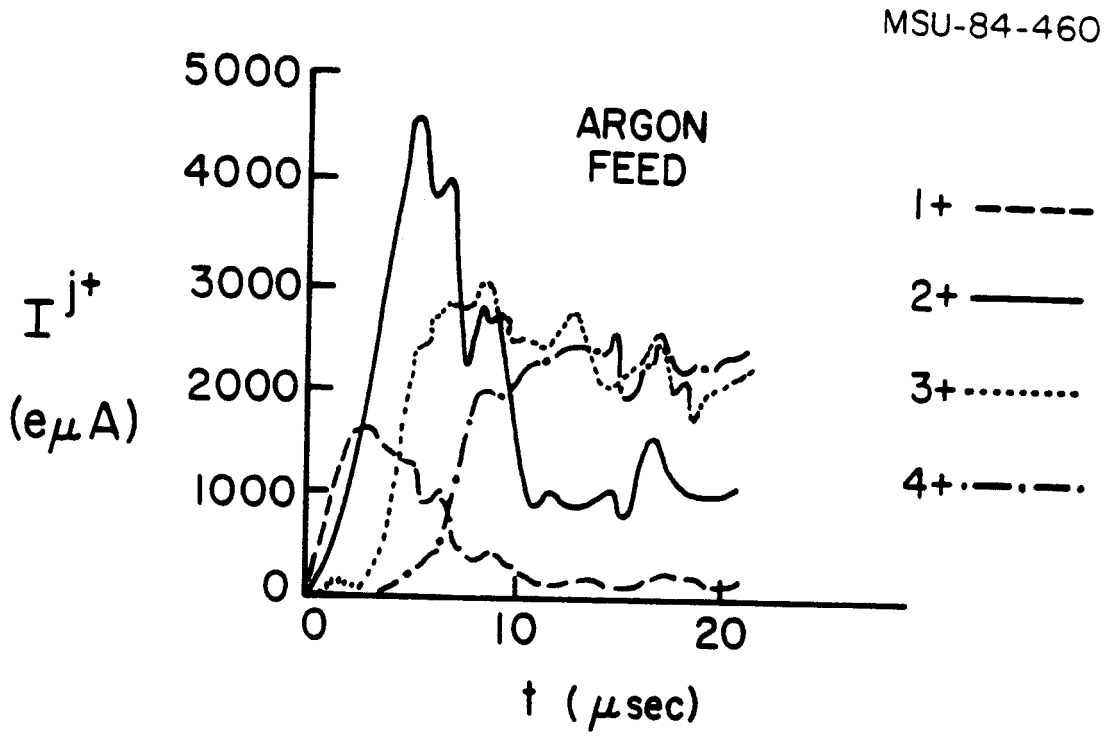

Figure 1.5. The rise time of argon 1+ through 4+ ions as a function of time is shown for a pulsed argon arc discharge from reference [Pa 72]. The time t=0 corresponds to the arc current coming on in the source.

In general, we are interested in obtaining an ion A^{j+} from a neutral atom A with as large a j as possible. In practice, the effective maximum usable j is determined by the resultant intensity that can be accelerated and extracted from the cyclotron. That is, high j ions must appear in the source output in sufficient quantities to produce useful beam currents. Starting from a neutral atom, one can consider many different reaction processes to obtain ion A^{j+}. Two extreme processes are summarized in Eq. (1.2).

$$A + e \longrightarrow A^{+} + 2e.$$

$$A^{+} + e \longrightarrow A^{2+} + 2e.$$

$$\vdots$$

$$A^{(j-1)+} + e \longrightarrow A^{j+} + 2e. \qquad (1.2a)$$

$$A + e \longrightarrow A^{j+} + (j+1)e \qquad (1.2b)$$

Eq. (1.2a) represents the successive impact model, while Eq. (1.2b) shows in a single step a total of j electrons being removed. In general, the cross-sections for ionization decline as the level of ionization increases [Wi 78].

There are fundamental differences in the signatures of these two ionization processes. First, with increasing charge, the cross-sections for multiple electron removal decline much more rapidly than for single electron removal [Wi 78]. Part of this difference can be ascribed to the increasing energy required to produce higher charges. Figure 1.4 shows the total ionization potential for the removal of Q electrons from neon or argon [Ca 70]. One sees that the energy required to remove the next electron is a very sharp function of the number of electrons removed. For example, the removal of the eighth electron from neon requires 400 eV, which is about 40 % of the total energy required to make a Ne^{8+} ion.

It is also obvious that if single electron collisions dominated the production of multiply-charged ions, then high-charge-state ions would appear in the source output as soon as ionizing electrons are present. The available data indicate on the contrary that the charge states appear sequentially, with lower charge states appearing before higher charge states [Pa 72]. This is shown in Figure 1.5, where argon 1+ to 4+ ions are seen to rise sequentially in time. Note also that the lower charge states actually decline with time, indicating their probable conversion to higher charge states. This is a very graphic demonstration of the successive impact ionization model.

There is however, a problem connected with successive impact ionization being the dominant ion production process. If the lifetime of an average ion in the plasma is less than the time required to produce ions A^{j+}, the output percentage of A^{j+} may be too low to be useful. The lifetime is dominated by charge exchange with neutral gas atoms, and it is then a balance of ionization and recombination that sets the average charge state achieved in an arc discharge.

1.2 The Design of the K500 Cyclotron PIG Ion Source and the Operating Environment

The final ion source design, the properties of which are the subject of this thesis, was established through a sequence of stages. The basic design was carried over from the discharge-heated PIG source operated in the MSU K50 cyclotron in the mid-1970's. Testing of that same source in the K500 cyclotron magnet with dc ion extraction occurred in 1976 and 1977. The dc testing established that a PIG source could indeed operate in a high magnetic field with the same extracted currents of multiply-charged ions as PIG sources operated at lower field levels have in the past.

There followed a period of inactivity in which the laboratory effort centered on completing the K500 cyclotron. During that time modifications were made to the source

design to accomodate it within the K500 central region. Fabrication of the first ion source specifically for the K500 cyclotron was completed in October 1981, and we went back to the then de-commissioned K50 cyclotron magnet to test this ion source, in parallel with the first operation of the K500 rf voltage system. In late 1981 these tasks were successfully completed and internal beams were obtained.

In 1982 this first ion source was operated exclusively, while the mirror image source for the other center plug was being fabricated. During this time the design underwent several modifications to improve operation, and these were incorporated in all succeeding sources. The second ion source was commissioned in January 1983, and in 1983 we employed both for the production of cyclotron beams. In December 1983, four additional ion sources of this design went into operation.

1.2.1 K500 Cyclotron PIG Ion Source Design

A schematic diagram of the ion source "head" is shown in Figure 1.6. This part of the ion source sits on the end of a six foot long shaft that is inserted axially through an air lock in the 7-inch diameter cyclotron center plug. The part of the source shown in Figure 1.6 is approximately

Figure 1.6. A sectional view through the anode of the head of the K500 PIG ion source is shown. Compare this to the schematic PIG source diagram in Figure 1.2.

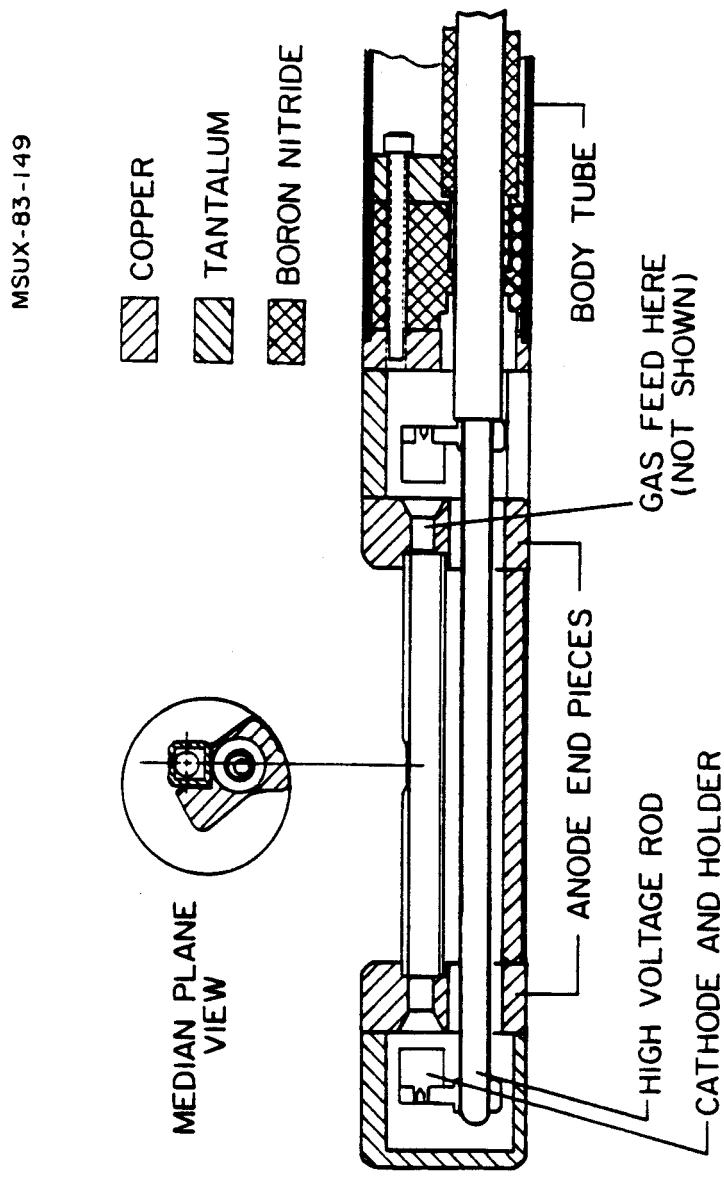
MSUX-83-149
COPPER
TANTALUM
BORON NITRIDE
MEDIAN PLANE VIEW
BODY TUBE
GAS FEED HERE (NOT SHOWN)
ANODE END PIECES
HIGH VOLTAGE ROD
CATHODE AND HOLDER

Figure 1.6.

7 inches long. Of course the axial magnetic field of the K500 cyclotron is quite large, so we have built the source without iron to allow insertion and removal during operation of the cyclotron magnet. The design of the first harmonic central region of the cyclotron, shown in Figure 1.7, fixes precisely the location of the ion source extraction slit and the shape of the ion source anode [Ma 81]. The ion source extraction slit resides 0.32 inches off the central axis of the cyclotron, with a 1 cm gap to the puller electrode on the end of the first dee. The ion source anode terminates the rf electric field in the center in a precise shape intended to boost the beam energy gain on the first turn to clear the ion source itself and the dee tip electrodes.

The ion source design emphasizes rapid recycling after the cathodes have worn out. Surfaces exposed to the arc will eventually wear out and hence can be removed for replacement. The core of the anode is a water-cooled copper part that is not intended to be replaced during ion source recycling. Replaceable copper end pieces define a .203 inch diameter anode aperture and seat the chimney. The tantalum chimney has a .250 inch square internal bore with a machined exit slit. We make chimneys out of 0.050 inch thick tantalum sheet stock, folded into a rectangular shape, TIG-fusing the resulting seam along one edge. When the exit slit has eroded away (typically after about 50 hours of

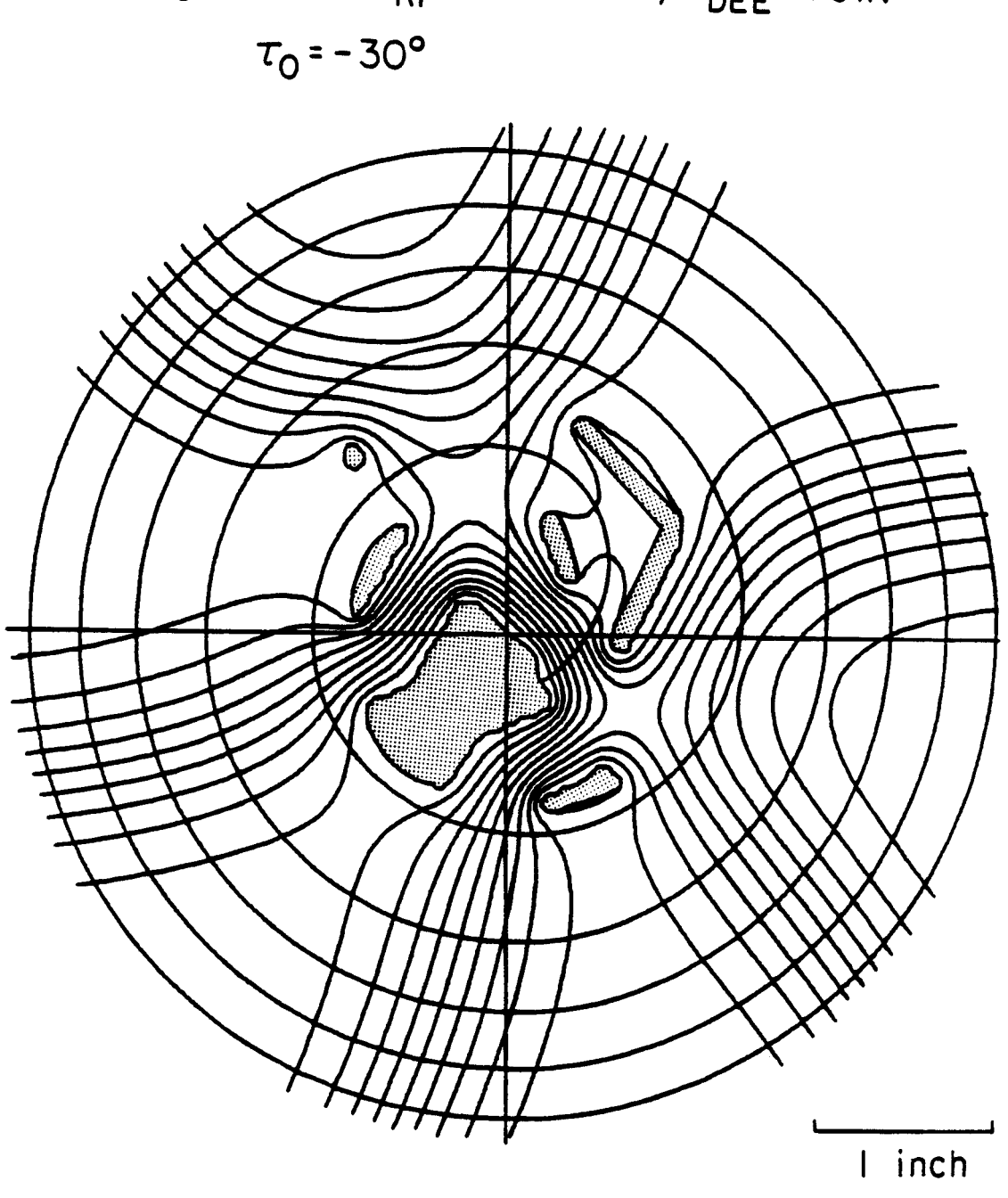

Figure 1.7. The central region geometry for first harmonic acceleration is shown. The ion source and electrodes crossing the median plane are shown as shaded areas. The equipotentials shown here correspond to all three dees having the same voltage and indicate the six acceleration gaps (from reference [Ma 81]).

of cyclotron operation) from the extraction of ions, we can just insert a new chimney. The 3/8 inch diameter cathodes are pressed into tantalum holders that slide over a water-cooled center conductor, we will refer to as the high voltage rod, that provides the cathode voltage bias for source operation.

The arc discharge is struck in this source when the voltage is raised to 1.5-3.5 kV and about 5 cc/min of gas is bled into the chimney. We then reduce the gas flow to 1-3 cc/min for normal operation and raise the arc current to 1.5-4.0 A. Multiply-charged ions will then appear in the source output. Figure 1.8 shows the inverse dependence of the arc voltage on gas flow and arc current, a characteristic signature of the arc discharge mode of operation (compare with Figure 1.3).

1.2.2. K500 Ion Source Commissioning Experience

The source design used for this thesis was the result of an extended period of development in the K500 cyclotron. That development work will be briefly reviewed here. Several physical properties of the source operation are demonstrated.

The ion source designed for the K500 cyclotron was first tested in the de-commissioned K50 cyclotron. The

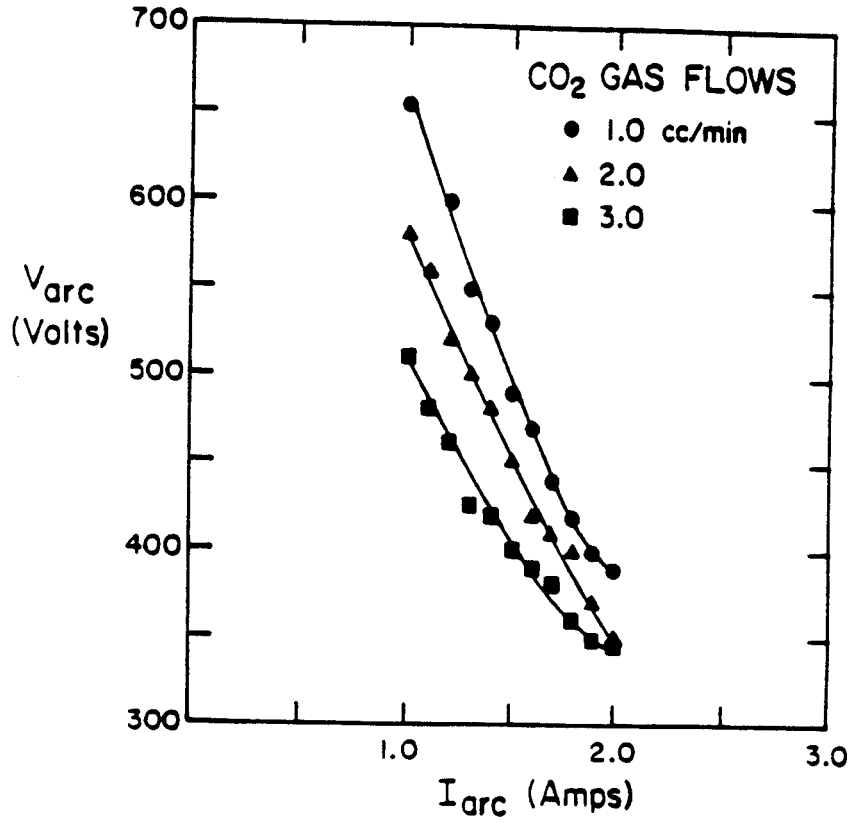

Figure 1.8. The dependence of the arc voltage on the arc current and gas flow is shown for the K500 cyclotron PIG ion source, for a carbon dioxide arc. The decreasing voltage with increasing arc current or gas flow is characteristic of this discharge mode.

major difficulty encountered with the source there was the failure of the vacuum voltage feedthrough; the power and water cooling are brought in to the vacuum through an alumina insulator at the other end of the ion source, so that the inside of the ion source is under vacuum, but the feedthrough insulator itself is 5.5 feet from the main source of pumping-- the cyclotron beam chamber. We found that the pressure inside the source body was high enough to initiate a glow discharge inside the ion source near this insulator and the power dissipated by the glow caused the insulator to crack. This problem was eliminated by drilling holes in the side of the source shaft to vent it to the center plug interior, and then to pump on that space to improve the vacuum.

Several improvements in the way we prepared and operated the source during 1982 resulted in a significant improvement in source lifetime. The histogram in Figure 1.9 shows the steady improvement in source lifetime with the total number of source runs during that period. The data include both source and cyclotron terminated runs, with the intrinsic source lifetime higher than the values in this histogram by about 25%. The first runs in the K500 cyclotron could be characterized as being dominated by failure in the source head of the center conductor, its support insulators, and parts of the anode that absorb arc power. Generally these problems were the result of the

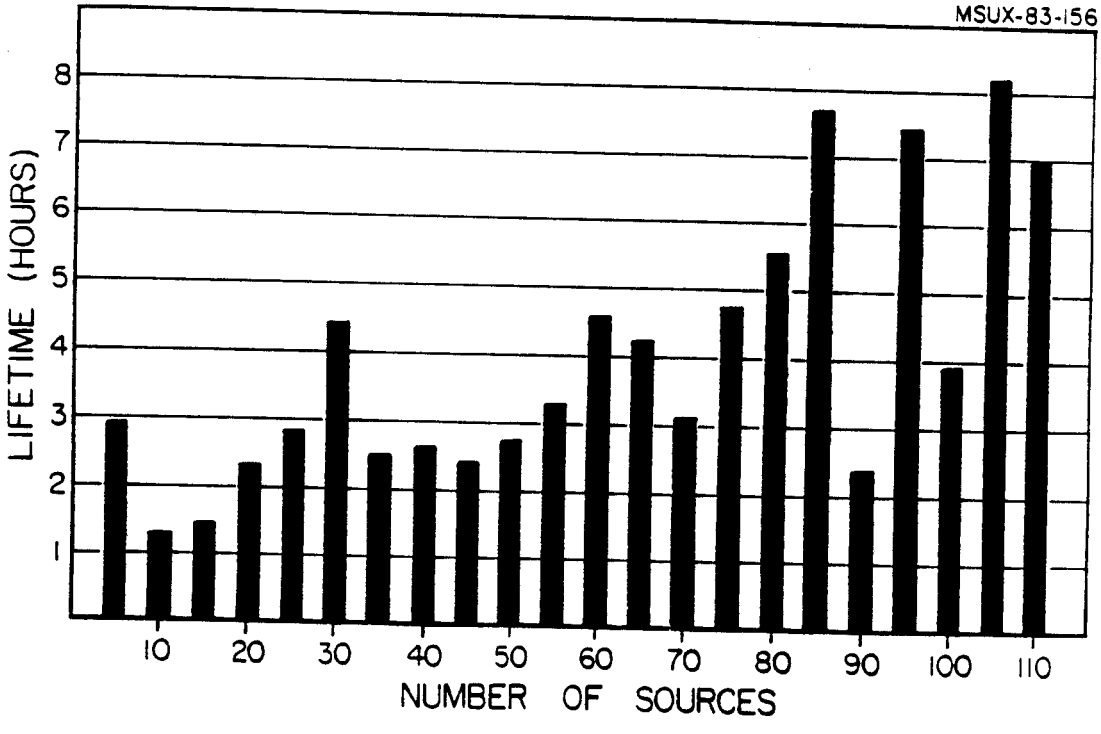

Figure 1.9. The increase in the average ion source lifetime with the number of runs, during the early development of the source is shown.

conflict between the requirement that the ion source have a small cross-section for the clearance of ions on the tight first orbit in the cyclotron, and the requirement that voltage, current and water cooling be passed through the small median plane cross-section to feed the cathode on the other side--which is necessary in an axial ion source design. This is of course a problem characteristic of both the highly optimized central region design and the large magnetic field at the center, which makes the first orbit diameter small. Many small modifications to the high voltage rod and insulators pushed the lifetime to about four hours average after 30 sources. The source design in Figure 1.6 includes those modifications.

In the next phase we were running mainly carbon beams in the cyclotron, and the source lifetime was a poor 2.5-3 h. Source operation with CO or CO_2 degrades the resistance of the boron nitride insulators, through the build-up of a conducting carbon layer on the surface, and after a short time the source shorts out. After about 55 sources we started tracking the center conductor resistance-to-ground during cathode changes and replacing the insulators when the voltage holding threshold went below 1000 V. The source lifetime improved, and then more typical failures resulting from deep craters in the cathodes or arc shorting from cathode material build-up in the apertures,

the normal failure modes for PIG sources, began to determine the average lifetime.

One final change was made in the operation to boost the lifetime above 6 h average. At about 80 sources we started supporting the arc on N_2 during carbon runs, and bleeding in only enough CO to produce adequate beam intensity. This reduced the rate of carbon deposition on the insulators.

The dip in the histogram at 90 sources was due to start-up work after a 1.5 month shut-down, and that at 100 sources was due to the commissioning of the second ion source. After that we could get 8-10 h lifetime for most light ions up to nitrogen, and charge states up to 4+. This was the status of the ion source development when the work that is discussed in the dissertation was begun.

1.3 Publications in Connection with this Research

The following publications have appeared in the literature in connection with this research:

A. K500 Cyclotron Central Region Design

1) E. Liukkonen, J. Bishop, S. Motzny and T. Antaya, Design of the Central Regions for the MSU 500 MeV Superconducting Cyclotron, IEEE Trans. Nucl. Sci., NS-26 (1979) 2107.

2) F. Marti, M.M. Gordon, M.B. Chen, C. Salgado, T. Antaya and E. Liukkonen, Design Calculations for the Central Region of the NSCL 500 MeV Superconducting Cyclotron, Ninth International Conference on Cyclotrons and Their Applications, Caen, France (1981).

B. Cyclotron Central Region Activation

1) M.L. Mallory, T. Antaya, F. Marti, and P. Miller, Radioactivation of a Heavy-Ion Cyclotron Central Region, Nucl. Instr. and Meth, 222 (1984) 431.

C. K500 Ion Source Development

1) T.A. Antaya, M.L. Mallory, and J.A. Kuchar, Operating Experience with an Ion Source in a Superconducting Cyclotron, IEEE Trans. Nucl. Sci., NS-30 (1983) 2716.

2) T.A. Antaya, J.A. Kuchar, M.L. Mallory, P.S. Miller and J. Riedel, The Development of Heavy Ion PIG Sources for the NSCL K-500 Superconducting Cyclotron, Tenth International Conference on Cyclotrons and Their Applications, East Lansing, Michigan (1984).

3) T.A. Antaya and P.S. Miller, Extended Lifetime and Other Beneficial Properties of Hafnium Cathodes in Heavy-Ion PIG Sources, Tenth International Conference on Cyclotrons and Their Applications, East Lansing, Michigan (1984).

CHAPTER 2

PULSED ION SOURCE OPERATION; NEON AND ARGON BEAM PRODUCTION

During the initial operation of the K500 cyclotron, extracted beams of more than a few nanoamperes of Ne^{5+} and Ar^{6+} could not be achieved. A survey of other laboratories indicated that in many instances beams of these ions were produced via a pulsed arc discharge. The general view was that peak arc currents much higher than could be maintained dc due to power dissipation limitations were possible, and this led to an increase in the production of multiply-charged ions. Modification of the K500 ion source power supply for this purpose was possible, and in a short time we were able to make the source run pulsed. The development of ion beams via pulsed operation and a study of the properties of the pulsed PIG arc discharge are the subjects of this chapter. After modifying the power supply, many beams were attempted with the ion source running pulsed, with the most important application ultimately being

N^{5+} with hafnium cathodes, the discussion of which will be deferred to the next chapter of this thesis. Ne^{5+} and Ar^{6+} beams on the other hand have proved to be the most difficult cases, and will be discussed herein.

This chapter will start with a review of the use of pulsed PIG discharges at other laboratories for the production of multiply-charged ions. Since the implementation of pulsing from an engineering standpoint is a question of changing the operation of the ion source power supply and not the ion source itself, the power supply modifications, made by the laboratory electronics group, will be discussed. Next, the more important pulsed PIG source operating characteristics that became evident during the development of K500 cyclotron beams will be introduced via selective examples and the performance of the pulsed source for Ne^{5+} and Ar^{6+} will be compared to dc operation. An empirical model for the mechanism by which the higher ion currents of multiply-charged ions are obtained will be introduced and discussed. Finally, attempts to alter the low source lifetime that seems to come with pulsed discharges will be reviewed.

2.1 Review of the Process and Anticipated Gains

The most extensive study of pulsed PIG discharge characteristics was performed in the 1960's by Pigarov and Morozov [Pi 61a, Pi 61b]. Ions of N, O, Ne, Ar, He and H were studied in a test stand with dc ion extraction and a magnet to analyze the charge-to-mass ratio. In this work it was shown that ion current does increase with the arc current in a pulsed discharge. The highest charge ions of a particular species generally required more arc current, and the lowest charge ions actually declined with increasing arc current. Since the arc went out between pulses, the time dependence of the ion formation could be observed, and it was found that there was a regular sequence of evolution in which the lower charge ions always appeared before the highest charge ions. This latter result served for many years as the primary physical evidence for successive impact ionization collisions with electrons being the main mechanism for the production of multiply-charged ions in PIG sources.

Pulsed arc discharges were used extensively in Europe in the 1970's for the production of multiply-charged ions. This generally followed the development of the indirectly-heated cathode PIG sources at Karchatov [Ma 76], and the subsequent application of that source design at many other laboratories including Bonn, Ganil and GSI-Darmstadt

[Ag 79, Sc 76, Ba 79]. However, in this type of PIG source one of the cathodes is heated by an auxillary electron emitting filament and has some different operating principles; for example, the auxillary electrode is the main source of cathode heating and not the discharge, so that there is no requirement that sufficient gas flow be maintained to stabilize the arc. Therefore detailed consideration of the pulsed operation of these sources was not made.

Pulsed discharge-heated PIG sources were developed at two American heavy-ion laboratories, LBL and Texas A&M, during the 1970's. The K500 ion source is of this type, wherein the cathode heating is coming from the discharge itself, and so these PIG sources were considered in some detail. At LBL, the ion source is generally run dc, but when required, pulsing at 20-20,000 Hz and a 20-50% duty factor is used to increase intensity [Go 79]. Ne^{5+} and Ar^{6+} are obtained from the 88-inch cyclotron there with extracted currents of 4-5 eμA [Cl 81]. At Texas A&M, pulsing is used for the highest charge state of each species accelerated [Sa 79]. A pulse width of 0.3 to 7 ms, and a maximum arc current of 18 A are available. It was shown that the extracted current of multiply-charged ions increased with pulsed operation at arc currents of greater than 10 A. The intensity seemed to have an optimum for a

pulse on-time of approximately 1 ms and an off-time of 2 ms, giving a duty factor in the range of 33%. The currents of low charge ions were higher with a dc discharge. One important observation was that the gas flow required to stabilize the discharge was much lower for pulsed operation: 0.2-0.5 sccm for Ne or Ar feed over approximately 2 sccm dc.

In all of these cases, it appeared that going to pulsed operation allowed a much higher arc current in the ion source, and that this is important for the production of multiply-charged ions, even though this higher current can only be maintained for a shorter time interval. Coupled with this higher arc current is a reduced requirement for support gas to stabilize the arc, apparently because the high arc current is taking over that function. A lower gas flow would reduce the recombination rate inside the source and the transmission through the cyclotron for an additional improvement in beam current.

At another major heavy-ion laboratory in the United States, ORNL, multiply-charged ions were being produced with intensities comparable to LBL and Texas A&M, but without the use of pulsing [Hu 75]. Instead, there it was found that the cyclotron vacuum had indeed a significant impact on the beam attenuation during acceleration due to charge exchange with residual gas atoms, and that large increases in beam intensity could be obtained by improving the cyclotron beam

chamber pumping . Since pulsing evidently allows arc stability at reduced gas flow rates, the gas load that the cyclotron sees from the ion source decreases, and so in that sense these two different experiences are in agreement.

The plan for the implementation of pulsing at MSU included the modification of the power supply arc current regulation, and boosting the peak supply output current,with initial testing for the production of Ne^{5+} and Ar^{6+} beams at 25 MeV/n and 10 Mev/n, respectively. The dependence of beam current on arc current, duty factor and gas flow were to be studied.

2.2 Power Supply Operation for PIG Sources and Modifications to Implement Pulsing

A schematic diagram of the ion source power supply circuit is shown in Figure 2.1. The negative impedance of the mode two arc we employ for ion production must be stabilized by the inclusion of a positive ballast resistance in series with the ion source and the dc power supply. The Eimac 400CW100D power tetrode can be viewed as such a ballast, with a variable resistance ranging from a few hundred ohms to infinity at cut-off.

The operation of this circuit will now be described. The current flowing through the ion source to ground must equal the current collected on the plate of the tetrode. This current is itself proportional to the grid bias voltage, since the tube is operated at a fixed screen voltage of +1 kV. At this screen voltage, a grid bias of -300 V should in principle cut-off the plate current completely, and then rasing the grid voltage from that value allows current emitted from the heated filament to reach the plate. Hence grid bias adjustment is the mechanism for controlling the current flow in the ion source circuit. One further point-- since there is a resistor between the tube filament and ground, when the tube draws current the filament potential rises from ground, reducing the net grid bias slightly. This bit of negative feedback helps stabilize the tube current.

With the above characteristics in mind, it is now possible to briefly discussion how the arc discharge with heated cathodes is obtained. Since the tube current is not completely cut off, at a grid voltage of -300 V, nearly the entire power supply voltage (V_s) appears across the ion source. It it would not be desirable for this voltage to appear instantaneously, as a high voltage conditioning period is often required initially for the source to hold high voltage. Therefore a resistor (R) is added in

Figure 2.1. In this schematic diagram is shown the ion source power supply circuit. On the right there is an Eimac 400CW100D tetrode and its filament, grid and screen supplies, for the purpose of regulating the current for the high voltage supply V_s that powers the ion source.

MSU-84-404

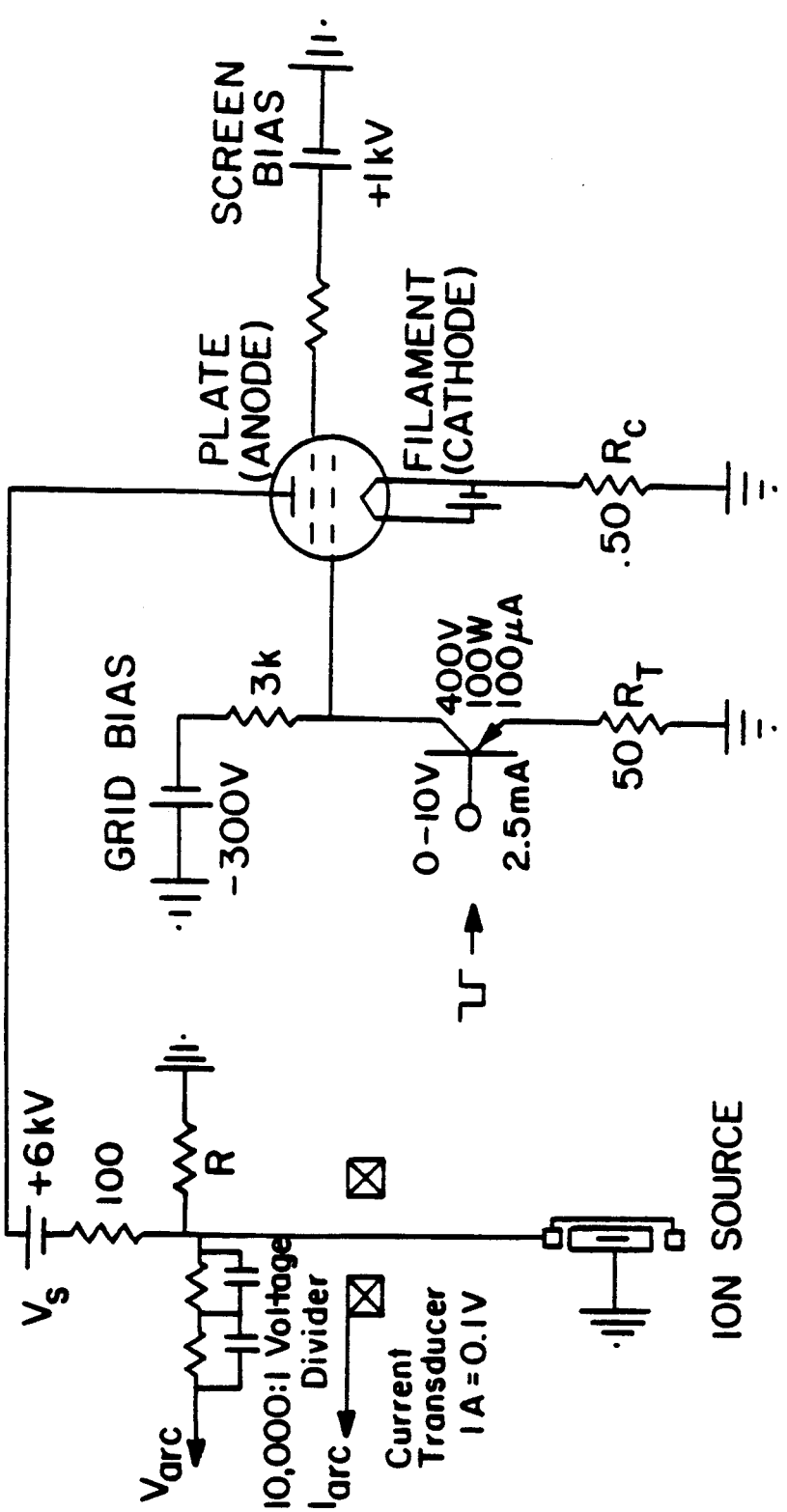

Figure 2.1.

parallel with the source to limit the turn-on voltage to approximately 750 volts. Subsequently raising the grid bias allows current flow, and the arc voltage rises from this initial value. The addition of some gas to the source at this time results in some ionization by field emitted electrons. The cathodes are hit by positive ions and the cathode temperatures rise. More electrons are produced via secondary electron emission as a result of this ion bombardment, feeding the process, and the ion population, cathode temperature and electron emission current density all increase until thermionic emission from the cathodes predominates and we say that a mode 2 arc has struck. The tetrode provides arc current regulation and stabilization once the mode 2 arc discharge has been reached.

In order to pulse the arc current, the grid bias voltage must be pulsed. This is accomplished using a circuit developed by J. Riedel [Ri 84]. A negative square wave signal of amplitude 0-10 V, variable frequency and duty factor is supplied to the base of a bipolar junction transitor, allowing current to flow through the transitor and causing the grid voltage to rise above the -300 volt value with the same frequency response and duty factor. The result is a pulsed output current from the tube.

For diagnostic purposes, both the instantaneous arc voltage and arc current are made available. The arc voltage

is obtained via a frequency-compensated 10,000:1 voltage divider circuit. The arc current is taken off a transductor having a dc to 1MHz frequency response through which the cable going to the ion source passes. A transductor output of 1 V equals 10 A. These signals are best displayed on an oscilloscope. They are also connected to a multiplier whose output is displayed on a meter reading average power input to the ion source.

2.3 Pulsed Operating Characteristics for Ne^{5+} and Ar^{6+}

The most obvious result of pulsing the arc is an increase in the number of adjustable parameters, as shown in Figure 2.2. Apart from the gas flow, one has only the arc current to adjust with a dc arc, with the arc voltage following changes in either. The two new parameters are the duty factor and period, or, alternatively, the on-time and off-time. One has also to introduce peak and average arc current and voltage values, but of these only the peak arc current is directly adjustable. It turns out that this increase in parameter space allows more control over the characteristics of the arc.

When running the source pulsed, it becomes immediately apparent that the beam current is sensitive to the duty factor. We are going to consider some curves showing the cyclotron extracted current of $^{22}Ne^{5+}$ ions versus ion source

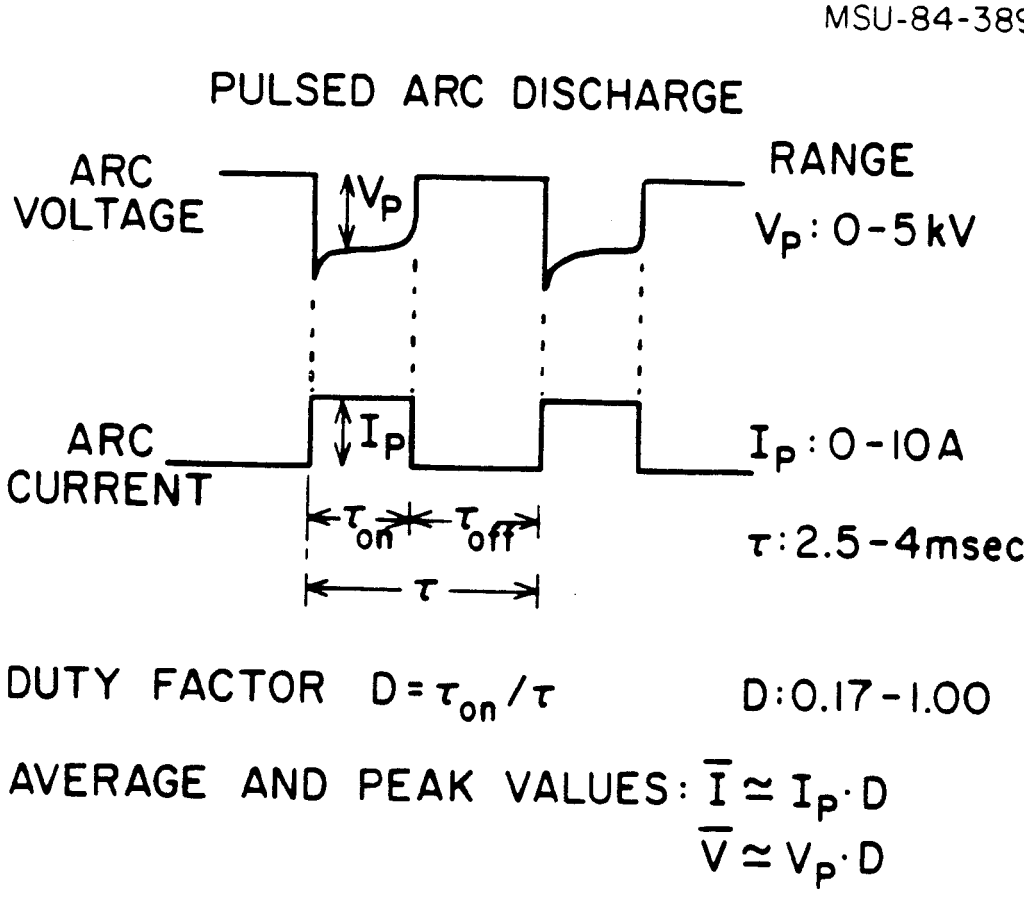

Figure 2.2. Pulsed ion source arc voltage and arc current waveforms.

parameters. The extracted beam current is only proportional to the ion current in the source, since the extracted current depends on the central region acceptance of the cyclotron, the transmission efficiency during acceleration, and the cyclotron extraction efficiency. As a result these curves have only a relative value. That is, only if they are taken under the same conditions at the same time can one make relative comparisons. This is one of the main limitations of studying ion sources in a cyclotron. (However one does get an unambiguous beam current as a result of the resonant acceleration generally, and also ultimately the ion source must perform well in the cyclotron, since getting it to work there eliminates intermediate steps.) Figures 2.3, 2.4 and 2.6 display datataken during one early cyclotron run for developing a $^{22}Ne^{5+}$ beam using a pulsed ion source. The A=22 isotope of neon was obtained via 70% ^{22}Ne enriched neon gas.

Ne^{5+} is a representative multiply-charged ion, and we find that the beam current is sensitive to the duty factor, as shown in Figure 2.3. The extracted current is plotted versus the pulse on-time for a fixed period of 3.0 msec. With the period held constant, varying the on-time changes the duty factor. With an arc current of 6.0A peak, the beam maximizes at an on-time of 1.0 msec, for a duty factor of 33%. However at an arc current of 9.5A peak, the beam

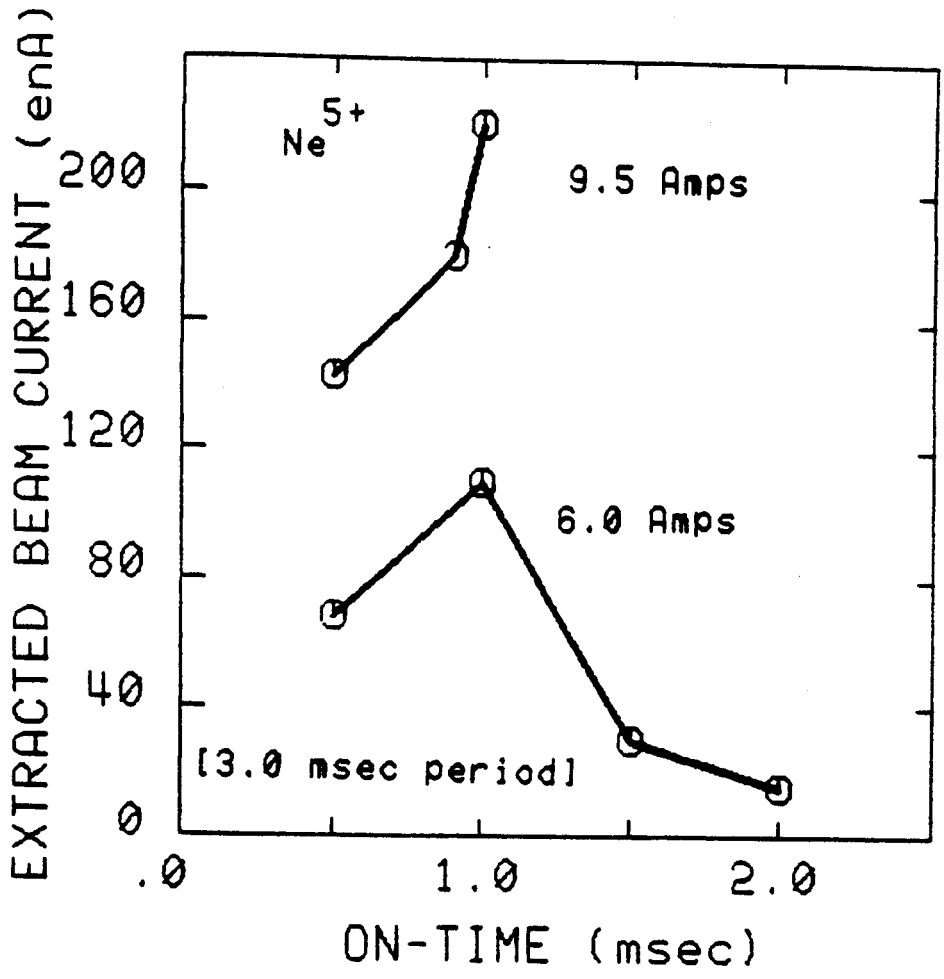

Figure 2.3. The dependence of $^{22}Ne^{5+}$ beam current on the pulse on-time is shown for a fixed pulse length of 3.0 msec and arc currents of 6.0 and 9.5 A.

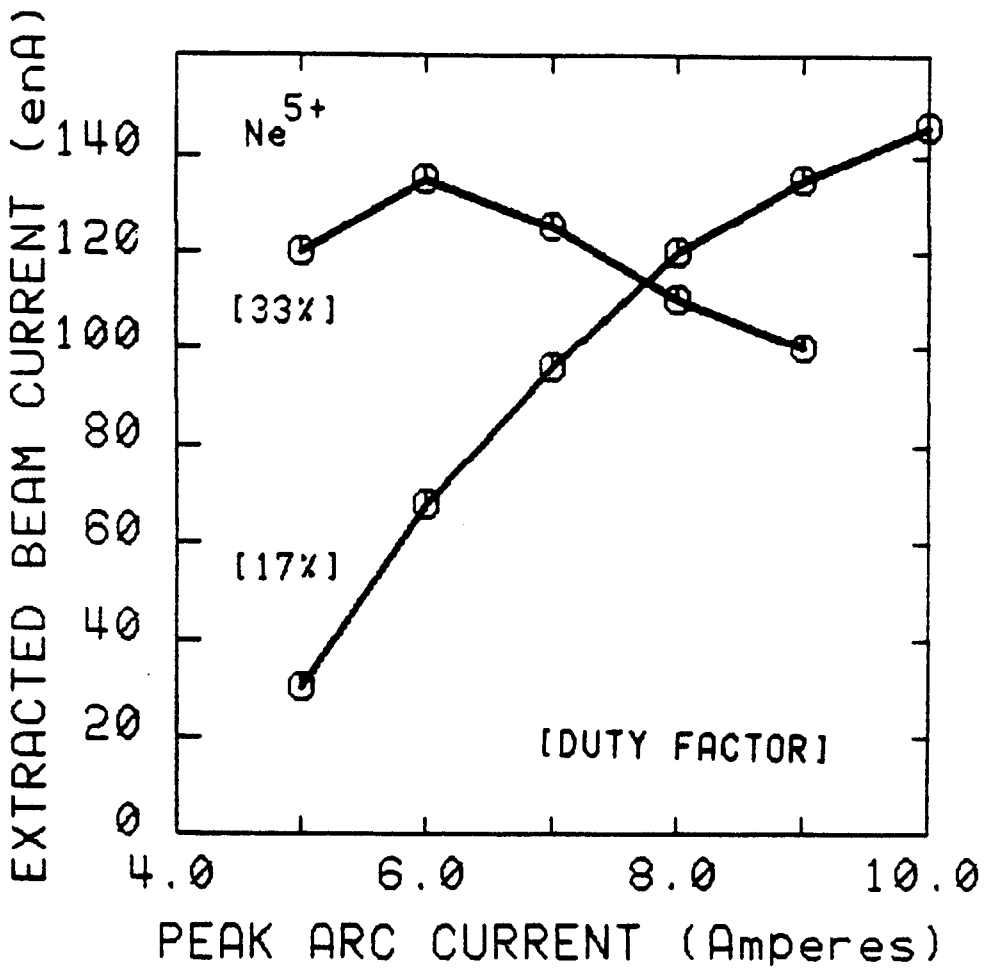

Figure 2.4. The dependence of the $^{22}Ne^{5+}$ beam current on the peak arc current is shown, for fixed duty factors of 17 and 33%.

The sharp rise in beam current at a low duty factor like 17% is consistent with an additional observation-- a pulsed arc has a surprising number of unstable modes, and therefore is quite sensitive to changes in operating parameters at low duty factors. Oscillograph (B) in Figure 2.5 shows normal pulsed arc voltage and arc current traces at a 20% duty factor and an arc current of 7 A. The arc voltage shows a leading high voltage spike peak of 1.0 kV and a voltage spread of 100 V. (It should be mentioned that this spike increases as the duty factor decreases, eventually reaching 5 kV at something like 10%, indicating that the arc is essentailly restriking each cycle!) If we cut the gas flow to less that 1.0 sccm, we often see an instability like that in oscillograph (A) in Figure 2.5. It has the disconcerting characteristic that it grows in time and will result in the arc discharge dropping out unless it is corrected. After about one-fifth of the on-time, the arc current collapses into oscillations which the tetrode can no longer stabilize, and the arc voltage goes back to 5 kV. The ion output for the source is unstable when these oscillations are occurring. Fortunately it can be corrected by increasing the gas flow and/or the duty factor. Both of these will result in an increase in the cathode temperature, via increased ion bombardment, and that seems to be what is necessary to stabilize the arc.

Figure 2.5. The discharge heated PIG source operating can be separated into regions of stability and instability during pulsed operation. Oscillograph (B) shows normal arc current and voltage waveforms. Oscillograph (A) results from a large decrease in the gas flow. This condition is unstable- eventually the arc drops back to the cold cathode mode and the production of multiply-charged ions will cease. Oscillograph (C) results from a large increase in the arc current. Evidently this large arc current is not neutralized by positive ions from the plasma, and twice during each pulse the plasma column is seen to collapse.

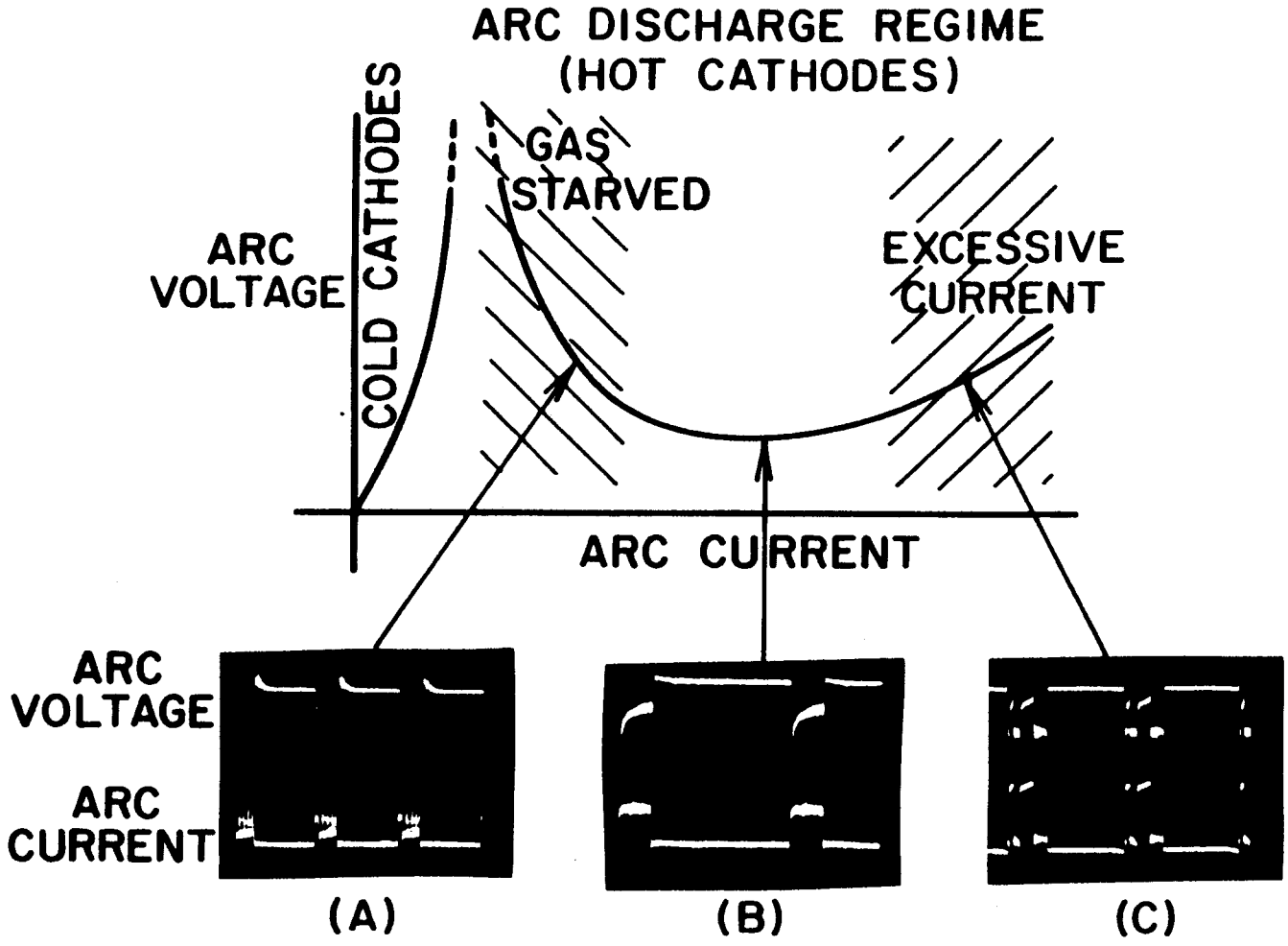
ARC DISCHARGE REGIME
(HOT CATHODES)
COLD CATHODES
GAS STARVED
EXCESSIVE CURRENT
ARC VOLTAGE
ARC CURRENT
ARC VOLTAGE
ARC CURRENT
(A)
(B)
(C)

Figure 2.5.

Another unstable mode can be obtained with excessive arc current, and is shown in oscillograph (C) in Figure 2.5. Under normal operating conditions, the electron emission is space charge compensated by the positive ions in the plasma. If the electron emission is excessive, there is a lack of compensation and the arc discharge collapses into the Penning discharge with a subsequent decrease in the beam current also. This is eliminated by simply reducing the arc current or increasing the gas flow. These two particular instabilities are the most commonly observed, and correspond to definite regions of the PIG source operating diagram, as indicated in the upper portion of Figure 2.5. The region of low gas flow borders on the transition between the pure Penning discharge with cold cathodes and the arc discharge, whereas the high arc current region is on the far edge of the arc discharge region, often exhibiting again some positive arc impedance. The average ion current produced by the source maximizes somewhere between these two extremes, and that is where we try to run the ion source.

An important feature of pulsed operation is that the high instantaneous arc current stabilizes the discharge at much lower gas flows. For reference, a gas flow of less than approximately 2 sccm, for a dc discharge, is not stable and would result in the shift to the cold cathode Penning discharge. This is important because, as shown in Figure 2.6, gas flow has a significant effect on beam

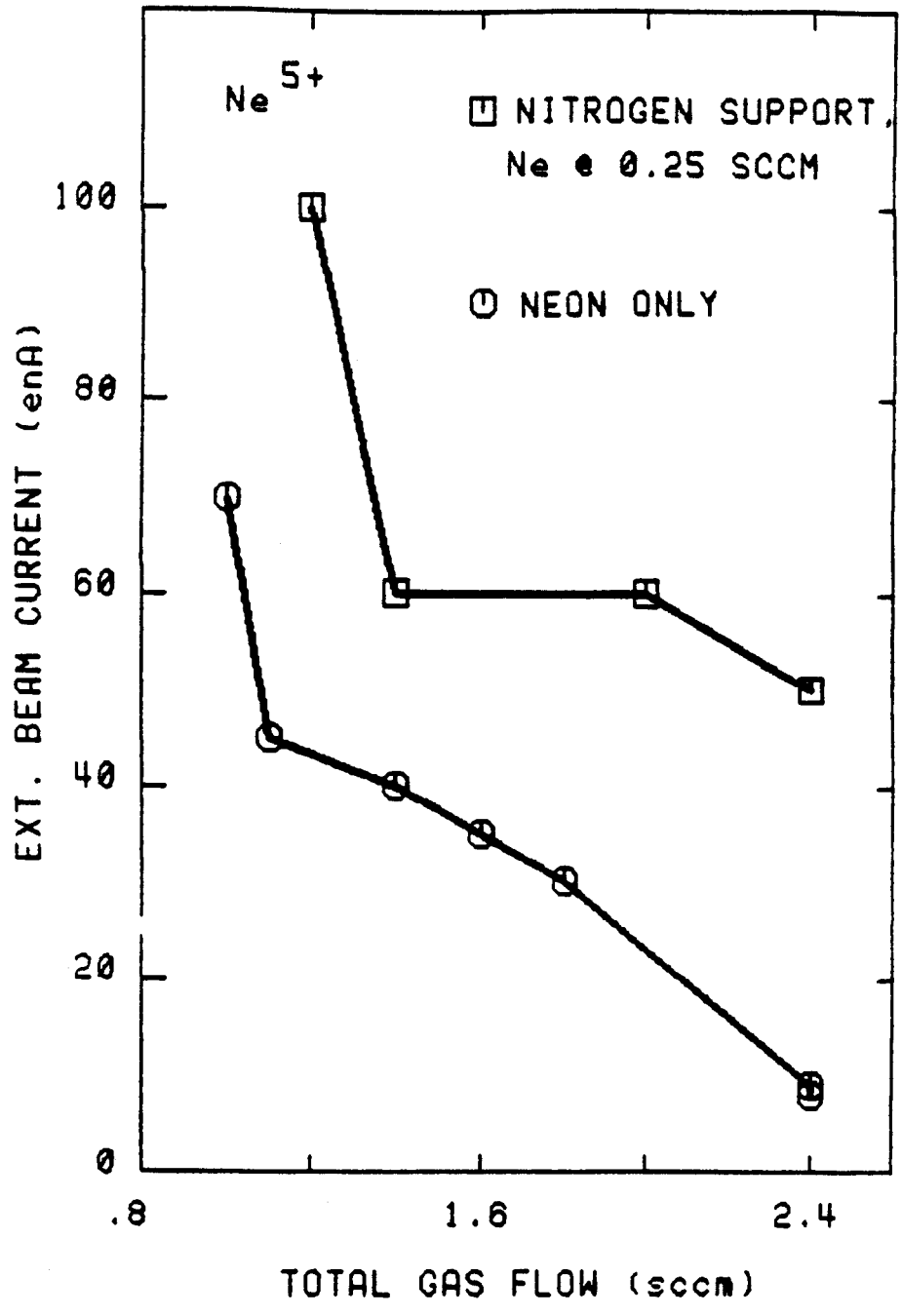

Figure 2.6. The gas flow rate into the ion source is a sensitive parameter for the production of multiply-charged ions. In this case the $^{22}Ne^{5+}$ extracted beam current is shown for neon gas (70% enriched 22-neon) source feed, and also for an arc supported by nitrogen with a constant neon flow of 0.25 sccm.

current. We return to the case of the production of $^{22}Ne^{5+}$ ions as in Figures 2.3 and 2.4. Two cases are illustrated. In the lower curve the source is being operated on neon only, and the beam current is seen to fall 70% from a gas flow of 1 sccm to 2 sccm. In the upper curve, the arc is now primarily operated on nitrogen gas, with neon bled in as an auxillary gas to produce the ion beam. This curve also shows a sharp increase in beam current at low gas flows. The lower overall level of beam current in the case of pure neon flow is due to poorer beam chamber vacuum. Nitrogen is more easily pumped by the vacuum system, and an increase in beam current due to a reduced attenuation at the center of the cyclotron results from replacing some of the neon with nitrogen. Since it happens that nearly all of the neon can be so replaced, the charge exchange in the cyclotron has clearly a large effect on the final extracted Ne^{5+} current!

As previously mentioned, the N^{5+} beam is probably the most important application of pulsed source operation at MSU, but Ne^{5+} and Ar^{6+} have proved more difficult from the standpoint of source operation and useful beam currents for nuclear physics experiments. Table 2.1 shows the results of operating ion sources for the production of 25 Mev/n $^{22}Ne^{5+}$ and 10 MeV/n $^{40}Ar^{6+}$ in the K500 cyclotron. In both cases there were approximately 50% more trials than

indicated in Table 2.1, particularly for dc operation, but many were early in the first operating period of the cyclotron, however, and have been obscured by non-source difficulties. In one very tight period both beams were operated dc and pulsed when the transition to pulsed operation was made, and it is that data summarized in Table 2.1. As before, the feed gas for the $^{22}Ne^{5+}$ beam was 70% enriched ^{22}Ne, with the remainder ^{20}Ne. For both beams in Table 2.1, the beam current obtained dc averaged less than 10 enA. It can be seen in Table 2.1 that pulsed operation at 15-33% duty factors does result in a large increase in beam current. In that respect the implementation of pulsing can be regarded as a success, since the extracted beam current is raised to a more useful level. At this time there are two other features of Table 2.1 that are important:(1) the lifetimes are quite low for these beams, both pulsed and dc, and (2) the average arc power during pulsed operation is less that half the dc arc power, and yet the beam currents are much higher! These features of pulsed operation will be addressed in the next two sections of this chapter.

Table 2.1. The characteristics of $^{22}Ne^{5+}$ and $^{40}Ar^{6+}$ beams extracted from the K500 cyclotron with dc and pulsed arc discharges in the ion source. The standard deviation is given in parentheses.

Species	Cath Type	Duty Factor	Aver. Power (kW)	Lifetime (h)	I(BSO) (enA)
$^{22}Ne^{5+}$	Ta	100	1.0(.11)	3.8(1.0)	5.2(2.3)
	Ta	30	.45(.09)	1.1(.20)	26.(19.7)
	Hf	15	.20(.06)	3.3(1.1)	77.(6.4)
$^{40}Ar^{6+}$	Ta	100	1.0(.05)	1.8(.04)	8.3(5.6)
	Hf	33	.39(.02)	2.02(0.3)	59.(19.2)
	Ta	33	*	1.8(.11)	*

*Runs for lifetime only- beam not extracted.

2.4 The Mechanism for Multiply-charged Ion Production in Pulsed Arc Discharges

A chief difficulty with the dc discharge is that, owing to the negative impedance of the arc, the arc voltage sags as the arc current increases. Both are important--the arc current is important in setting the rate of ionization and the arc voltage sets the maximum ionizing electron energy. Eventually one reaches a condition where the cathodes are emitting a lot of electrons (high arc current), but the multiply-charged ion production falls anyway because of a low electron energy (low arc voltage). Multiply-charged ions require a higher electron energy to remove the more tightly bound inner electrons, and the sagging arc voltage sets one important limit on the highest practically attainable ionization state by setting the electron energy limit. In this section it will be shown that pulsing introduces a mechanism whereby the usual negative impedance of the arc discharge can be "effectively" positive, and that this occurs because the arc voltage increases as the duty factor is reduced.

The relationship between the arc current and arc voltage can be altered in a dc arc by reducing the gas flow. In fact, the arc voltage rises as the gas flow is reduced. With lower gas flow the flux of ions to the cathodes decreases and the cathodes must cool. The arc voltage must then rise to maintain the same arc current, which is being

held constant by the power supply. This has the further advantage of reducing the ion recombination rate by reducing the gas pressure inside the source and also the cyclotron beam chamber. Of course, lowering the gas flow eventually puts the arc discharge out.

It is easy to write a set of ideal requirements for the production of multiply-charged ions in a PIG source. We would like to raise the arc current, keeping the arc voltage up at the same time, but also in such a way that allows a low gas flow and also keeps the average arc power low to protect the ion source against melting. Pulsing the arc current on a millisecond time scale as we have now done accomplishes this! At a fixed arc current, decreasing the duty factor of the pulse lowers the average arc power and the cathodes cool, with a subsequent rise in the arc voltage to maintain the constant arc current. Reviewing the pulsed cases in Table 2.1 confirms that the average power dissippated in the source has significantly decreased. For example, the entries for Ar^{6+} show that in going from dc to 33% duty factor, the average power drops by a factor of 2.5, but at the same time the beam current has increased a factor of 8.5. This has come about in part from the need to have a stable arc. If only the duty factor is lowered, the arc discharge would eventually drop out because of cooling cathodes. Therefore, the arc current must at the same time

be raised to increase the total ion production rate to stabilize the arc. In this way it turns out that both the arc current and arc voltage during the on-time have been raised far above dc levels, so that the time-averaged ion production rate is well above the dc level in spite of the low duty factor. This is why pulsing works.

Recently N^{4+} beam current in the K500 cyclotron was observed as a function of arc power, arc current and arc voltage, at fixed duty factors of 50, 75, and 100%, as shown in Figures 2.7- 2.9. These curves demonstrate the main features of the above argument. In Figure 2.7, there is a remarkable linear dependence of beam current on average arc power, and also the three curves can be nearly partitioned into separate regions of low, intermediate and high average arc power. We can say that for a constant duty factor the beam current increases linearly with arc power, and yet the beam current at 200 watts and 50% duty factor is more than twice as large as the beam current at 500 watts and 100% duty factor. So the average arc power consumed by the source is not as important as how it is obtained. If we look at the peak arc current during the pulse, in Figure 2.8, we see that this again separates on the basis of duty factor, and with the beam current increasing with arc current in all three cases of duty factor. Observe that for approximately the same peak arc current, the beam current is

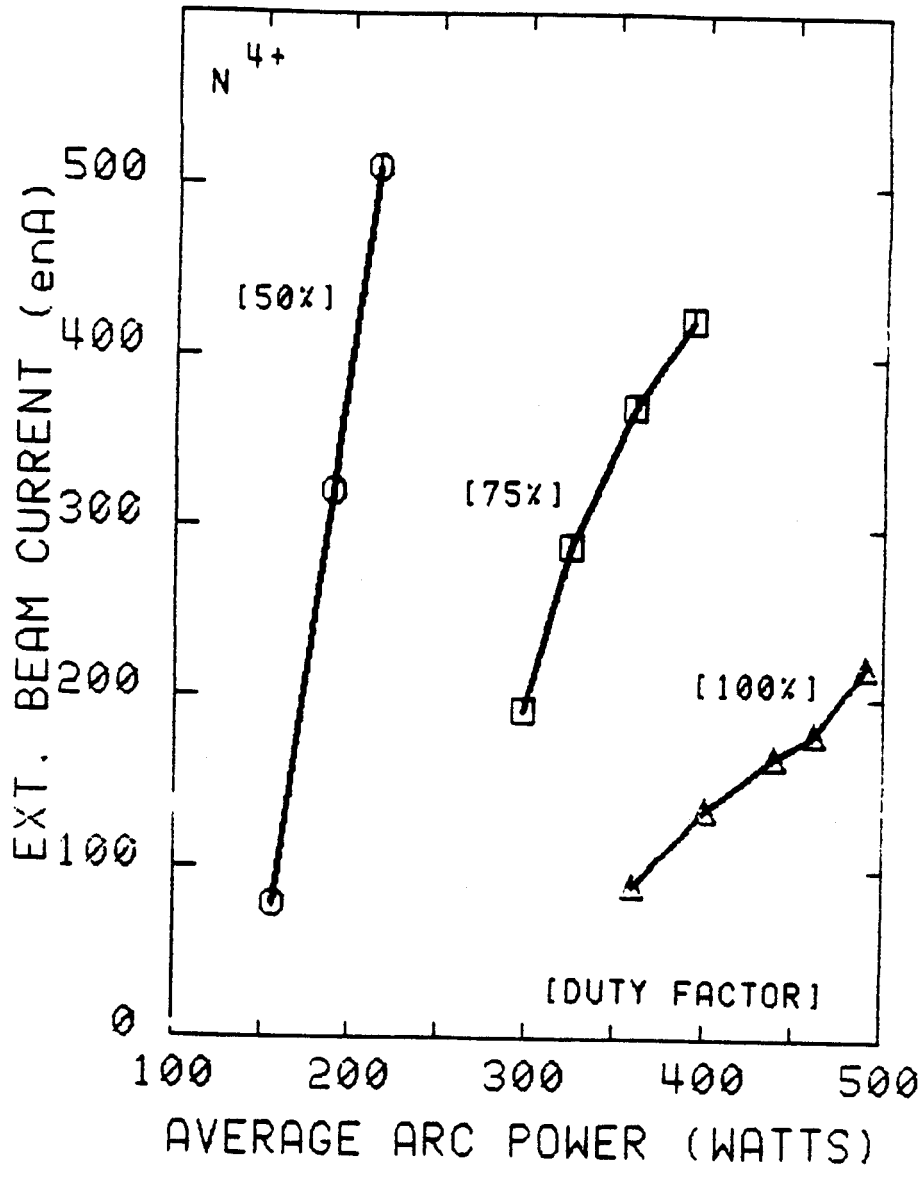

Figure 2.7. N^{4+} extracted beam current is plotted versus average arc power, for fixed duty factors of 50, 75 and 100%.

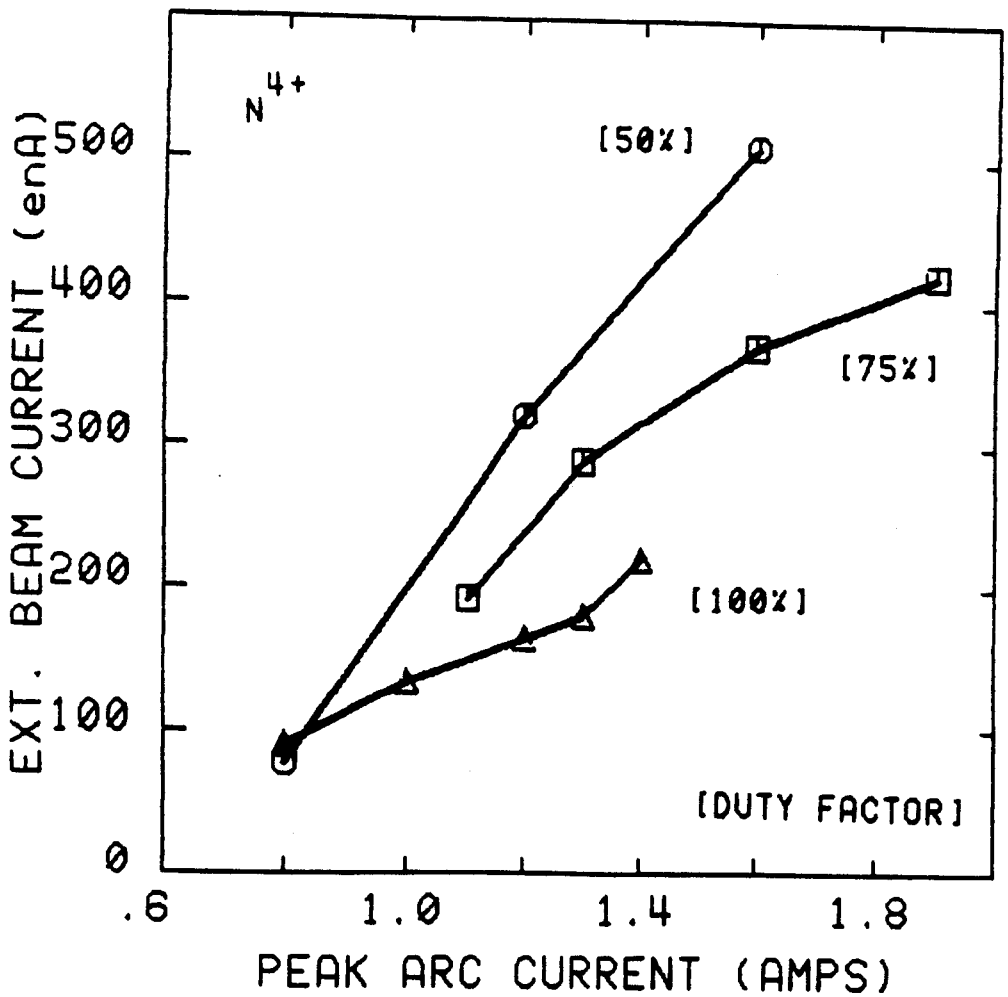

Figure 2.8. N^{4+} extracted beam current is plotted versus peak arc current for 50, 75 and 100 % duty factors, corresponding to those same cases in Figure 2.7.

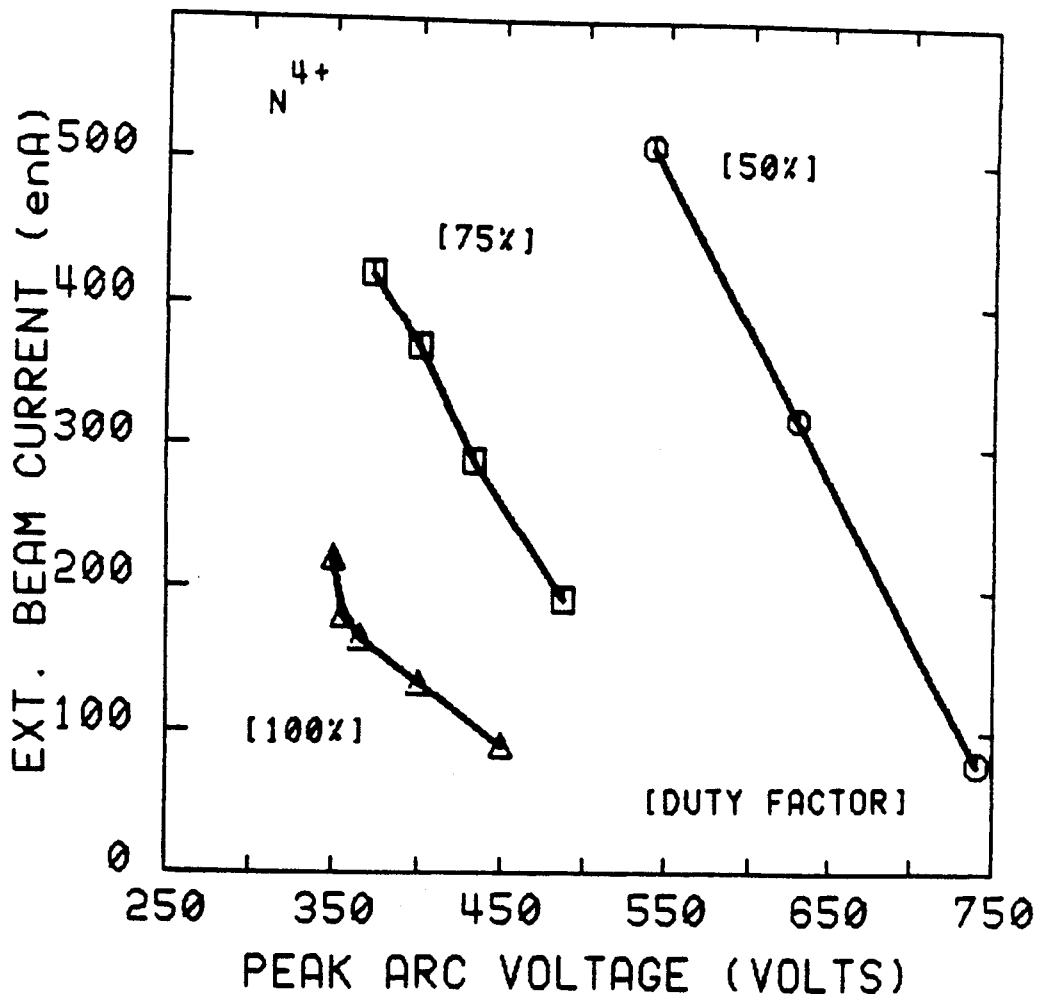

Figure 2.9. N^{4+} extracted beam current is plotted versus peak arc voltage for duty factors of 50, 75 and 100%, corresponding to those same cases in Figure 2.7.

higher for a lower duty factor. The explanation of this effect comes from Figure 2.9, in which the beam current is plotted as a function of the peak arc voltage. The arc voltage is increasing rapidly with the decreasing duty factor, so that for the same peak arc current the product $I_p x V_p$ is much larger for a lower duty factor. So at low duty factors both the arc current and arc voltage are allowed to be large, and that is compensating for the reduction in the on-time to such an extent that the total beam current still increases. Also in Figure 2.9, observe that at a constant duty factor the arc exhibits the usual negative impedance, so that the basic character of the arc discharge has not been altered. One final point about the curves in Figures 2.7-2.9: the beam current varies more rapidly with all parameters at low duty factor--implying less stability and more critical tuning.

2.5 Source Lifetime with Pulsed Neon Discharges

For the production of Ne^{5+} ions with tantalum cathodes and a 33% duty factor, Table 2.1 shows that the source lifetime is only about 1 h. This low lifetime exacts a heavy source maintainence cost whenever this beam is attempted, and it would certainly be attempted more if the lifetime was improved. We decided to try to boost the lifetime by making changes in the arc geometry and would like to review that

work here. As is always the case with PIG source operation, the strong coupling of the various parameters makes it difficult to alter the operation of any one independently. This is particularly true of the source lifetime. For example, increasing the duty factor has been observed to reduce the sputtering rate, but often the beam current goes down as well. Increasing the gas feed would also help by lowering the arc voltage, and therefore the energy at which positive ions bombard the cathodes, but the gas flow is one of the most sensitive parameters with regard to beam current, and we find for instance, that beam current decreases rapidly with increased neon flow (see Figure 2.6).

One obvious approach would be to stop the formation of the deep crater, since this is what is making the arc go out, and a study was made in that direction, based on a review of a successful approach made at Texas A&M.

According to Sakurada [Sa 79], the lifetime of the Texas A&M PIG was improved by reducing the diameter of one cathode to no more than 1 mm greater than the diameter of the plasma chamber aperture. Evidently with this change a deep depression does not form in this cathode, and the electron emission is maintained until some other limiting process comes into play. The lifetime for Ar^{8+} was given as

8 h and as much as 14 h for Ne^{6+}. With this change the useful source lifetime becomes more a question of beam attenuation due to a build-up of sputtered cathode material in arc defining apertures and the extraction slit than arc stability, so that making both the cathodes the smaller diameter gave no additional benefit. The geometry of the TAMU PIG is very similar to ours, with the main differences being the larger overall diameter and the location of the vacuum feedthru near the arc chamber. Table 2.2 below summarizes the differences between the two geometries for tantalum cathodes, assuming the lower ion source configuration in our case, with "outer" referring to the cathode at the end of the high voltage rod.

Table 2.2. Comparison of cathode sizes and plasma aperatures in the Texas A&M and MSU ion sources.

	TAMU	MSU
Inner Cathode Diam.	13 mm	9.5 mm (.375 in.)
Outer Cathode Diam.	7.5 mm	9.5 mm
Plasma Aperature	6.5 mm	5.2 mm (.203 in.)

Ten tantalum cathodes of 6.4 mm (.250 in.) diameter were fabricated in order to test whether this technique could be used to improve the lifetimes of our pulsed argon and neon beams. This cathode diameter is 1.2 mm larger than the MSU

plasma aperture, and hence just outside the prescribed range according to the TAMU data, but we have the additional problem of setting manually the rotational position of the cathode, and the increased diameter was viewed as an appropriate safety factor there. In addition, since the position of the inner cathode in our source is more stable, it was thought that locating the smaller cathode there would insure that the arc would not fall off the side, should the alignment be off or the position of the high voltage rod move. During a 22 Mev/n $^{22}Ne^{5+}$ run, two trials were made with a small inner cathode, each after a run with a normal cathode size.

Operation was found to be the same as with normal cathodes--that is, if you did not know that there was a small cathode in the source, nothing in the behavior during striking and operation would lead you to believe that there was some difference. In the first trial we were over-confident, reducing the neon gas flow to 1.0 cc/min and cutting out the nitrogen support altogether, and after one hour lost the source because of low gas flow. Inspection revealed a well centered and shallow crater on the small cathode, with a similar sized depression on the other cathode as well. The second small cathode trial lasted 1:50 h, with the failure being the arc instability associated with cathode erosion. Inspection revealed a deep,

well centered depression in the small cathode with thin side walls. Obviously the reduced diameter was still too large! Both normal runs ended in the usual way with the arc dropping out and attempts to restrike being unsuccessful. Table 2.3 summarizes the results of the four runs made. In this table "d" is the depth of the cathode depression and "w" is the corresponding width.

Table 2.3. Cathode wear characteristics with neon feed.

	LIFETIME (hr:min)	INNER CATH. d (inches)	INNER CATH. w (inches)	OUTER CATH. d (inches)	OUTER CATH. w (inches)
1. Normal	1:41	.147	.236	.135	.236
2. Small	0:52	.050	.168	.081	.224
3. Normal	1:25	.152	.222	.144	.218
4. Small	1:50	.128	.220	.122	.220

Without getting too carried away with the numbers, it is interesting to note that the lifetimes of sources 1,3 and 4 are correlated to the inverse of the average crater depth, as shown in Figure 2.8, while the widths are a reasonably constant .22 - .24 inches. (Of course, source 2 was inadvertently gas starved out and therefore will not correlate.) Since we have established that we can run the small cathodes, the expected gain in lifetime ought to be

there; we just picked a diameter slightly too large--something like .220 inches would work better. Alternatively, increasing the plasma aperture would have the same effect. In future work both of these options should be explored.

2.6 Summary

Operating the ion source with a pulsed discharge has given us Ne^{5+} and Ar^{6+} beams of sufficient intensity to use for nuclear physics experiments. The advantages of pulsing include having more source tuning parameters for improved control, the use of higher arc current without at the same time reducing the arc voltage, less gas flow to the source and achieving a lower average arc power. The disadvantages include low source lifetimes for some beams, new instabilities and more critical tuning, especially at low duty factors. At low duty factors, the need for more arc current from the power supply is evident, and in that regard the K500 supply with a 7-10 A maximum current does not exploit the full potential of pulsed operation, and may be a contributing factor in the low lifetimes.

In addition, it seems that not all experiments can tolerate the additional time structure that goes with pulsed operation, for when the arc current goes out on each cycle,

the beam current shortly follows. This is particularly true for coincidence experiments. Consider a single coincidence experiment, where the simultaneous measurement of events E_i and E_j are made. The rate of accidental coincidences (R_a) will depend upon individual reaction rates R_i and R_j, and the time resolution of the measurement $\Delta\tau_{ij}$,

$$R_a \propto R_i R_j \Delta\tau_{ij}, \qquad (2.1)$$

but the rate of each event must be proportional to the instantaneous beam current (I_{beam}), and so Eq. (2.1) can also be written as:

$$R_a \propto I_{beam}^2 \Delta\tau_{ij}. \qquad (2.2)$$

At the same time the rate of true coincidences (R_t) must also be proportional to the beam current, which we express as

$$R_t \propto \sigma I_{beam}. \qquad (2.3)$$

Hence the ratio of true coincidence events to accidentals, obtained by dividing Eq. (2.3) by Eq. (2.2) is

$$\frac{R_t}{R_a} \propto \frac{1}{I_{beam}} . \qquad (2.4)$$

During pulsed operation, a much higher beam current is produced during a shorter time interval, and so the ratio of trues to accidentals must then decrease according to Eq. (2.4). In practice one finds that this difficulty limits the lowest permissible duty factor in coincidence experiments to 50-80%.

CHAPTER 3

HAFNIUM CATHODES AND NITROGEN SUPPORTED ARCS

When PIG ion sources are used to produce heavy ions, the source lifetime becomes a major issue. The costs of ion source maintenance can be large, and ion source recycling can become a significant fraction of the accelerator operating time [Ba 72,Hu 73]. For a PIG source with discharge-heated tantalum or tungsten cathodes, lifetimes generally fall in the range of 5-20 hours, with the lowest lifetimes resulting from operating conditions aimed at producing the highest charge states of the heavier elements [Sh 81,Go 79,Ke 72,Ba 72]. Experience here has shown that source lifetimes fall in the range of 2-10 hours with tantalum cathodes in the K500 internal PIG sources [An 83, An 84]. The lowest lifetimes have occurred during the production of neon and argon beams, while the highest have been for C^{3+} and N^{4+} beams.

The finite lifetime is due principally to the sputtering of the cathodes by ions from the discharge, as illustrated schematically in Figure 3.1. Any one of the following consequences of the cathode sputtering can destroy the ion output.

1. An arc short resulting from the build-up of sputtered material in the gap.

2. Low output as a result of sputtered material choking the discharge defining aperture or the source extraction slit. One observes a slow beam attenuation with time and finally the run is terminated.

3. Arc instabilities that result from the formation of deep craters in the cathodes which tend to extinguish the arc-- especially during pulsed operation at low duty factors, where the arc literally has to restrike on each cycle.

The worst effect of the formation of a crater is a lowering of the surface electric field of the cathode, which must be high initially to switch the pure Penning discharge to the high power arc required for the production of multiply-charged ions. If the arc goes out for some reason, it will not restrike if the crater has become deep, and the

source must be rebuilt. This is the primary cause of maintainence difficulties associated with the operation of PIG sources, and it is clear that any increase in source lifetime would be desirable. Unfortunately the ion bombardment that causes these problems is also the source of cathode heating, which is essential for the thermionic emission of electrons that sustains the arc.

In this chapter the initial testing and development of hafnium cathodes in the K500 PIG sources will be presented. The motivation for this switch from tantalum is extremely long lifetimes that have been obtained as a result. This study was accomplished in the context of the operation of the K500 during the production of beams for experiments and also during the development of new beams. The advantage has been a rigorous testing of the limits of applicability of hafnium cathodes under the conditions of actual use, but the major disadvantage is the lack of precise test conditions as would have been possible in an ion source test stand. As a result only the most evident properties will be discussed.

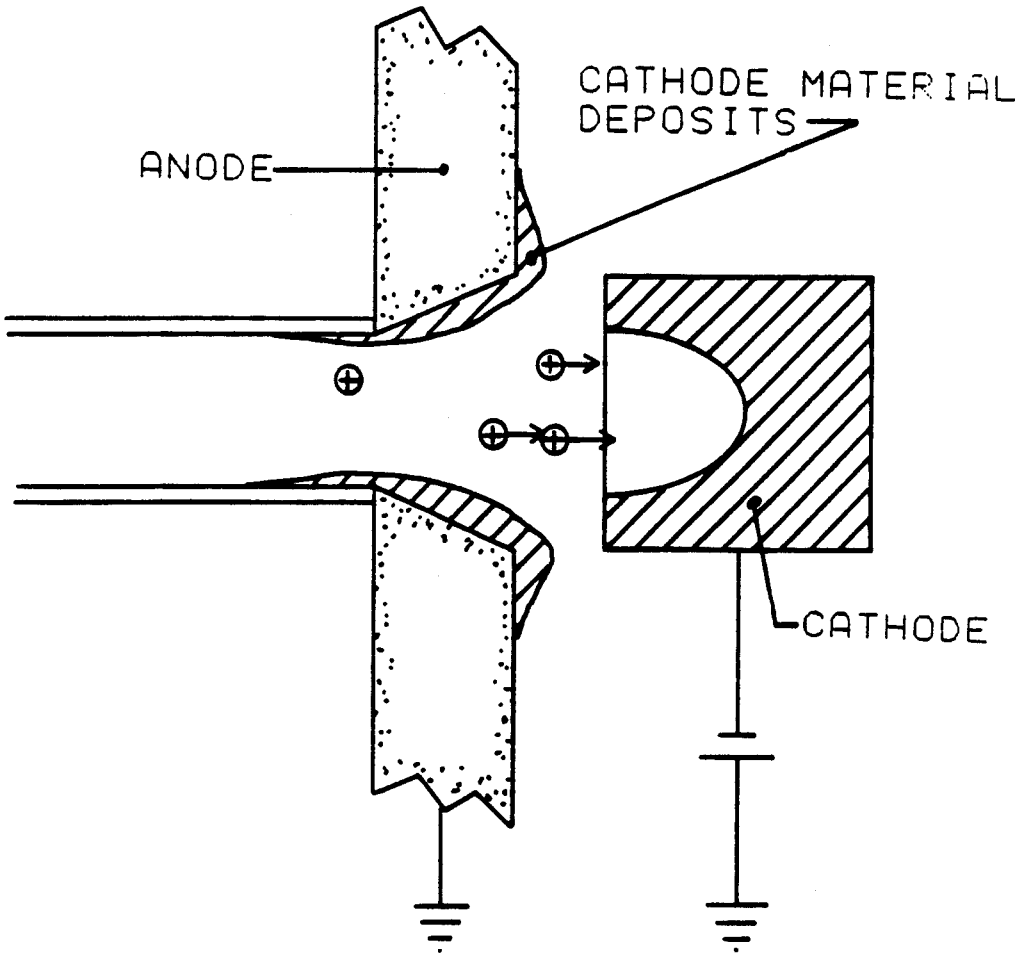

Figure 3.1. A schematic representation of one end of the PIG arc geometry, showing the anode end, arc defining aperture, and the cathode. The effects of cathode sputtering are illustrated.

3.1 Choice of Cathode Materials

Good cathode materials for PIG sources must possess low sputtering rates and high thermionic emission current densities. Refractory metals are usually the material of choice for PIG sources, since they best meet these two requirements. Cost, availability and workability are also important.

Consider the sputtering rate first. In a PIG source large fluxes of positive ions bombard hot cathodes, and we want to know what materials will give the longest lifetimes under these conditions. The most extensive study of the variation in sputtering yield (ejected atomsper bombarding ion) was made by Wehner with 30-400 eV mercury ion bombardment first [We 57], and then the noble gases over the energy range 50-600 eV [La 61,Ro 62]. Fortunately the data span the energy range of positive ions in a PIG source. The sputtering yields were found to vary nearly linearly with bombarding energy in this range and to increase slightly with bombarding mass. Some of the elements found to have relatively low overall sputtering yields, and have also higher densities, which determines the volumetric sputtering rate, were Ti, Mo, Nb, Hf, Ta and W. These "pure" atomic physics facts are in good agreement with the experience gained during the operation of PIG sources with various cathode materials [Be 72]. In Wehner's studies, hafnium,

the subject of this chapter, had a slightly higher sputtering yield generally than Ta or W, so only a slightly higher sputtering rate would be expected. On that basis hafnium cathodes would be expected to show lifetimes somewhat shorter but comparible to tantalum and tungsten in PIG sources.

In addition, cathodes for PIG sources must be efficient electron emitters at high temperatures. Thermionic emission from pure metals follows Dushman's Equation [Bl 74]. In its simplest form:

$$J = AT^2 e^{-b/T},$$

where J is the emission current density in Amperes/cm^2,

A is a quasi-constant of 120.4 Amperes/cm^{2}deg^2,

T is the absolute temperature, and

b is the absolute temperature equivalent of the work function.

The work functions of the above metals do not vary significantly, so that temperature is the dominant parameter, and as a cathode material, metals with high melting points are favored. On that basis Ta and W from the above list, with melting points of 3269 K and 3683 K, respectively, would appear to be the best cathode choices

for high power PIG sources. In this regard hafnium has a larger emission current versus temperature as tantalum [Ha 67], but has a much lower melting point (2495 K), so the maximum J is less. This is shown graphically in Figure 3.2. In practice, the lower melting point would translate into a lower arc power limit for an operating ion source.

3.2 Initial Use of Pure Hafnium Cathodes- A Review

On the basis of the above considerations, as a cathode material hafnium would be expected to perform like the other refractory metals--but not as well as tantalum and tungsten at high arc powers, where the lower melting point sets a limit.

3.2.1 MSU K50 Cyclotron

As a result of an observation that hafnium targets were difficult to produce by sputter deposition, in 1978 tests were made of hafnium cathodes in a heavy ion PIG source in the K50 cyclotron, which was still running at that time.

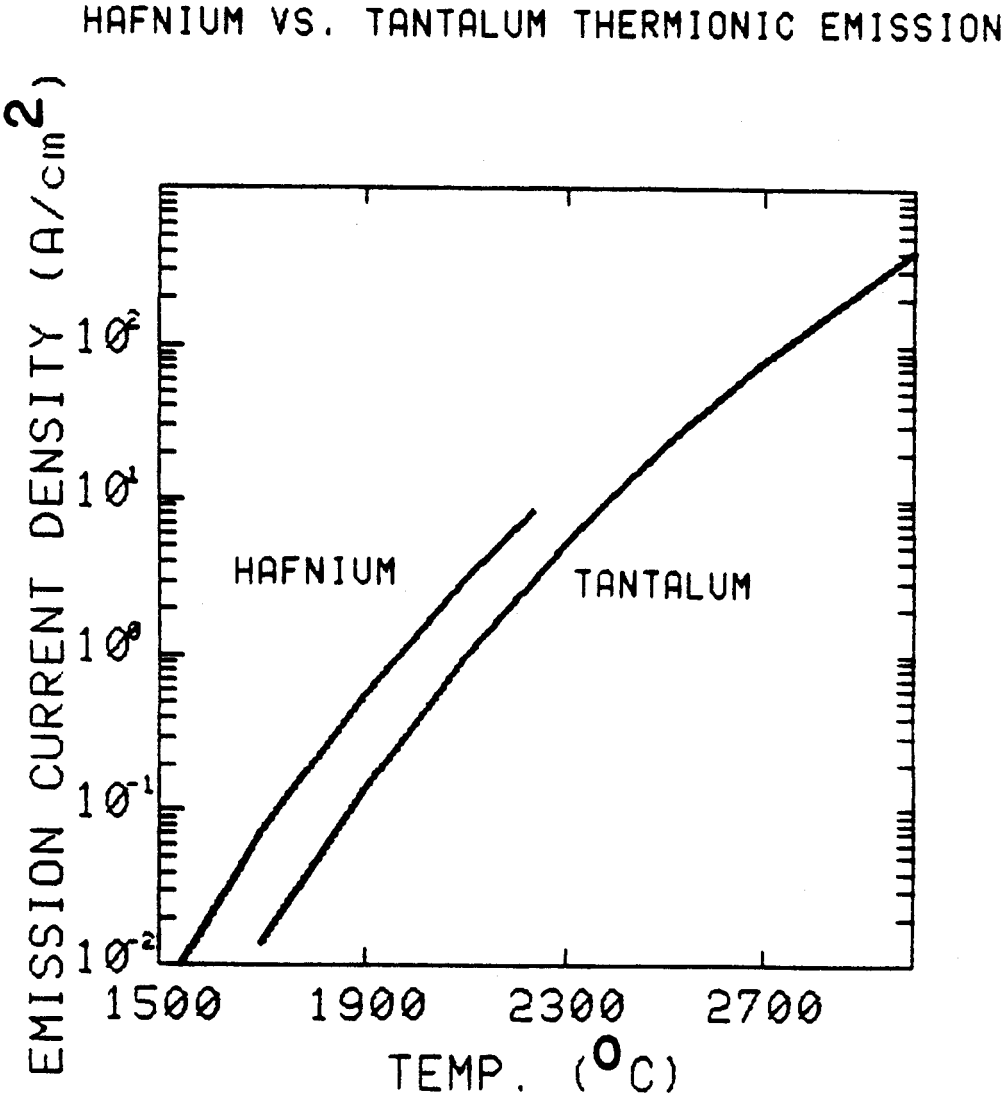

Figure 3.2. The thermionic emission currents densities of pure hafnium and tantalum are compared over the temperature range of 1500-3000 °C.

Only a few runs were possible, but some operating characteristics quite different from those of tantalum cathodes were observed [Mi 79]. With CO feed, a 24 h lifetime was obtained, as compared to 2-3 h for a normal tantalum run, albeit at the expense of lower beam current. One experiment in March 1979 took 1 eμA of 70 Mev C^{4+} ions on target for 24 h from a single source equipped with hafnium cathodes [Ha 84]. For comparison, with tantalum cathodes the extracted beam current was 15-30 eμA. The lower extracted current was thought to be due to a lower maximum cathode operating temperature, as a result of the lower melting point of hafnium. The order of magnitude increase in lifetime was however a surprise, and since the lifetime enhancement was not observed with nitrogen or neon arcs, it was attributed to the formation of a HfC layer on the surface of the cathodes. Hollow tantalum cathodes filled with pressed-in HfC powder were tried, and longer lifetimes were obtained, but the arc operation was erratic and gave unstable beam output.

Since high beam intensities are not always required, it was speculated at that time that hafnium cathodes might find application in the K500 cyclotron when run in the injector mode, where the charge states required for acceleration would usually be low.

3.2.2 Experience At Other Laboratories

Other laboratories certainly tried hafnium cathodes after 1979, but generally could not see any advantage over tantalum. The experience at Texas A&M was typical [Wa 84]. A longer lifetime was found, but intensities were low for the highest charges states where difficulties were encountered in maintaining high arc power without melting the hafnium cathodes, in agreement with our experience.

Since higher beam energies, and hence higher charge states, is generally more important than source lifetime, hafnium cathodes did not come into wide use.

3.3 Hafnium Cathodes in K500 Cyclotron PIG Sources

A review was made of the testing of hafnium cathodes in the K50 cyclotron, and on that basis it was expected that for low-charge-state-carbon beams, an increase in ion source lifetime over tantalum could be expected without a reduction in beam current. Ten pairs of hafnium cathodes of the same design as the normal tantalum cathodes were machined, for use in the K500 cyclotron in order to make a comparison of operating characteristics with tantalum. The very first test was made with a C^{4+} beam, and a factor of three increase in lifetime was observed with hafnium without

significant beam attenuation. This success encouraged trial of hafnium cathodes for nearly all of the K500 beams. Table 3.1 presents data on the lifetimes of sources operated with hafnium cathodes for ion production in the K500 cyclotron, and Table 3.2 summarizes the operating characteristic of hafnium sources.

The largest increase in lifetime is seen for N^{4+} and N^{5+} beams. To get a feel for the magnitude of the lifetime effect, at the end of the first cyclotron operating cycle in June 1983, 340 h of N^{5+} beams had beeb obtained using only 13 sources, and the same result would have required about 53 tantalum sources! Figure 3.3 shows samples of the long-lived cathodes from a N^{5+} source, which exhibit many of the characteristics of used hafnium cathodes.

Generally hafnium cathodes flake or crumble upon removal from the cathode holders, and as a result measurement of the amount of material sputtered during source operation contains a large uncertainty. In addition, the large variation in arc parameters that occurs during

Table 3.1. K500 operation with Hf cathodes. Lifetimes for tantalum cathodes are given where available.

ION	GAS	HAFNIUM		TANTALUM
		t_{mean}(h)	t_{max}(h)	t_{mean}(h)
$^{4}He^{1+}$	1% He+N_2	12.9	20.5	
$^{6}Li^{2+}$	96% ^{6}LiF pellet+N_2	37.3	67.6	
$^{7}Li^{2+}$	LiF pellet +N_2	16.0	42.5	
$^{12}C^{3+}$	CO,CO + N_2	10.6	19.0	
$^{12}C^{4+}$	CO,CO + N_2	14.1	31.6	9.6
$^{14}N^{3+}$	N_2	15.4	27.8	
$^{14}N^{4+}$	N_2	23.4	55.0	5.8
$^{14}N^{5+}$	N_2	24.9	55.1	6.4
$^{16}O^{4+}$	O_2 + N_2	10.8	13.9	
$^{20,22}Ne^{5+}$	Ne	3.3	4.6	2.5
$^{40}Ar^{6+}$	Ar	2.0	2.4	1.8

Table 3.2. A summation of the main characteristics of K500 ion sources operated with Hf cathodes.

1. Extended lifetime.

The best case is with N_2 feed, with CO + N_2 almost as good, and CO the next best. The emergence of N_2 feed as giving the longest source lifetimes was quite a surprise. The lower lifetime with CO results from carbon deposits that form on insulators, making the arc unstable, and not specifically cathode wear.

2. Source striking.

The source strikes at a lower arc voltage- ~1000 volts versus 2500-4000 volts for tantalum. Normally it is not possible to restrike a tantalum source after more than 1 hour of operation. Hafnium sources restrike after many hours. This is difficult to quantify, as adequate statistics have not been kept, but the interval is greater than 20 hours for an N_2 fed source and greater than 10 hours for a CO fed source. Multiple source restrikes are also possible in these cases.

3. Cathode wear.

Very shallow craters form in the cathodes when operated DC.

4. Beam attenuation.

Less sputtered material builds up in the anode bore, resulting in slower beam attenuation with time.

5. Noble gas feed.

Same behavior as tantalum cathodes for Ne or Ar gas feed- deep craters form in the cathodes and no significant improvement in lifetime is observed.

6. Cathode-feed gas reactions.

Used cathodes show strong chemical changes after operation with N_2, CO or O_2 gas feed. The cathode color is glossy gold for N_2 feed, burnt black for CO feed, and dark gray for O_2 feed. Often the cathode is found to have fragmented, and for O_2 feed exhibits swelling. No reaction to noble gas feed is observed (ofcourse!).

Table 3.2.(cont'd.).

7. Temperature effects.

There is often evidence of partial cathode melting, especially at the cathode center. With more than about four amperes of arc current DC, hafnium cathodes in K500 sources have melted.

8. Pulsed ion source operation.

Roughly the same beam currents can be obtained as with Ta cathodes, but at much lower duty factor. Depending on the duty factor, the lifetime enhancement is still possible however.

9. Normal failure mode.

For long lived hafnium cathode sources, the cathodes crumble and the source dies in a short.

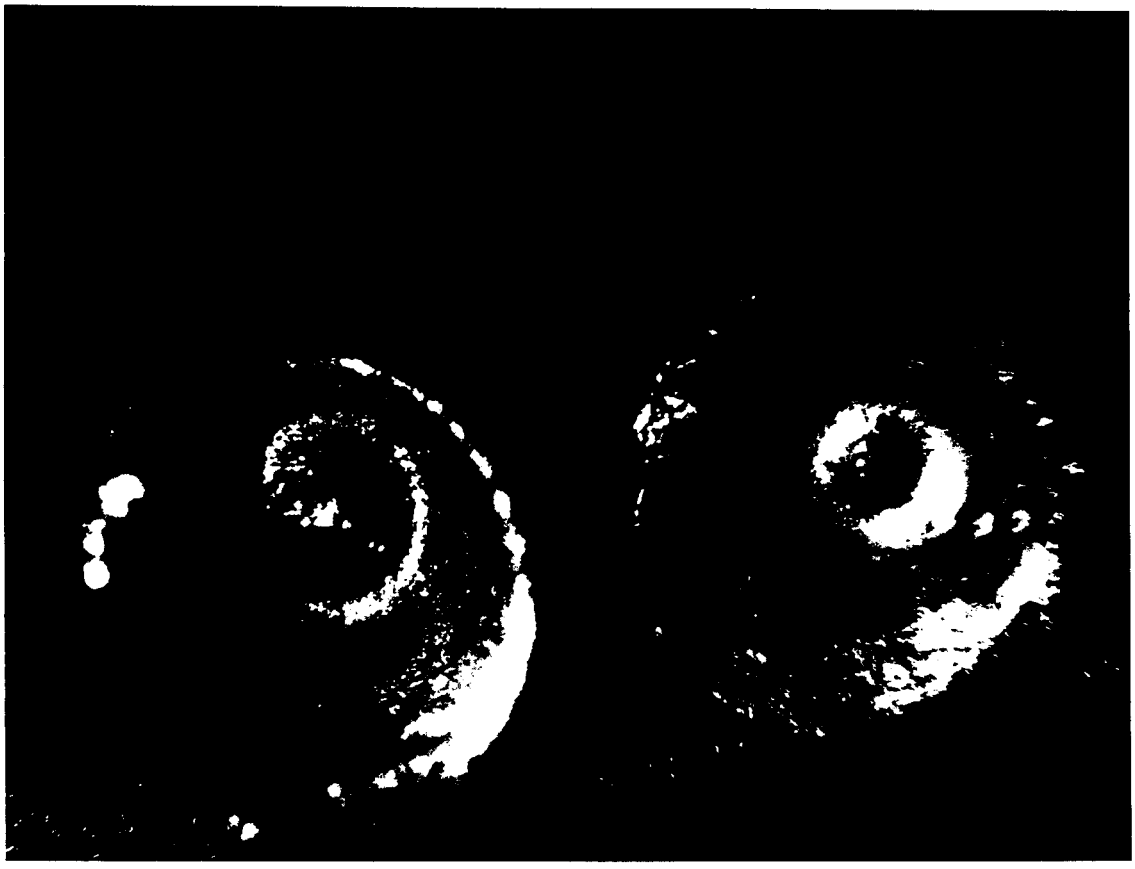

Figure 3.3 55 hour lifetime hafnium cathodes for N^{5+} show small molten domes at the base of the craters and crumbled edges- the latter evidence of a structure changing reaction of the hafnium and nitrogen gas. New hafnium cathodes resemble other refractory metals.

normal operation eliminates the possibility of relating cathode wear to arc parameters. Finally, there are not many cases in which hafnium and tantalum cathodes are run under the same conditions and so, comparing the rate of wear to that for tantalum cathodes is not possible for all the cases in Table 3.1.

During the development of an Ar^{6+} beam, however, both tantalum and hafnium cathodes were used under the same conditions. Since hafnium does not react with argon, the cathodes remained hard and could be removed intact. The sputtering rate was measured in this case and the results are given in Table 3.3.

Table 3.3. Hafnium and tantalum cathode sputtering rates with argon gas feed for 10 sources, used during the development of Ar^{6+} ions.

Material	Cases	M (mg.)	T (min.)	S (mg./min.)
Hf	6	855	140	6.10
Ta	4	740	80	9.25

The tantalum sputtering rate is 1.5 times the rate for the hafnium in these cases with argon feed. This is in good agreement with the ratio of the average lifetimes of hafnium and tantalum sources with argon feed, as given in Table 3.1. On that basis one can estimate that the tantalum sputtering

rate with nitrogen feed is four times the sputtering rate of hafnium.

Up to this point, we been considered only the lifetime performance of sources with hafnium cathodes. The source output current is, of course, also affected. For low charge state beams (Li^{2+}, C^{3+}, N^{3+}, N^{4+}), there is no difficulty in obtaining cyclotron extracted currents greater than 10 pnA, (which statisfies minimum requirements for nuclear physics experiments) with hafnium cathodes. For N^{5+} beams under certain conditions, hafnium cathodes still provide adequate current, but for Ne^{5+} and Ar^{6+}, tantalum cathodes must be used. N^{5+} was run pulsed or dc, with hafnium or tantalum cathodes. These data are summarized in Table 3.4.

Table 3.4. Nitrogen 5+ beam currents with hafnium and tantalum cathodes. N_2 feed is assumed in all cases.

CATHODE TYPE	DUTY FACTOR (%)	EXT.CURRENT (enA)	MEAN LIFETIME (h)	MAX. LIFETIME (h)
Hf	30	120	24.9	55.1
Ta	100	100	6.4	10.6
Ta	80	150	5.5	7.6

As can be seen in Table 3.4, three basic operating modes can be distinguished. In the first, Hf cathodes are

used to obtain long life, but pulsing at a low duty factor is required to maximize the beam current. In the second mode, Ta cathodes are used, the beam intensity is roughly the same as in the first case, though obtained dc, but the average lifetime is 4 times lower. This mode is necessary when the experiment cannot tolerate the pulse structure, such as in coincidence experiments. If a small amount of pulsing can be tolerated, then a third mode with Ta cathodes is used, and there is about a 50% increase in the extracted beam versus dc.

In connection with the data in Table 3.4, the arc parameter ranges for N^{5+} production with hafnium and tantalum cathodes operated DC are presented in Table 5. For the same gas flow and arc current, the arc voltage is significantly lower for hafnium cathodes operated dc than for tantalum cathodes under the same conditions. This will be discussed in Section 3.4.

Table 3.5. Comparison of the range of dc arc parameters for sources equipped with hafnium or tantalum cathodes, when used to produce N^{5+} ions in the K500 cyclotron.

CATH. TYPE	ARC VOLTAGE (Volts)	ARC CURRENT (Amps)	ARC POWER (KW)	EXT. CURRENT (enA)
Hf	200-300	2.0	0.4-0.6	20-40
Ta	500-700	2.0	0.8-1.4	75-150

3.4 Analysis of Lifetime and Beam Current Effects

3.4.1 Cathode lifetime

The dominant cause of these effects is the significantly lowered sputtering rate over tantalum or pure hafnium for N_2 or CO feed and the same operating conditions.

The key observation is that when a non-reactive gas such as neon or argon supports the arc, hafnium cathodes show the same deep crater formation as tantalum cathodes, with the arc eventually going out in the usual way. With the noble gases, what we are seeing is the sputtering of pure hafnium, which differs from tantalum only in a small way, so cathode lifetimes must also be similar. As seen in Table 3.1 for Ar or Ne beams the average lifetimes for hafnium are slightly larger than for tantalum, by factors 1.14 and 1.33 respectively.

On the basis of the sputtering yield data for pure hafnium, no enhancement in the lifetime would be expected for nitrogen or carbon dioxide supported arcs. However, the source lifetime with nitrogen feed is four times longer when hafnium cathodes are used. For CO, the picture is not so clear because cathode wear is generally not the cause of source failure, as mentioned in Table 3.2. Furthermore,

K500 sources for carbon ions have been run with a mixture of CO and N_2 to reduce the build-up of carbon on support insulators. We will therefore concentrate on the nitrogen feed case, which is the main new result, knowing that the previous K50 cyclotron testing of hafnium cathodes reported a lifetime effect for CO feed. The present study has seen lifetimes for CO feed longer than those previously reported, so that the analysis here will also be applicable in principle to that case as well.

Since the sputtering yield data for pure hafnium would predict a sputtering rate about the same as tantalum, the preponderance of evidence points to the reaction of the hafnium with the arc support gas, and the subsequent formation of a layer with a much lower sputtering rate at these energies. This kind of lifetime enhancement has in fact been observed before, with a different set of elements. In a early study, extended lifetimes were noted in a pulsed low power PIG source, when aluminum oxide or beryllium oxide cathodes were used in place of pure aluminum or beryllium cathodes [Go 53]. In addition, pure aluminum cathodes, initially exposed to pure oxygen in an arc, had the same lifetimes as aluminum oxide cathodes. In this case it is the nitride and carbide, rather that the oxide that gives the longest lifetimes with hafnium cathodes. In that regard, it is no coincidence that hafnium nitride is the

highest melting point nitride, and hafnium carbide is the most refractory binary compound of all [Ha 74]. As a further corroboration of this effect, HfC cathodes have been used at Karlsruhe and other laboratories since 1972, where it was found that their performance was superior to other materials for production of Li^{3+} in a high power PIG arc [Sc 84]. There the high melting point of HfC is exploited, with the lithium vapor coming from a small oven built into the source, and so the lifetime increase with N_2 or CO feed could not be known.

3.4.2 Hafnium Cathodes and Beam Current

The best comparison between hafnium and tantalum cathodes on the issue of beam current can be made for the production of N^{5+} ions, and Tables 3.4 and 3.5 are relevant. Hafnium cathodes in a dc ion source give a much lower beam current than tantalum. The puzzle here is that if one starts with a hafnium source pulsed at low duty factor, no combination of arc parameters can be found that will allow this same beam current, but without some pulsing. On the other hand, if one starts with a hafnium source running dc, and then adjusts arc parameters so as to maximize the beam, one ends up with a low duty factor! The required duty factor itself is not a fundamental quantity, and depends on the balance achieved between gas flow rate and arc current.

Nevertheless, the trend is clear-- hafnium cathodes are unsuitable for the production of N^{5+} when operated dc. This can be illustrated in several ways. Figure 3.4 shows the dependence of beam current on duty factor for an arc current of 0.6 A and a N_2 gas flow of 1.5 sccm. The beam current steadily declines as the duty factor is increased, to about half the peak value at 80 %. Furthermore, if one plots a scattergram of optimum beam current versus duty factor for all N^{5+} beam runs in a one year period, as in Figure 3.5, no correlation between duty factor and optimum current is seen, as the extracted current depends on source parameters and non-source parameters as well, but there is a definite clustering of the hafnium runs at low duty factor and the tantalum runs at nearly a dc operating level.

At first one would expect that the lower melting point of hafnium sets a lower thermionic emission current limit, and that this then is the reason for the poor performance. However, we have run tantalum cathodes at low power dc, where the emission currents are similar, and yet the beam current is still higher with tantalum than for hafnium cathodes.

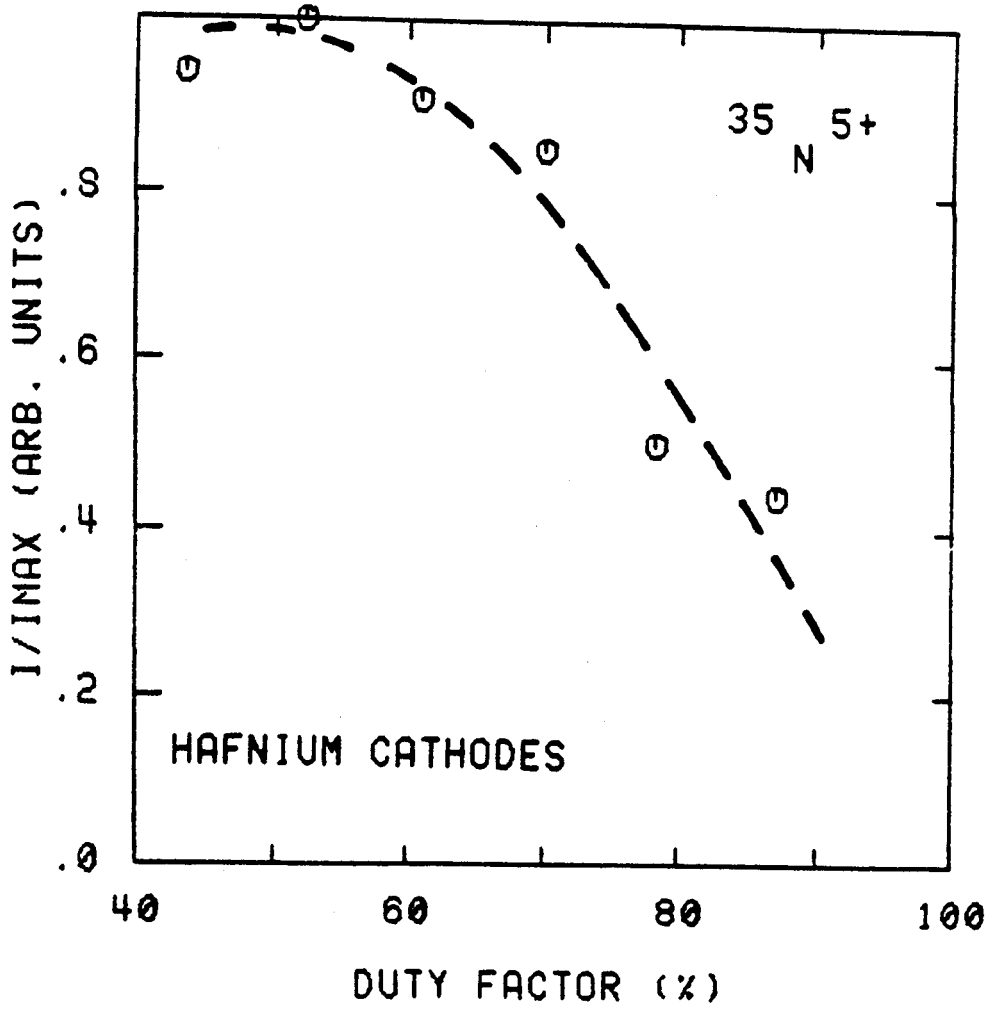

Figure 3.4. With hafnium cathodes, the N^{5+} current drops with increasing ion source duty factor. In this case, the N_2 flow rate was 1.5 sccm and the arc current 0.6 A.

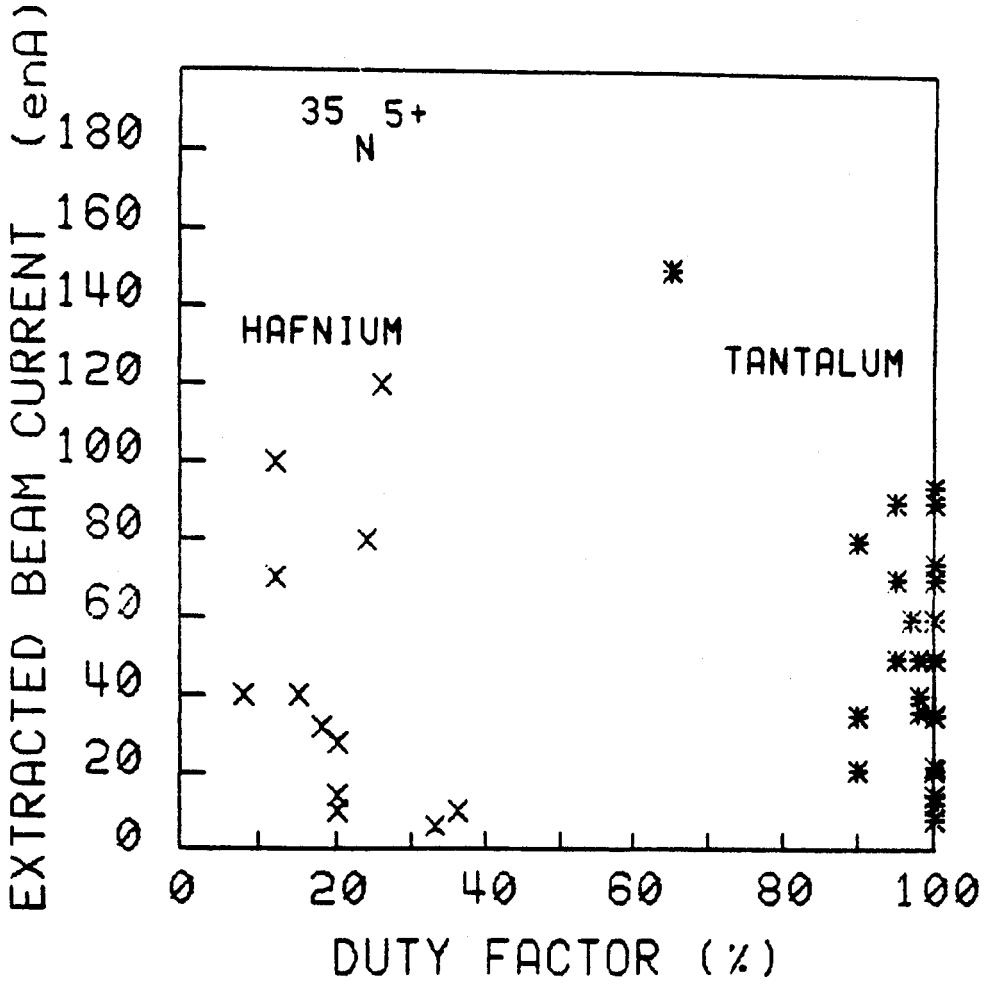

Figure 3.5. A history of the maximum cyclotron extracted beam current versus source duty factor for N^{5+} runs and hafnium or tantalum cathodes in K500 cyclotron PIG sources, over the period March 1983 to January 1984.

The explanation of this effect requires the introduction of another important cathode property-- the cathode contribution to the source gas pressure. This must be low for high charge states to appear in the source output current, because the charge exchange losses are lower [Ma 76]. The arc voltage is indirectly proportional to the internal source pressure, as can be easily seen by turning up the gas flow rate. What we find is that for the same arc current and gas flow, the hafnium source runs at a significantly lower arc voltage than a tantalum source, as was shown in Table 3.5. The difference in arc voltage at the same arc current and gas flow implies that the pressure inside source is higher for a hafnium source. As a further corroboration of this effect, the cyclotron beam chamber pressure is higher when hafnium cathodes are used for N^{5+} ion production, as shown in Figure 3.6, where the vacuum is plotted versus gas flow rate for the same cases as in Figure 3.5. One sees that the beam chamber vacuum declines as the gas flow increases, but that for the same gas flow rate there is large difference in vacuum on the basis of cathode type alone. We infer that the higher pressure results from a higher vapor pressure as a function of temperature for hafnium than for tantalum under the same conditions. A comparison of vapor pressures of hafnium and tantalum in the range of 2000-2500 °C, in Figure 3.7, shows that the hafnium vapor pressure is 5 orders of magnitude

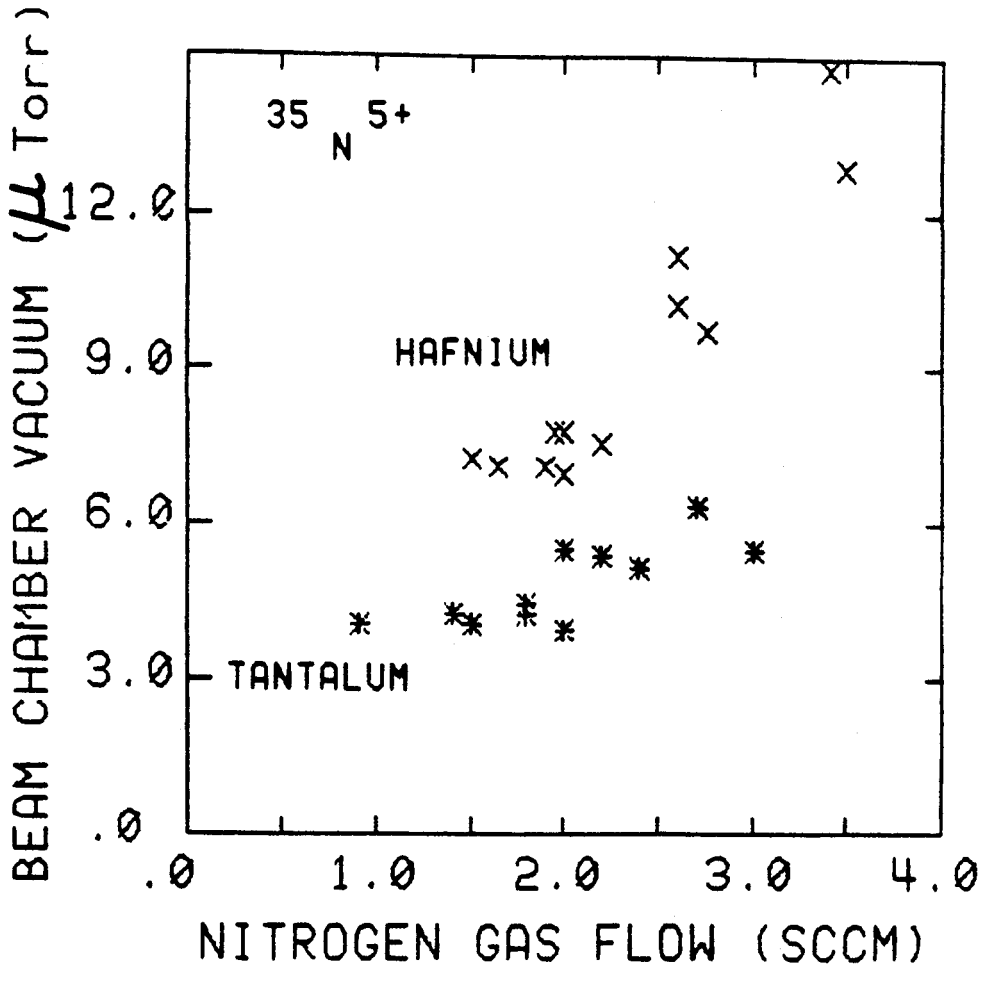

Figure 3.6. Hafnium sources (X) operate at higher pressures than tantalum sources (*), for the same gas flow, as shown or the same group of N^{5+} as in Figures 3.4-3.5.

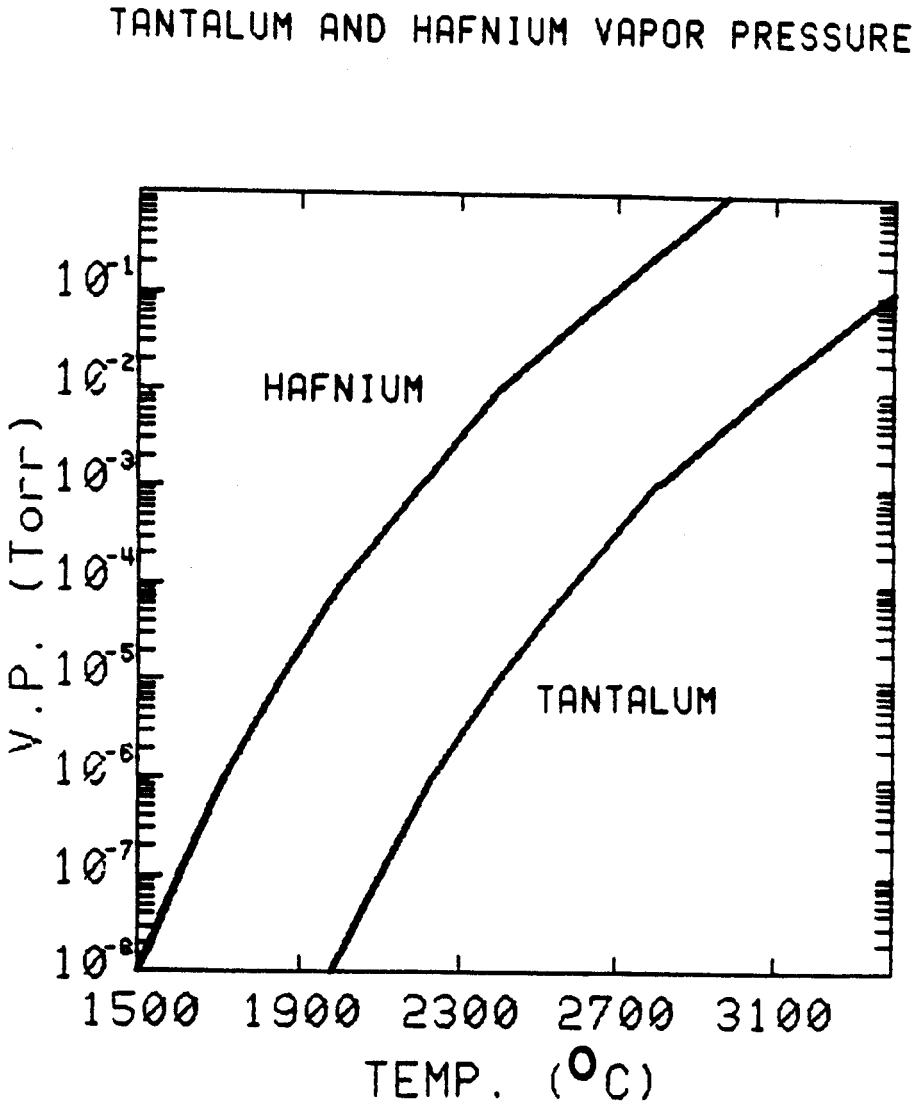

Figure 3.7. A comparison of the vapor pressures of hafnium and tantalum over the range of 1500-3400 °C [Ro 63].

larger at the same temperature [Ro 63]. Since one of the main effects of lowering the duty factor is to lower the average cathode temperature, there would also be a decrease in the source's internal pressure as the duty factor is lowered. The cathode temperture is not a directly knowable quantity, but must depend directly on the average arc power dissipated in an operating source, and one would expect that the average arc power must decrease with decreasing duty factor-- for the hafnium vapor pressure to be the cause of the lower currents when operated dc. As Figure 3.8 shows, this is indeed the case. Hafnium sources run at less than half the average power level of tantalum sources for the production of N^{5+} beams.

3.5 Summary and the Impact of Hafnium Cathodes

By replacing tantalum cathodes with hafnium, one obtains longer lifetime in exchange for lower extracted current. Pulsing the arc, when permitted, partially compensates by increasing the beam current. The higher vapor pressure of hafnium best explains this observed difference in performance. A factor of four increase in source lifetime is observed with N_2 feed, and about half that for CO feed. These longer lifetimes would not be expected on the basis of sputtering yield data for pure hafnium, and must instead be due to the formation of

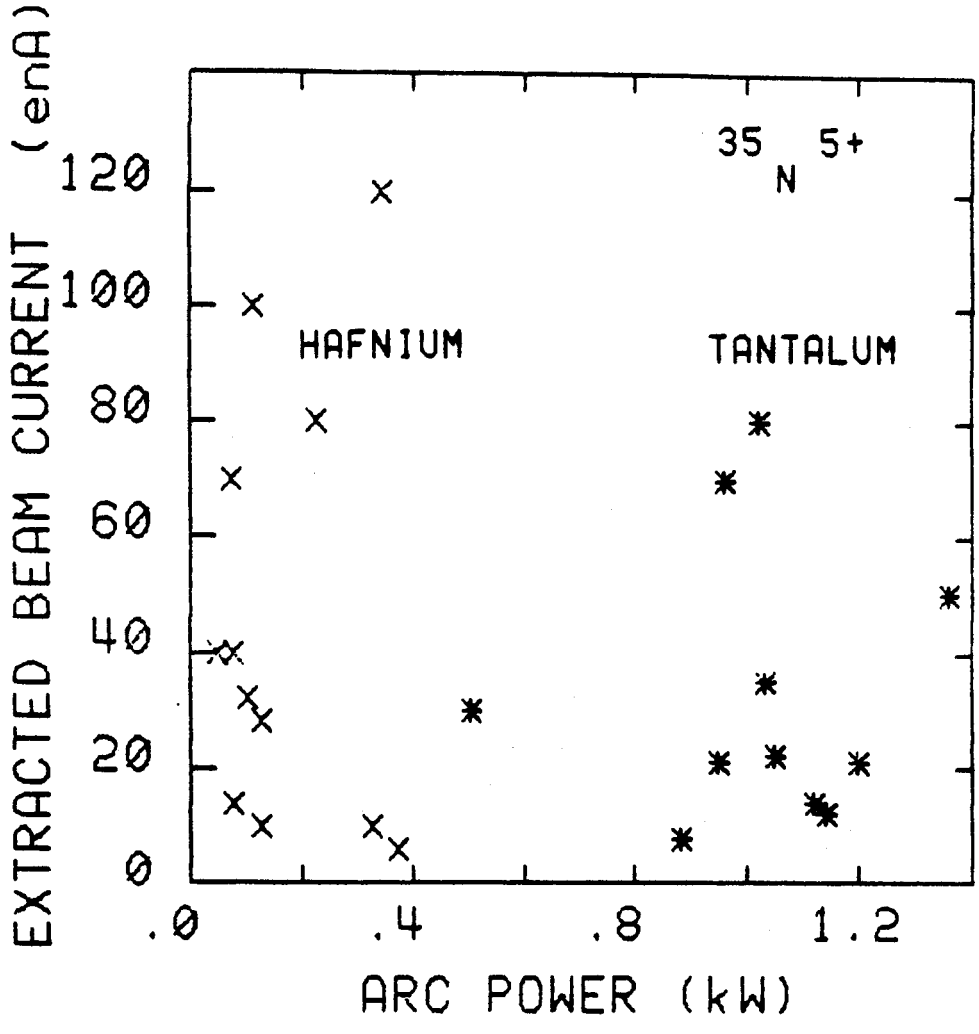

Figure 3.8. For N^{5+}, hafnium cathodes are found to operate at low average arc power when compared to tantalum cathodes. Note the lack of correllation between beam current and power.

compounds of the feed gas and the hafnium. In other cases where N_2 can be used to partially support the arc, some degree of lifetime enhancement usually results.

On an absolute scale we have had many nitrogen sources that ran in excess of 50 hours. In addition, hafnium sources can be restruck many times, and after many hours. Sources are often turned off during energy changes, and left in the cyclotron to be restruck, and this further reduces the number of required source changes. Under those conditions, the ion source ceases to be an important operational issue. This carries over to situations in which nitrogen can be used to partially or completely support an arc used to produce other ions. As will be discussed in Chapter 5, the production of ions of metals and other solids has been added to the K500 sources via back-bombardment sputtering, and for $^{6,7}Li^{2+}$ ions the arc can be supported with nitrogen, and thereby very long source lifetimes are obtained as with nitrogen beams. We see the lifetime effect also with CO feed, but CO has a deleterious effect on the HV stand-off insulators in the source, as carbon deposits form on the surface and shorts result. However, by mixing in some N_2, this process can be controlled and the lifetime increased.

CHAPTER 4

ION SOURCE RADIOACTIVATION CORRECTION

In the early K500 cyclotron runs, we were mainly accelerating carbon and nitrogen 3+ and 4+ ions, and we soon encountered a serious ion source activation problem with these beams. Activities of a few hundred mrem/h were typical, and some rates higher than 1 rem/h were observed. In one case, shown in Figure 4.1, a 56 hour long run of 30 MeV/n $^{14}N^{4+}$ resulted in an average level of over 100 mrem/h on the source, with the highest activation on surfaces protruding the most from the cyclotron center.

At that time we had only two ion sources, and often a hot ion source had to be recycled right away to support the cyclotron operation. Eventually it was determined that the accelerating ions were stripping to the next higher charge state through an interaction with the residual gas. The subsequent "walk" of these off-centered trajectories through

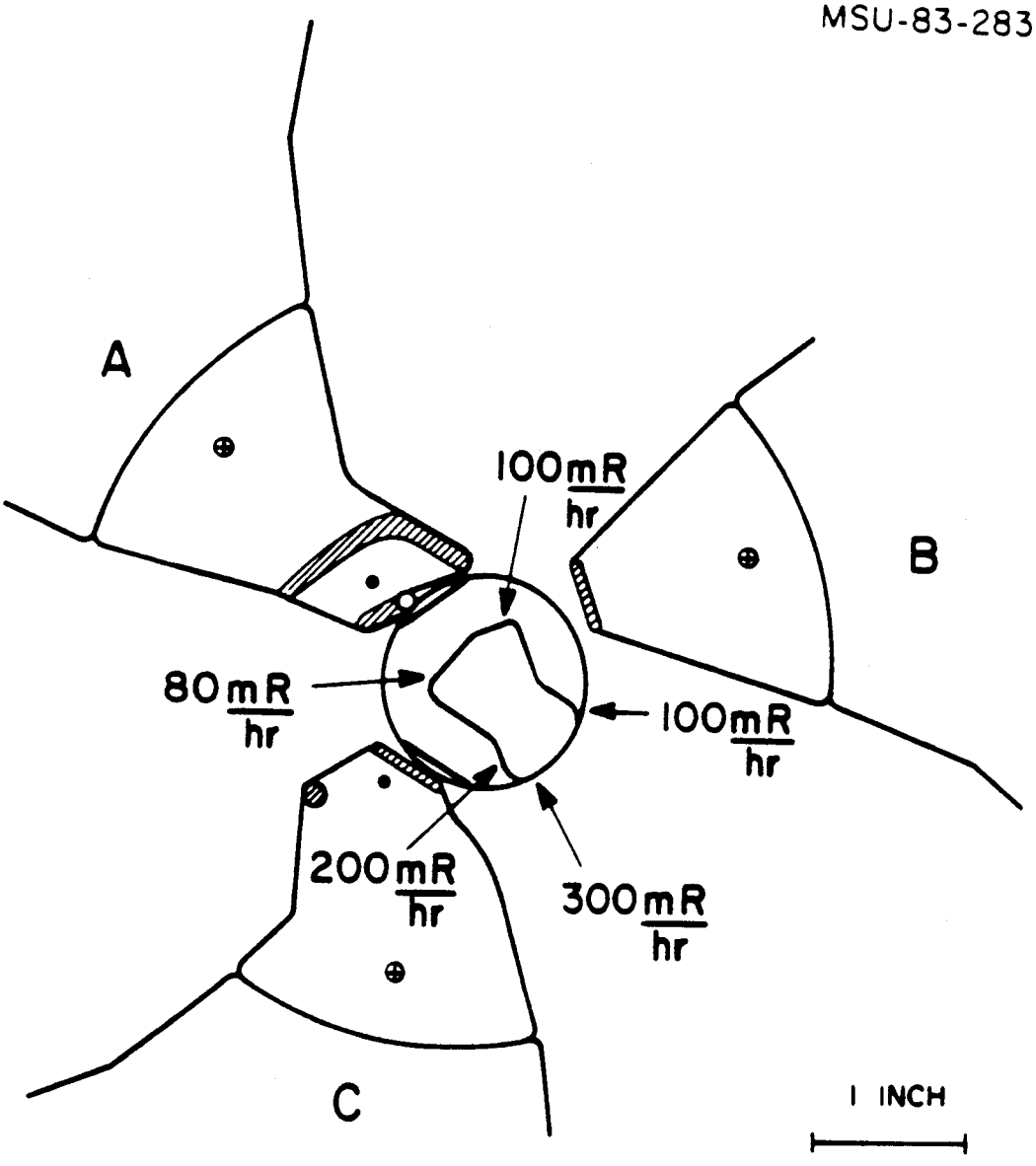

Figure 4.1. The activation of the K500 PIG source is shown after a 56 h run of 30MeV/n N^{4+} ions. The arrows with numbers at their tails indicate measured radiation levels in mrem/h. The ion source back protrusion is not shadowed by the dee tips, and becomes more activated.

the cyclotron central region resulted in a bombardment of the ion source. Since the internal energy of K500 heavy ion beams easily exceeds the coulomb barrier for copper, such activation is possible. This process also makes the dee tips hot, but since they are not routinely removed from the cyclotron the hazard is not as great.

The analysis of this problem led to an analytical formulation of the systematics that showed a dependence on the cyclotron K factor [Ma 84], and thereby explained why this is such a problem in the K500 cyclotron, where the K of 500 is about three times that of room temperature heavy-ion cyclotrons. This chapter will start with a brief review of that analysis. The paper also included a suggestion for a method for reducing the hazard to personnel handling the sources, and it is the main purpose of this chapter to demonstrate how that works. The solution is to cover the median plane surfaces of the ion source with thin tantalum shields that can be removed during handling to a safe shielded area. These shields, now in place, are not however thick enough to stop the highest energy K500 beams, and we will demonstrate that as well. Finally, after analyzing the problem here, we observed in a report from the RCNP Laboratory at Osaka University in Japan that they had encountered similar difficulties with the activation of their PIG sources when run in the 230 cm. cyclotron. An analysis was made that showed that this stripping process

could be the source of their ion source activation. One can show that there will be no activation at all if the copper anode surfaces are replaced with tantalum, since returning ions will not exceed the coulomb barrier on tantalum!

4.1 Review of the Ion Source Activation Model

The analysis of this problem has been the subject of a paper: [Ma 84], of which this student was a co-author. The details of the derivation of the condition for activation will not be repeated here. In summary, if an ion of charge qe and mass Am_o, is accelerated to an energy E(r) at a radius r where its charge is shifted to (q+1)e, then it can hit the central region if

$$E(r) \leq E_{max} = \frac{K(q+1)^2}{4A}. \qquad (4.1)$$

For activation to occur, the particle energy E(r) must be greater than the coulomb barrier (E_{cb}), which in the lab frame and evaluated in MeV is

$$E_{cb} = 1.44\left(\frac{A_1+A_2}{A_2}\right)\frac{Z_1 Z_2}{1.45\left(A_1^{1/3}+A_2^{1/3}\right)}. \qquad (4.2)$$

In Eq.(4.2) subscript 1 refers to the projectile and subscript 2 to the target, while Z_1 and Z_2 are the atomic numbers of the projectile and target, respectively. Here 1.45 fm is used for the coulomb barrier radius [Ev 82]. With this pair of equations one can study the ion source activation problem.

We have found several ways of demonstrating why the level of activation is high in the K500 cyclotron, and one of the best is shown in Figure 4.2. For the case of any 4+ ion stripping to 5+, the maximum energy for ions hitting the central region is calculated from Eq.(4.1). This is plotted in Figure 4.2 as a function of ion mass (A) for three different K values: 100, 300 and 500. The last case corresponds to our cyclotron, for a central field of B_o= 48 kG, while the region near K = 100 is where the conventional heavy-ion cyclotrons in this country operate. The coulomb barriers for Cu and Ta are also shown. The region above the Cu coulomb barrier for K=100 is small, corresponding to the lightest ions only, whereas it is quite large for the K=500 case. Figure 4.2 can be used to introduce the topic of the next section--since the coulomb barrier for tantalum is about twice that for copper, it is obvious that less activation will occur if tantalum is placed in the median plane elements of the ion source.

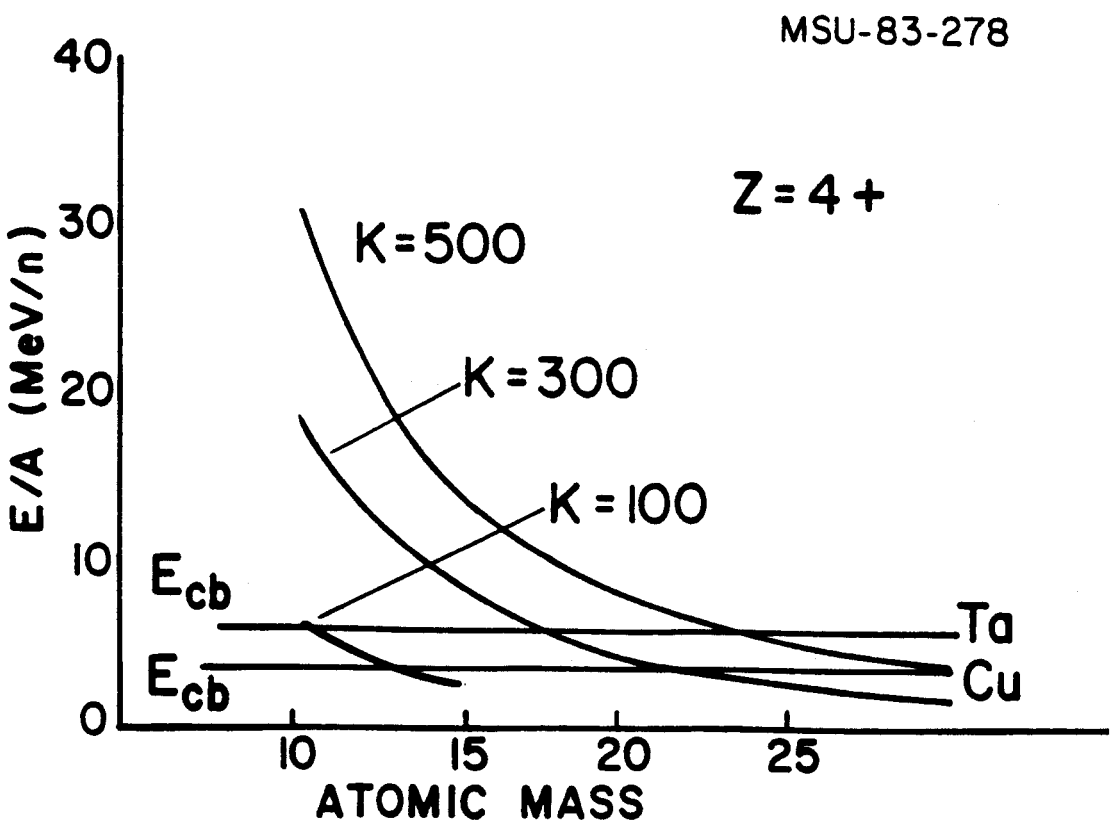

Figure 4.2. The maximum energy of particles that can hit the central region is shown for charge state 4+, and stripping to 5+ and for three different K values as a function of atomic mass. The coulomb barrier for copper and tantalum is also shown.

4.2 Removable Median Plane Tantalum Source Shielding

We took the simplest approach in dealing with this problem-- the median plane surfaces were covered by removable tantalum shields. First, the activity of the ion source copper is reduced because the tantalum stops some fraction of the ions, and second, the activation of tantalum is less than an equivalent thickness of copper because the coulomb barrier is higher. To do a complete median plane shielding, copper must be removed from the source surface to accommodate the shield, since this surface forms one side of the dee voltage gap. Also the ion source must pass through an alignment collar with a 0.001 inch clearance on the source diameter as it slides into position in the cyclotron, and no part of the median plane section of the source can protrude beyond that diameter. The only two sources available for the early runs were unfortunately too radioactive to allow this machining, and so they received thin (0.010 in. thick), partial surface shields. In later sources this shield was extended to cover all the exposed copper. The effectiveness of the tantalum shielding is shown in Figure 4.3 for the case of the initial partial shields, after the 56 h run of the 30 MeV/n $^{14}N^{4+}$ beam of Figure 4.1. As can be seen, the activity at the surface of the source is reduced by more than a factor of two after the

shields are removed. Figure 4.3 also shows why later sources had to have complete shields--the area of the highest activation was not covered by this partial shielding.

It is clear that some of the ions are getting through the thin tantalum shield, and as the energy of cyclotron beams is increased, one may have to accept increasingly greater transmission of the bombarding particles through the tantalum. We can use Eqs.(4.1)-(4.2) to determine how thick the shield must be to stop the bombardment in the tantalum over the whole range of stand-alone beams that the K500 cyclotron can produce. The maximum activation energy will occur for the case of the lightest mass species that can strip from q to (q+1) electrons removed (assuming also K=500). For these maximum bombarding energies (which were computed from Eq.(4.1) for various masses and charge states), mean ion depths were obtained from range tables for copper and tantalum [Li 80]. Figure 4.4 shows the results from the calculations of the stopping range in copper and tantalum at the maximum activation energy. A 0.5 mm (0.020 in.) tantalum shield, only twice as thick as that currently in use, would stop all but the lightest K500 cyclotron beams. This would substantially reduce the hazard to personnel handling the activated sources since nearly all of the activity would be gone when the shield was removed.

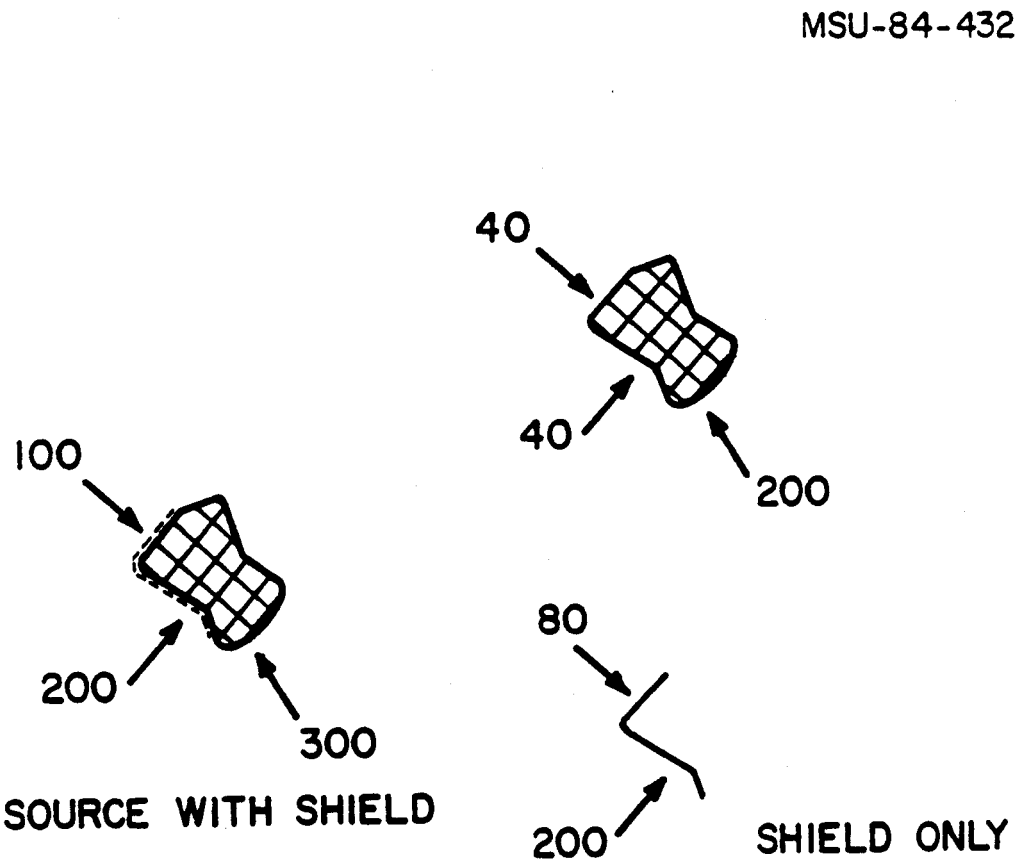

Figure 4.3. A median plane cross-sectional view of an activated ion source with tantalum shields in place and removed is shown. Much of the activity disappears when the shields are removed, thus reducing potential exposure.

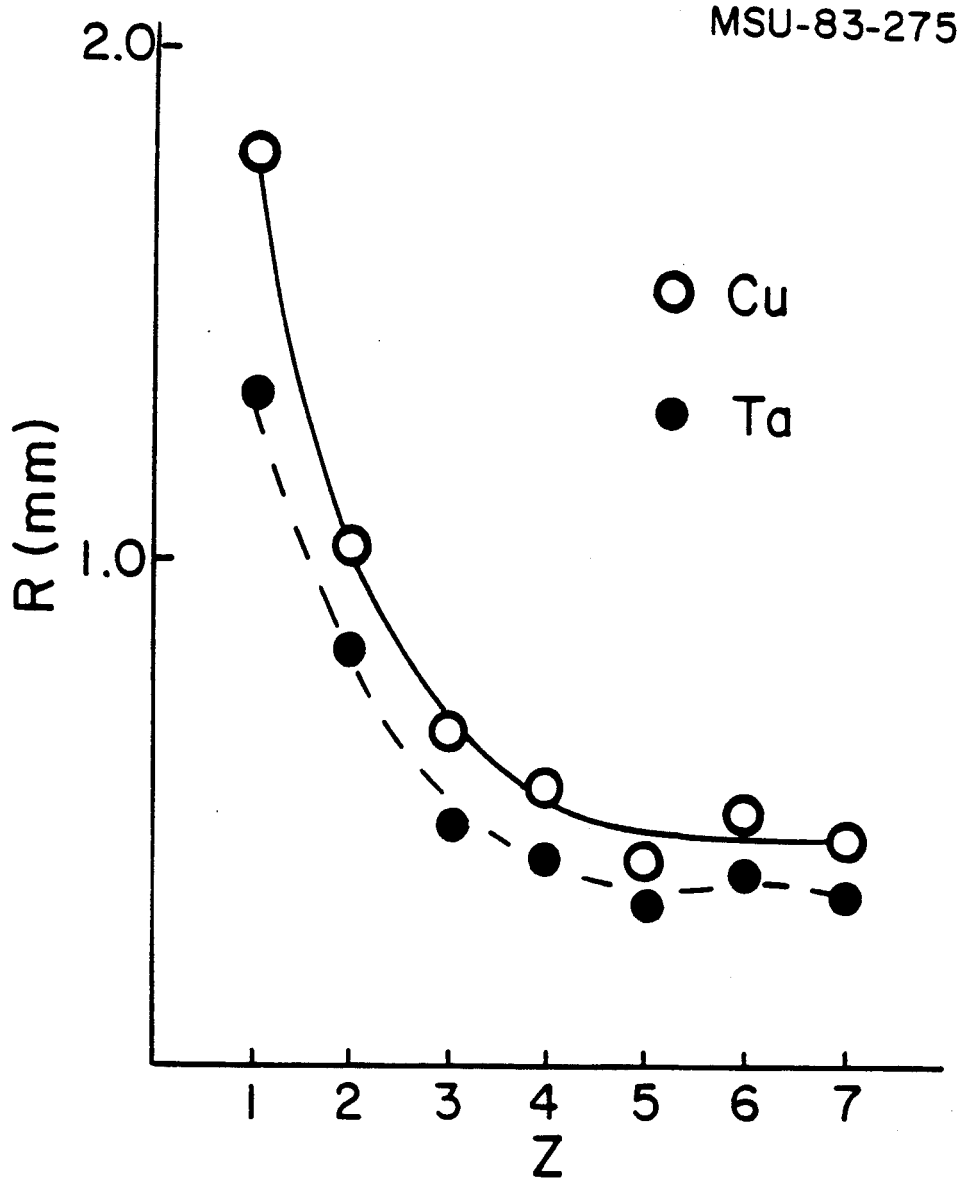

Figure 4.4. The stopping range in copper and tantalum for the maximum energy particles that can hit the central region plotted as a function of initial charge (q). The atomic mass for the lightest particle that could strip to the next higher charge and K = 500 was used.

Finally, after we had made an analysis of this problem at MSU, we came across a reference in section 8.3 of the 1982 RCNP Annual Report to source activation problems that were encountered after running heavy-ion beams in the K=120 cyclotron there. It turns out that the ion source anodes there are also made from copper. We decided to find out if this stripping process could be the source of their activation, and if so, how hard it would be to correct. Table 4.1 shows the results of applying the activation calculations to three of the beams listed in that annual report. It shows that $^{11}B^{3+}$ at 95 MeV and $^{12}C^{3+}$ at 80 MeV will both cause central region activation in that cyclotron while $^{14}N^{4+}$ at 135 MeV will not. Note however that no activation would occur if the copper ion source anode were replaced with tantalum. Note also that this situation is much more favorable than ours, since our K values are higher.

Table 4.1. Calculation of the activation expression of Eq.(4.1), with $E(r) = E_{cb}$, for selective beams of the RCNP Laboratory K=120 cyclotron, to determine whether that process could be the source of their reported ion source activation.

BEAM	ENERGY	COULOMB BARRIER		$E_{cb}/E_{max} \leq 1$?	
		On Cu (MeV)	On Ta (MeV)	On Cu	On Ta
$^{11}B^{3+}$	95	26.0	48.8	0.61	1.14
$^{12}C^{3+}$	80	32.8	58.3	0.90	1.63
$^{14}N^{4+}$	135	38.5	79.1	1.14	2.34

CHAPTER 5

THE PRODUCTION OF IONS FROM SOLID MATERIALS

Up to this point, consideration has been given only to the production of ions of elements that can be fed into the PIG source as a gas. This is in fact a rather fundamental limitation, since the design of the source and also the ion source power supply actually depend on the initiation of an arc in a low pressure gas. However not all elements are available in gaseous form, and in many other cases the gaseous form is highly toxic or corrosive and requires special handling techniques that preclude routine use. Since a large and important region of the operating diagram of a heavy-ion accelerator is potentially excluded, some method of making available gases or ions liberated from solid materials, must be developed for each PIG source.

Several methods have been developed for the purpose of converting solids to ions in PIG sources. Ovens connected directly to the arc chamber have been used to boil solid

materials to produce vapor for admission into the arc [Be 69, Jo 72, Va 69]. In this case there is very little control over the material consumption rate and ion intensities. Another approach has been to insert electrodes fabricated of the desired element directly into the plasma, where some erosion via ion bombardment sputtering takes place--to control the rate of sputtering the electrode can be biased [Ga 72, Ga 75, Pa 72, Sc 76]. These methods have proved successful but generally require the development of some complex auxiliary apparatus, and then one must find space in which to locate it.

The discovery by the ORIC Cyclotron Group at Oak Ridge National Laboratory that nonresonant ions returning to the source have sufficient energy to cause substantial sputtering of source structures [Hu 74, Hu 76], is the basis of another method. This seems ideally suited to requirements of a heavy-ion cyclotron ion source, in that the mechanism is provided by the existing rf field of the cyclotron and, in addition, changes in the source to accomodate the method are minimal. We chose to apply this back-bombardment sputtering technique developed at Oak Ridge for the production of ions from solids, and in this chapter the application of this technique in K500 ion sources will be explained. First, a brief review of the origins of the process and the subsequent development as a viable method for obtaining ions from solids will be reviewed. Next,

physical modifications made to the K500 ions sources to implement this technique will be introduced and justified, and the plan for testing those design changes will be presented. The main result of that work is that it has now become possible to accelerate lithium beams in the K500 cyclotron, and this opens up the possibilities for other species as well. An analysis of the ion dynamics at the center of the cyclotron that results in one of our beams, namely 22 Mev/n $^{7}Li^{2+}$, has been done, and will be discussed. The agreement between the calculations and the experimental situation is quite good.

We are concerned here with the first acceleration gap, which, for reference purposes, has been identified in Figure 5.1.

5.1 Origins of the Back-bombardment Sputtering Technique

A spurious beam with large beam current of 0.5 eμA was observed during the acceleration of a $^{130}Xe^{12+}$ beam in the Oak Ridge Isochronous Cyclotron. Subsequently this extra beam was identified as being $^{65}Cu^{6+}$, and coming most likely from an erosion pattern in the inside of the back of the ion source chimney [Hu 74]. Several studies were made of the properties of this beam. The replacement of the xenon gas

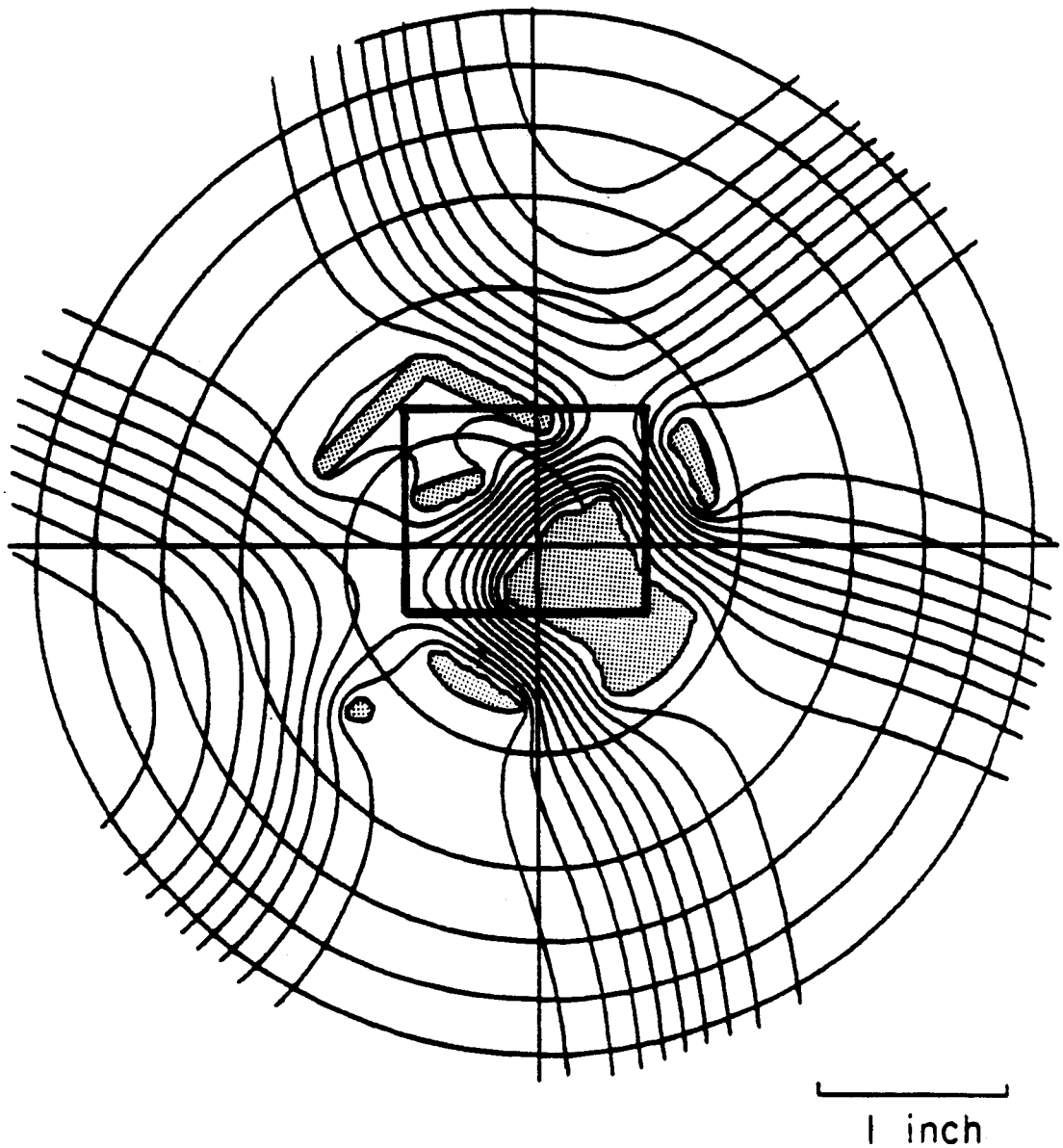

Figure 5.1. The central region of the K500 cyclotron is illustrated for reference purposes in subsequent discussions. The shaded areas indicate the median plane cross-section of the dee tip electrodes and the ion source, and gap voltage contours are shown. The electrode on the tip of the first dee after the ion source is called the "puller electrode" and the boxed region is the critical first accelerating gap.

in the source with neon cut the copper beam current a factor of 20, indicating that the mass of the ion source feed gas was important to the process. The replacement of the eroding copper section of the source with nickle completely eliminated the copper beam, confirming the copper "source". Orbit computations showed that low charge-to-mass ions were failing to cross the 1 cm accelerating gap between the source and the puller electrode for nearly all starting times during the negative voltage part of the accelerating cycle. These ions are accelerated back into the source when the voltage on the dee changed sign and struck the back with energies as high as 30 keV.

Additional studies at Oak Ridge expanded the range of elements in which ions were made this way by changing the material making up the back of the chimney, establishing the viability of the method in the process [Hu 76]. Further orbit computations, coupled with estimates of the sputtering effectiveness of different source feed gases, led to predictions that krypton and xenon would be the most effective for sputtering nickle. The measurement of the extracted beam intensity of $^{58}Ni^{5+}$ ions for several gases confirmed this.

5.2 Design Considerations for the K500 Ion Sources

In preparing a source to operate on this technique we felt the following issues were important:

(1) Compatibility with existing source design--allowing for easy change-over.

(2) Properly sized feed material insert. (This in part determines the useful lifetime, but not absolutely because the support gas species, its sputtering yield and the slit size also play a role.)

(3) Feed material inserts in a standard size, simple shape for all materials.

(4) Operation where possible of the ion source on nitrogen support gas with hafnium cathodes to obtain long source lifetimes (recognizing that whether nitrogen can be used will depend on its sputtering yield with particular feed materials.)

The solid to be sputtered must be placed in the chimney back. Then the key design constraint for us is the close proximity of the high voltage rod behind the chimney in our existing source design. Also, the feed material must come in contact with the chimney, which has an unknown

temperature, but has been observed to be incandescent on occasion. The design that we have chosen is shown in Figure 5.2. A double-tube high voltage rod end is traded for the standard .250 in. O.D. copper tube to open up the space behind the chimney. This allows a tantalum receptacle to be fused to a standard tantalum chimney for holding the feed material. With this design we can put 0.170 inch thick feed material inserts in a standard source. The design clearances between the high-voltage rod and the grounded chimney are within the range of acceptable clearances for holding voltage in the source, even when including typical assembly tolerances. This would change however if the high-voltage rod is not positioned parallel to the back of the chimney, as the resulting voltage holding asymmetry would certainly cause arcing.

The other important part of this development is the selection of suitable test beams. These are summarized in Table 5.1. The initial goal of the work was the development of $^{6,7}Li^{2+}$ beams, but since lithium fluoride melts at about 900°C, and the operating temperature of the conductively cooled tantalum chimney was not known (but on occasion observed incandescent), the first beam trial would instead be $^{11}B^{2+}$, using boron nitride as the feed material. After that, lithium beams were attempted. Lithium floride was available in powered form, with natural abundances of

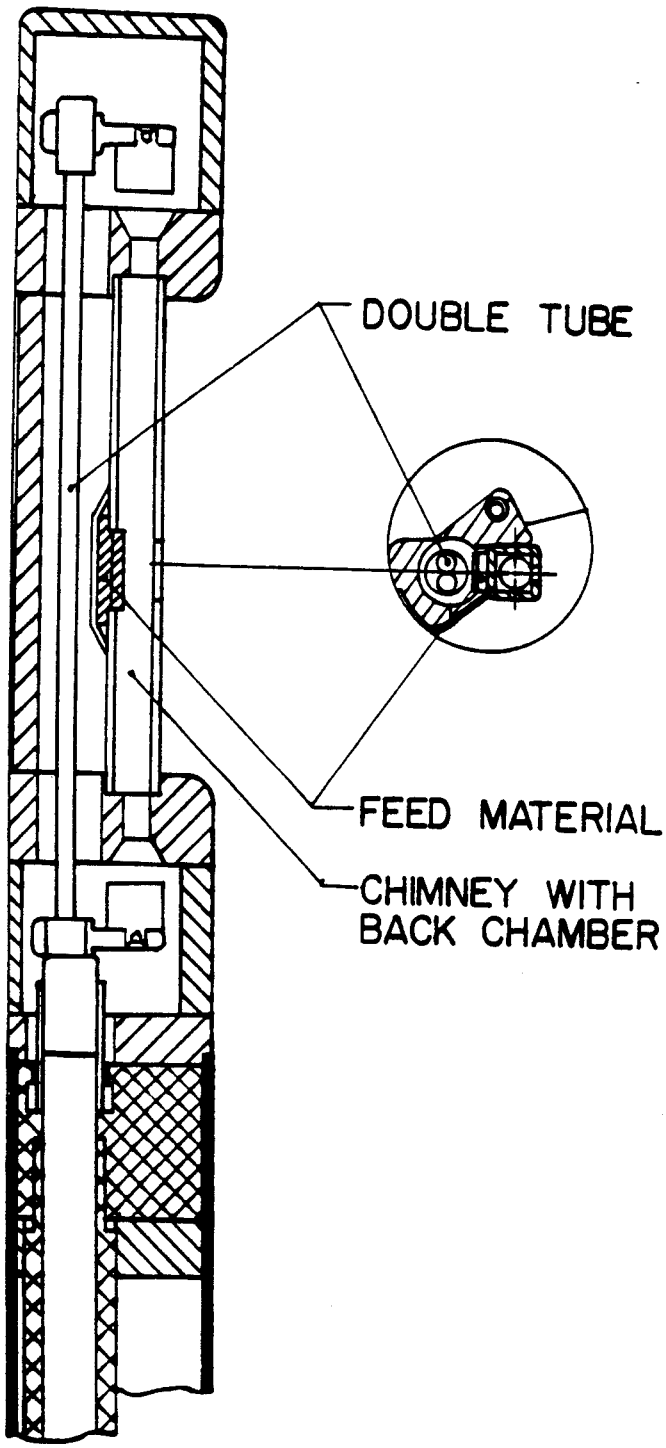

Figure 5.2. The conversion of the source for the production of ions from solids was accomplished through minimal changes in the design of the standard source. A chimney with a welded tantalum receptacle located in the back wall behind the extraction slit holds the feed material insert, and a double tube high voltage conductor, thin in the direction of the chimney, feeds the upper cathode in place of a larger diameter coaxial conductor.

isotopes ^{6}Li and ^{7}Li of 7.5% and 92.5 % respectively, or with the ^{6}Li in various enrichments. We started with lithium floride containing lithium isotopes in natural abundances. This was then packed in a carbon boat and heated to the melting point, where upon cooling it solidified. The ingots were then machined to get the required insert shape.

The $^{6}Li^{2+}$ and $^{7}Li^{2+}$ beam in Table 5.1 happen to be by choice analogs (same q/a) as two well developed beams of ions $^{12}C^{4+}$ and $^{14}N^{4+}$, respectively. By first optimizing the acceleration of the analogs and then making a frequency change, the lithium beams would be found. In that regard the expected frequency shift is -.044 MHz for $^{6}Li^{2+}$ and -.030 MHz for $^{7}Li^{2+}$.

5.3 Production of Boron and Lithium Ions

There was time to try only the first three beams entered in Table 5.1. The source modifications worked and the results of these trials are summarized in Table 5.2. In all three cases the run was stopped to switch to a new test of some other cyclotron component (the cyclotron was undergoing intensive development at that time that and the development of solid feed was only one aspect). There were

Table 5.1. Beams chosen for the initial testing of the source modifications made to incorporate the back-bombardment sputtering technique into the design.

ION	FEED MATERIAL	SUPPORT GAS	CATHODE MATERIAL	BEAM ENERGY	DEE VOLTAGE
$^{11}B^{2+}$	BN	N_2	Hf		38.1
$^{6}Li^{2+}$	LiF	N_2	Hf	30.0	60.4
$^{7}Li^{2+}$	LiF	N_2	Hf	22.0	67.0
$^{19}F^{3+}$	LiF	N_2	Hf	*	*
$^{27}Al^{4+}$	Al	Ne,Ar	Ta	10.0	50.9
$^{24}Mg^{4+}$	Mg	Ne,Ar	Ta	10.0	52.9

*Beam parameters not selected in advance.

Table 5.2. The first beams in the K500 cyclotron produced by back-bombardment sputtering of solid feed inserts.

ION	EXTRACTED BEAM CURRENT (enA)	SOURCE LIFETIME (h)
$^{11}B^{2+}$	>1.0	>13
$^{6}Li^{2+}$	12.0	> 8
$^{7}Li^{2+}$	400.0	> 9

no significant difficulties with the design during this testing period. Inspection after the boron run indicated that some arcing from the high-voltage rod to the chimney back had occurred. A greater effort was made to insure that the high voltage rod was straight for the two lithium runs, and no further arcing was observed. Certainly since that time the Li^{2+} beams have been used extensively, but this additional experience has not been included in this discussion. We will simply note here that with hafnium cathodes and nitrogen gas supporting the arc, we have obtained lifetimes in excess of 20 h and extracted beam current averaging 200 enA. The physical evidence that the ions are indeed being made via back-bombardment is shown in Figure 5.3, where an eroded LiF block is shown along with a fresh unused block.

Figure 5.3 In this photograph are shown both new and used LiF pellets. The sputtering of the used pellet is evident, and the curvature of this erosion pattern agrees well with the erosion pattern suggested by ion trajectory computations, as will be shown in Section 5.4.

5.4 Analysis of the $^{7}Li^{2+}$ Ion Production Dynamics

The case of $^{7}Li^{2+}$ at a final beam energy of 22 MeV/n has been selected for consideration here in detail. We want to show the interaction of the initial ion trajectories with the rf accelerating field.

In this case, the arc discharge in the ion source is being maintained by a flow of nitrogen gas at a few cubic centimeters per second. After the LiF has been sputtered there will be lithium and flourine ions also present, but the extracted beam current will be dominated by nitrogen ions. We first have to decide, on the basis of source output current and other factors, which nitrogen ions are likely to contribute to the sputtering process. Figure 5.4 makes a comparison of the nitrogen charge state distribution of three typical PIG sources. The data in Figure 5.4 were obtained with dc extraction from the sources at a fixed voltage, and then separated on the basis of M/Q by magnetic fields. Most of the output current is going into 2+ and 3+ ions, with a fall off by approximately 1/5 of those levels for 1+ and 4+ ions, and 5+ and 6+ ions by more than an order of magnitude below that.

According to Figure 5.4, something like 80-90 % of the extracted current from a nitrogen discharge will consist

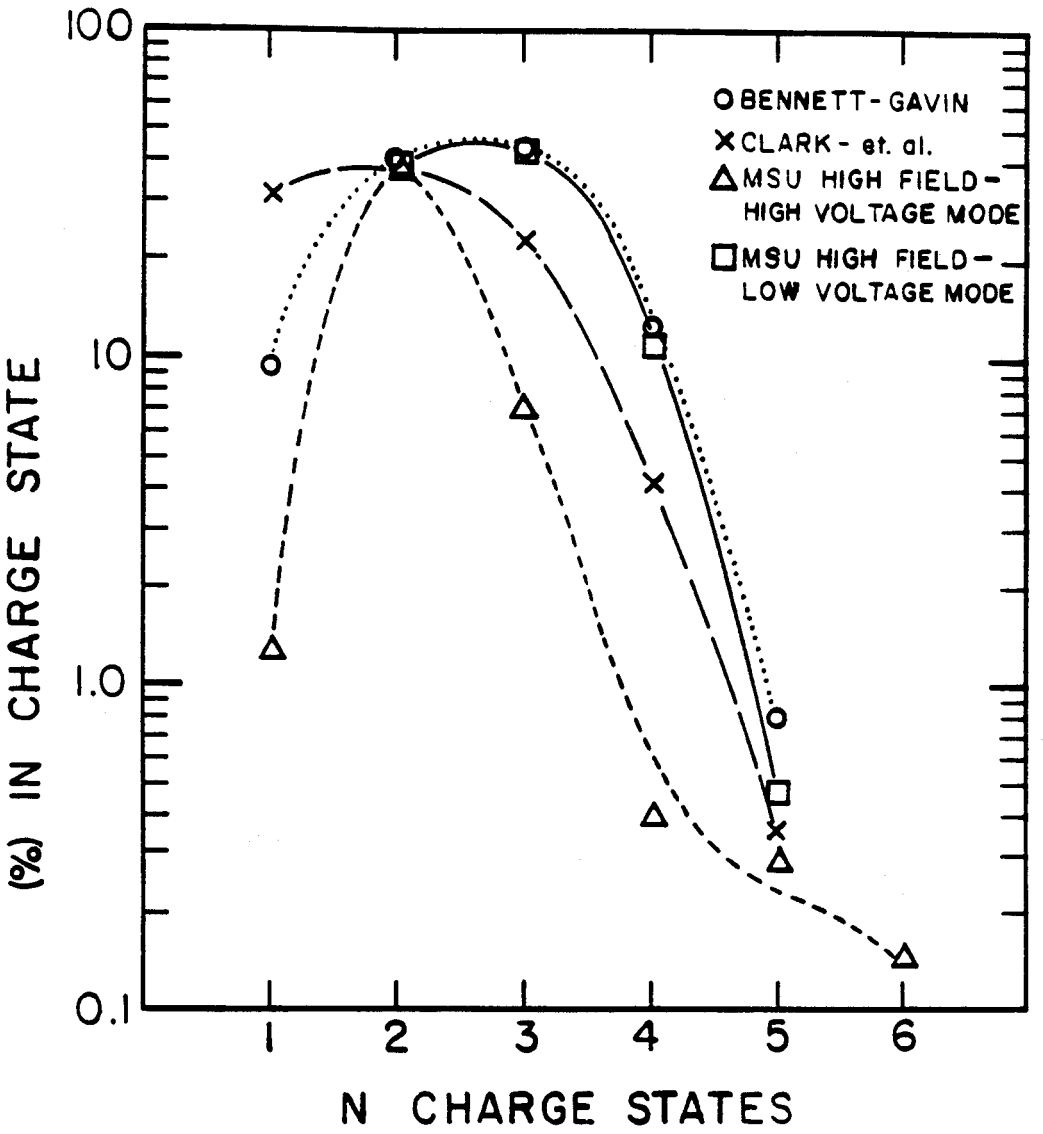

Figure 5.4. The charge state distribution for nitrogen ion production from discharge-heated PIG sources is seen by considering two sources from the literature [Cl 71, Be 73], and the MSU 50 MeV cyclotron PIG source also in the cold cathode (high voltage) pure Penning discharge mode [An 83]. As can be seen for the three sources operated in the arc discharge mode, ions of charges 2 and 3 will appear in the output with approximately the same intensity, with 1 and 4 within an order of magitude less than that.

of the first three charge states, and we will therefore only consider in detail the trajectories of these ions. Figure 5.5 and Figure 5.6 show the central region trajectories of the $N^{1,2,3+}$ ions for starting times near the peak voltage on the first dee. These we obtained via the computer program Supercyclone, developed at MSU to compute accelerated orbits in the superconducting cyclotrons, and used originally during the design of the K500 cyclotron central region [Ma 81]. Figure 5.4 shows only N^{1+} ions but includes more of the central region details. For reference, the area exhibited in Figure 5.5 corresponds to the boxed region at the center of Figure 5.1, which showed the positions of the ion source and dee tips. Starting times earlier than those plotted in Figures 5.5 and 5.6 correspond to orbits that reached the puller electrode before the voltage changed sign--these ions do not return to the source. For those trajectories plotted, many do return to the source slit, and it is likely that other orbits would also, but only trajectories of ions starting from the center of the source extraction slit were computed. These figures show the ions tracing out a curved trajectory inside the source, and as a result, preferential sputtering of the right side on the feed insert would be expected. This agrees well with the erosion pattern exhibited in Figure 5.3. The trajectories definitely show that the position of the feed material insert, dictated by the

available space, is not optimum. The right side of the chimney, as viewed down from the top, is an external wall of the ion source and although the feed insert would be better placed here, there is, unfortunately, no space for that purpose.

On the basis of the ion trajectory calculations, one can make an estimate of the energy that the ions will bombard the feed insert with. Figure 5.7 shows a plot of the final energy versus starting time for the ions exhibited in Figures 5.5 and 5.6. As can be seen, the width in time of the returning ions is decreasing with increasing charge, because the greater energy gain allows more higher charge ions to reach the puller. The final energy however is increasing with the charge.

In order to sputter a material appreciably, the mass and energy of the bombarding species are both important. Since nitrogen is a relatively light sputtering agent, the energy must then be high. While there is no available data on the energy dependence of LiF sputtering, a review of the situation for other materials [Ca 68] shows that energies of the order of a few keV for nitrogen should result in sputtering yields of 1-2 for nitrogen ions on metals. (A sputtering yield of 1 means that 1 sputtered atom is obtained for each bombarding ion.) Our energies are well above that.

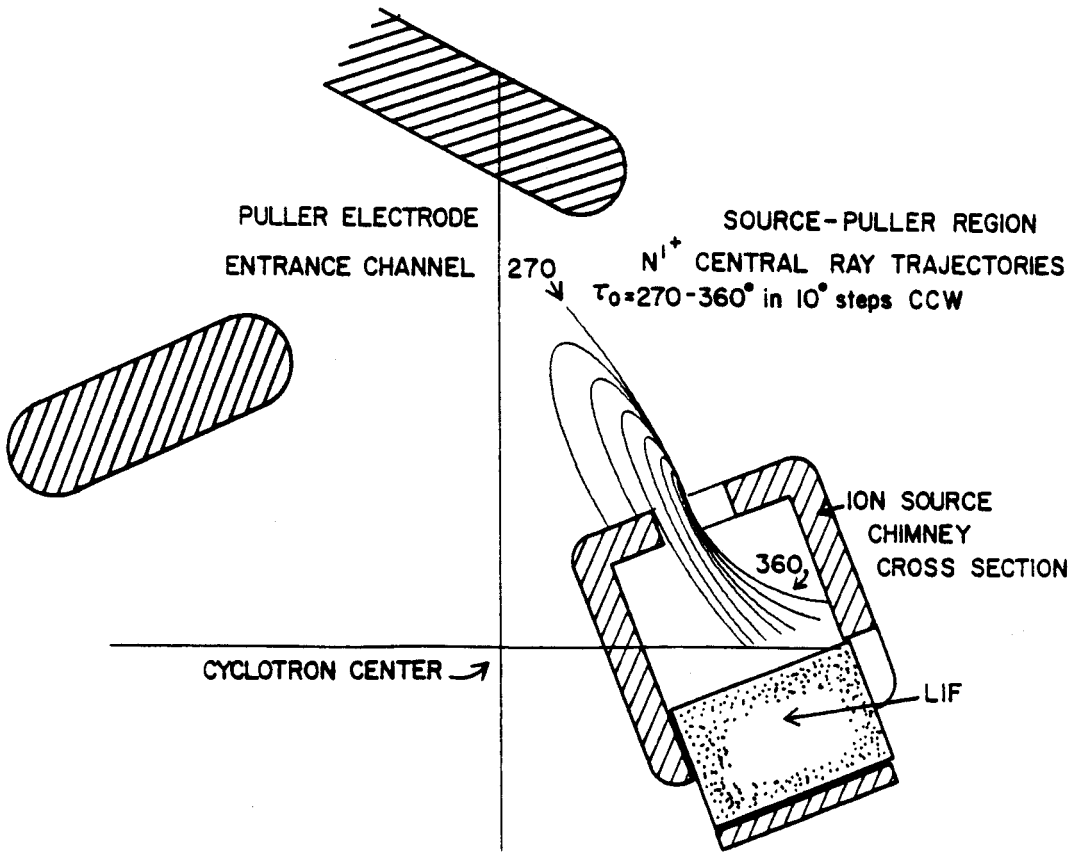

Figure 5.5. Orbit trajectories for N^{1+} ions staring after the peak voltage on the first dee are still in the gap when the voltage changes sign and so are accelerated back to the source. A sinusoidal time dependence is assumed for the voltage on the first dee, so that the peak voltage is occuring when $\omega\tau$=270? Though these N^{1+} ions were not the resonant species, the behavior that they exhibit here can be used to sputter LiF feed material located in the chimney back receptable, putting lithium ions in the arc for the production of the cyclotron resonant ion $^{7}Li^{2+}$.

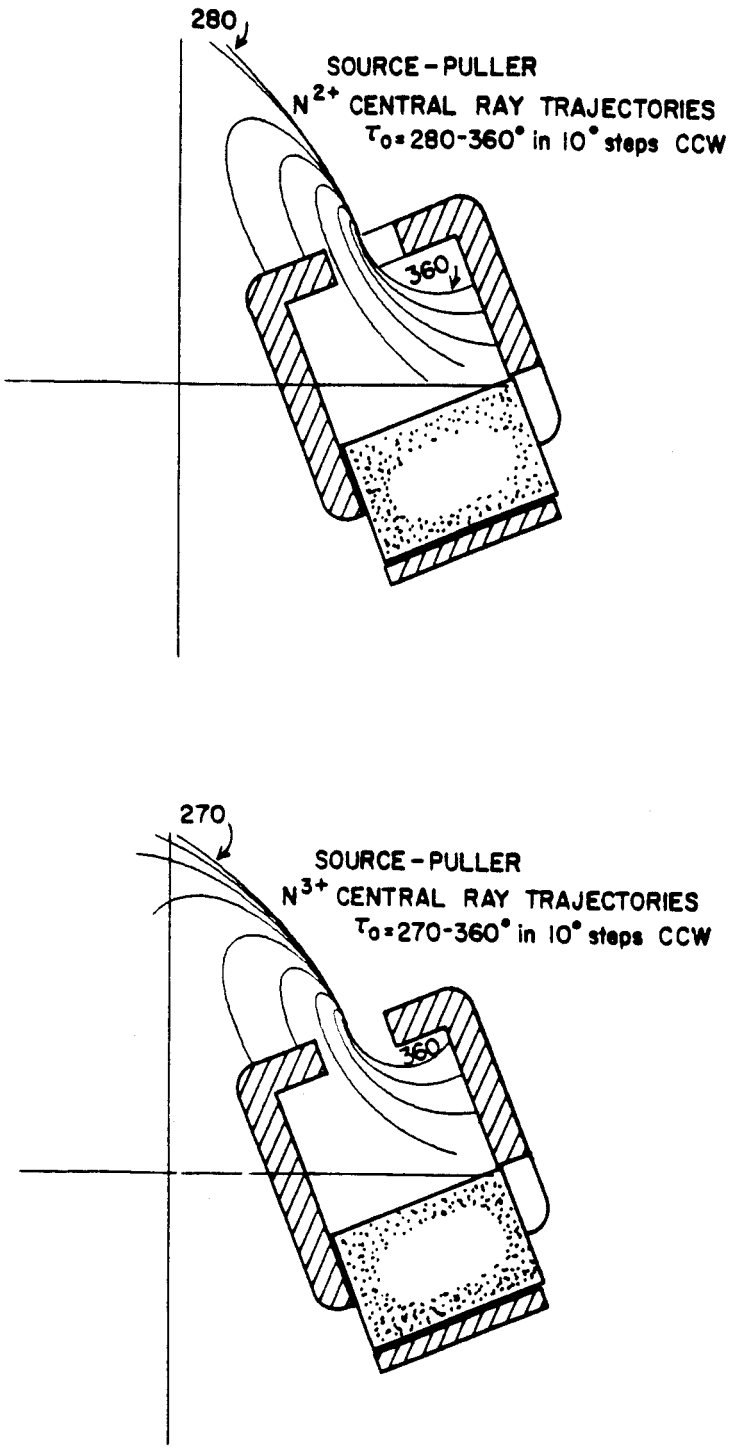

Figure 5.6. The trajectories of late starting N^{2+} ions, in (A), and N^{3+} ions in (B), show that these too come back into the source, with some striking the feed material insert.

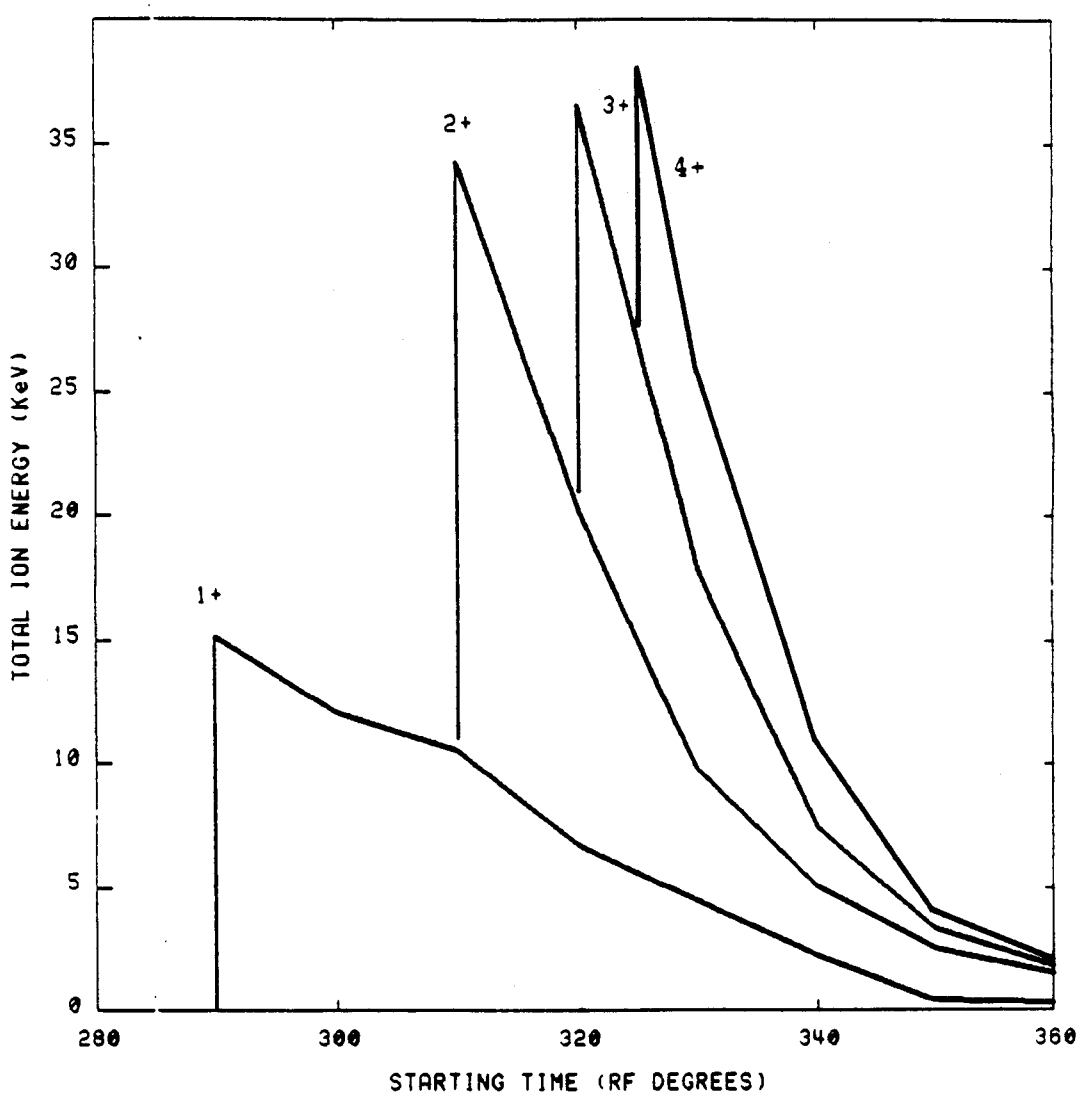

Figure 5.7. For the ion trajectories shown in Figures 5.4-5.5, and also N^{4+}, the final energy of nitrogen ions returning to the source is plotted versus the ion starting time. The truncation of the curves at the earlier starting times was made on the basis of whether the ion came back to the source. At 360° the dee voltage reverses sign and positive ions are no longer pulled from the source.

5.5 Summary and Conclusions

At the time of this writing, there have been approximately 200 hours of cyclotron beam time devoted to lithium beams using the design that we have been discussing, and so we can say that this development has certainly worked. However the erosion pattern in the feed inserts shows, and the orbit computations confirm that the design is not optimal--ideally the feed insert should be moved over to intercept more of the ion trajectories. But in this ion source there is no space to do this, except by replacing the side wall of the chimney with some other material of the same thickness. During the above-mentioned operating experience, we have found that the position of the high-voltage rod behind the chimney is critical, and errors in placement have resulted in arcing and some source failures.

We have found that there is good qualitative agreement with orbit computations, and these imply large return energies of more than a keV, which is quite good and will prove helpful when more difficult ions than Li^{2+} are attempted. In that regard, one future direction would be to attempt higher charge states, like, for instance Li^{3+}, where it might be found that some heavier gas than nitrogen is required to obtain adequate intensity. Pushing on in the

direction of doing some metal ions, one should try first perhaps the aluminum and magnesium beams originally proposed as test beams.

CHAPTER 6

MEASUREMENT OF ION SOURCE OUTPUT VERSUS CATHODE SEPARATION

The previous chapters have been concerned with ion source studies that have been important in the development of operating heavy-ion PIG sources for the K500 cyclotron. One question that we asked when the K500 cyclotron was under construction was: what will be different about the operation of an ion source in the high magnetic field ? Part of this was answered through the measurement of dc extracted ion currents in a test stand operated for a time in 1978 in the K500 magnet at high field [An 83]. That study showed that the charge state distribution was the same as for low field PIG sources (see for example Figure 5.4). Factors that would be expected to change at high field, like the electron gyro-radius and the radial magnetic pressure on the plasma, evidently are not fundamentally limiting.

The main purpose of the magnetic field in the PIG source is to guide cathode emitted electrons through the

arc. In that sense field curvature is more important than magnitude: if the magnetic field does not direct ions into the arc chamber a plasma will not form. This is because electrons tied to field lines that cross metal surfaces will be stopped at the surface, and will not reach the arc chamber to contribute to the ionization process. One more observation can be made about the field shape-- a diverging field passing through the arc would reduce the electron density there, and with it the ionization rate, and so a minimum requirement would be for a uniform magnetic field between the cathodes.

It is here that there is some difference between K500 axial magnetic field, and those from low field room temperature cyclotrons. The axial magnetic field of the K500 cyclotron, coming mainly from the superconducting coils, does not fall off as sharply along the axis at large distances from the median plane. Figure 6.1 shows a comparison of measured axial field of the ORIC cyclotron for B_o= 17.39 kG and the K500 cyclotron for B_o= 43.1 kG. The ratio B_z/B_0 is quite comparable for small z values, but drops to a low level for ORIC at large z values. Observe that at 20 inches the K500 magnetic field is ten times larger that in ORIC! In addition, the curvature of the K500 axial field is quite small. Figure 6.2 shows field lines

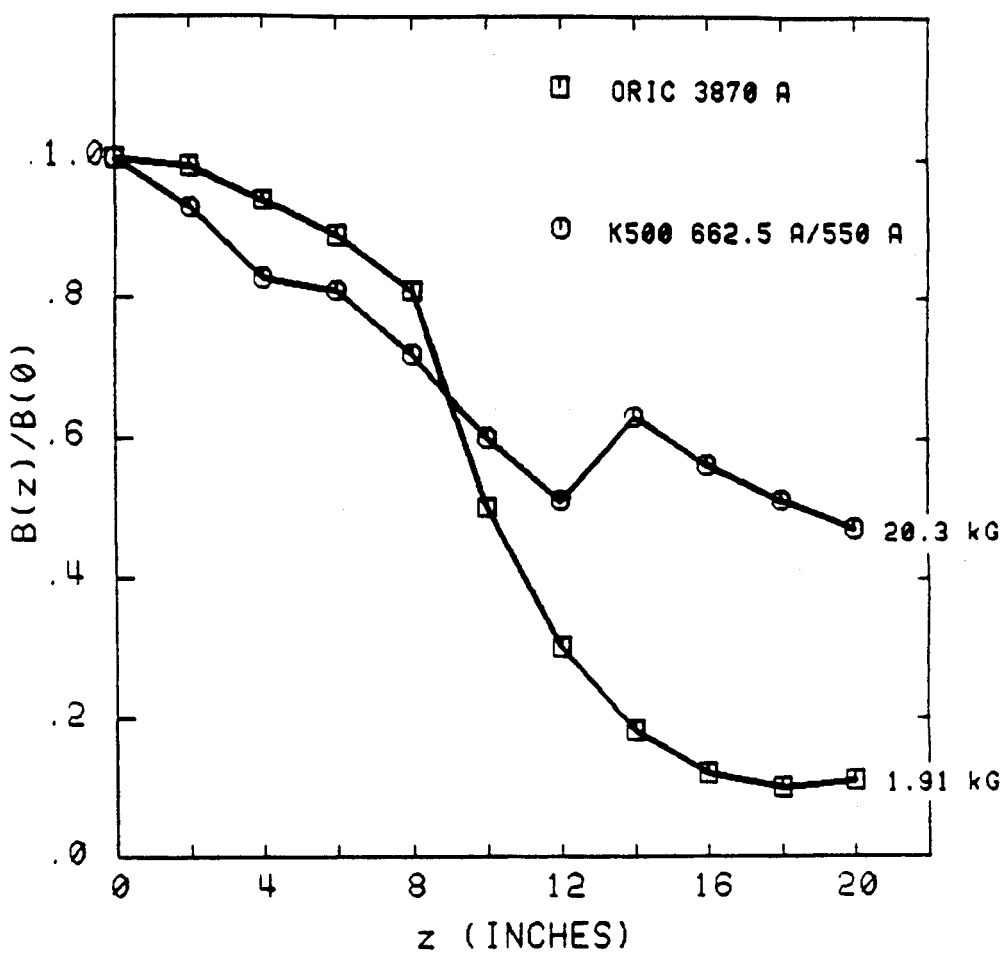

Figure 6.1. A comparison of a conventional cyclotron (ORIC), and superconducting (K500) axial magnetic fields is made. For ORIC B_o= 17.39 kG and for the K500 B_o= 43.1 kG.

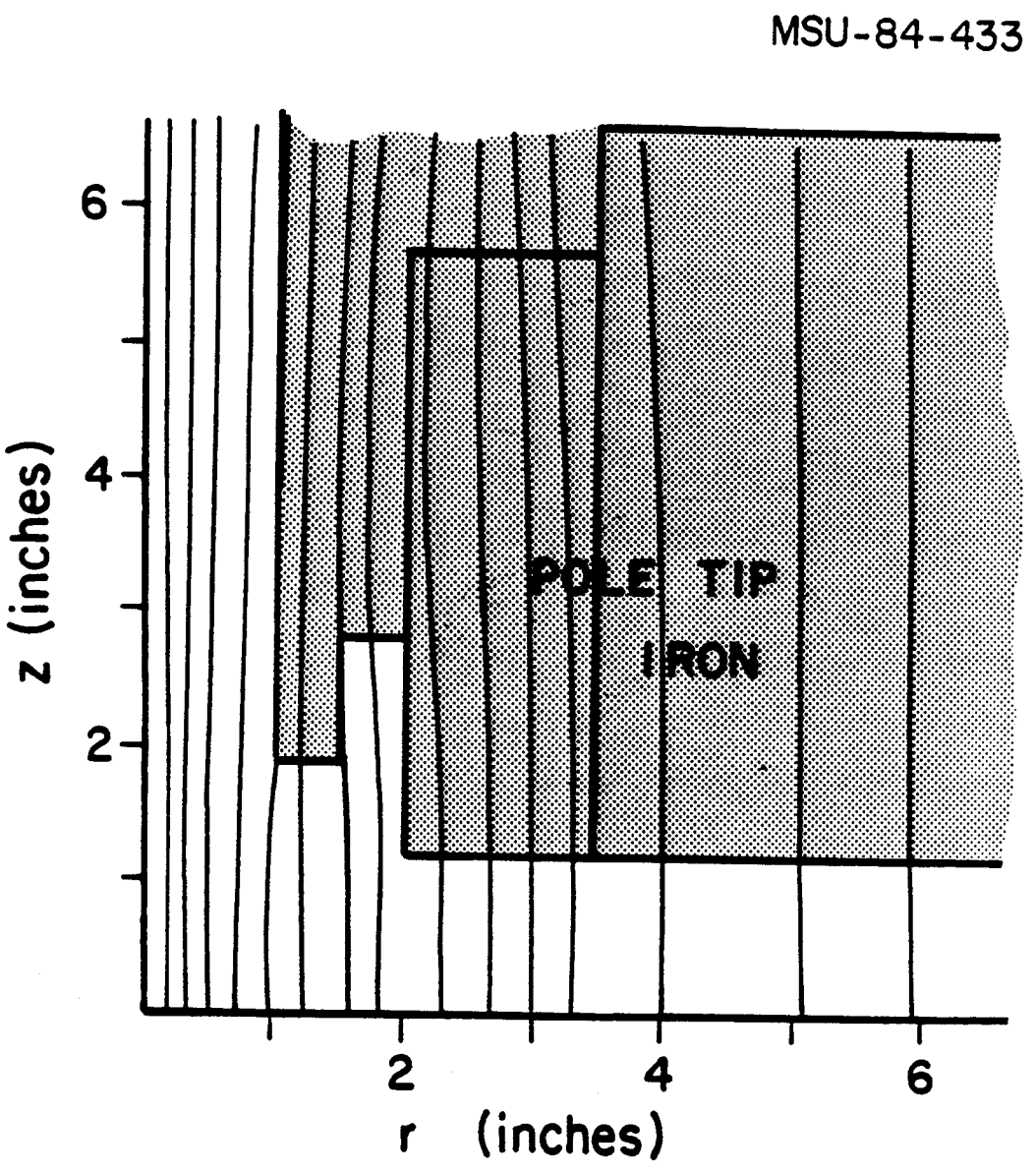

Figure 6.2. Magnetic field lines, obtained via a relaxation calculation and shown for the region above the media plane of the K500 cyclotron, for currents of 662.5 A/550 A in the small and large coils respectively.

in the cyclotron center for the K500 field plotted in Figure 6.1. These were obtained via the magnetic field calculating program POISSON, using a relaxation technique that includes both the coils and iron geometry [Ho 79]. Figure 6.2 shows that field uniformity at the center of the cyclotron, in the 2 inch diameter hole where the ion source resides is quite good.

It was conjectured that this large difference in the axial magnetic field might make it possible to build a longer ion source in the K500 cyclotron. This would be advantageous for several reasons. For one thing, at Dubna it has been shown that neutral cathode vapor in the arc reduces the percentage of high charge state ions from the feed gas [Ma 76]. This cathode vapor is highest near the cathodes, decreasing in the direction of the arc chamber center. Moving the cathodes away from the center might therefore result in a significant gain by reducing this charge exchange loss mechanism. Secondly, the high magnetic field has required that the central region of the K500 cyclotron be compact and this restricts possible changes that can be made to the ion source. Moving the cathodes away from the median plane would allow, for instance, larger cathodes, and might also result in a more reliable ion source, through the use of larger insulators, water cooling passages and voltage holding surfaces.

Two fundamental processes controlling the production of multiply-charged ions would be affected by increasing the ion source length. One can show that the probability that an electron, traversing the arc, will make an ionizing collision, is approximately

$$P = 1 - e^{-n\sigma\Delta\ell} \qquad (6.1)$$

where

n is the neutral gas density,

σ is the total cross-section for the reaction, and

$\Delta\ell$ is the separation between the cathodes.

The neutral gas density in the arc is about 10^{12} Atoms/cm^3, and ionization cross-sections are of the order of $10^{-16} cm^2$, which makes the collision probability for a single pass through a 10 cm arc of P=0.001. This would increase to P=0.005 for a 50 cm arc. The change is evidently in the right direction.

The second important physical process is the confinement time of the positive ions, which must be large for multiply-charged ions to appear in the output. In a PIG source unfortunately the positive ions have no real confinement, for in the axial direction the electric fields at the ends of the arc chamber draw positive ions to the

cathodes (this large ion flux to the cathodes being the important source of cathode heating), while in the radial direction the highly collisional ions can walk across the field lines, where they are lost at the arc chamber surfaces. If the axial drift time sets the effective ion lifetime, then increasing the length of the ion source should result in a shift in the charge state distribution toward higher charge values.

In order to study these effects, we built an experimental source for the K500 cyclotron that had a variable cathode separation, and measured the production of N^{4+} and N^{5+} ions as a function of cathode separation. In this chapter the design of this source, its operation and measured properties will be discussed.

6.1 Design of the Variable Arc Length Ion Source

The basic design of the variable arc length ion source is shown in Figure 6.3. This device can best be pictured as cutting the normal source design on planes through the arc chamber end plates into three separate elements for the purpose of allowing independent motion of the cathodes relative to the anode.

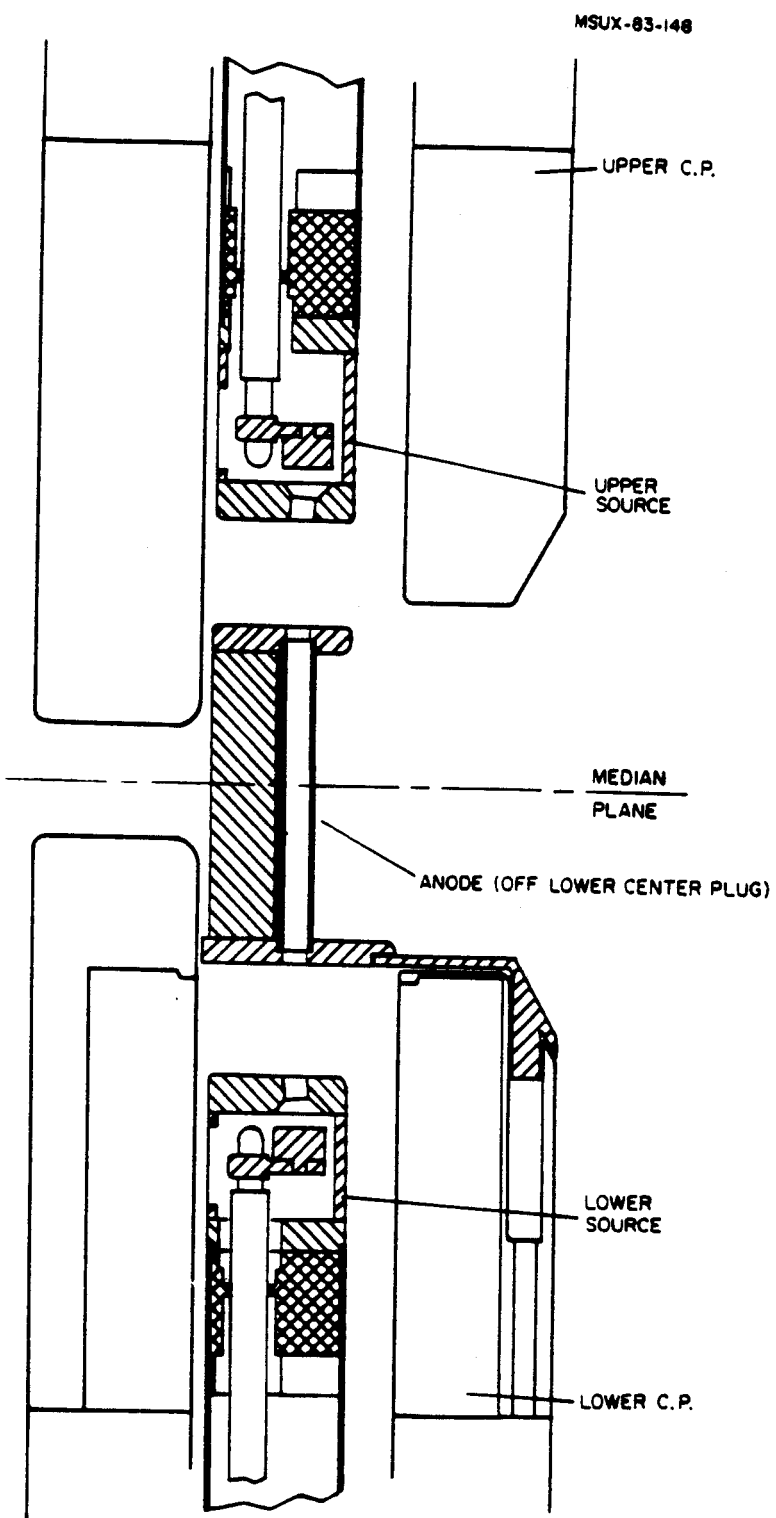

Figure 6.3. The central region elements of the variable arc length ion source are shown. See text section 6.1 for details.

The anode, mounted off the lower center plug, maintains the required central region shape of the ion source, as well as holding and shielding the plasma from the rf field. A slight median plane asymmetry had to be introduced into this anode in order that it fit into the center plug vacuum lock. The chimney mounted in this anode uses same type of square tantalum tube as for normal sources.

The other two elements of the source, which we will call the electron guns, house the cathodes and define the arc. An electron gun actually is a normal ion source with a shortened chamber housing only one cathode on a shortened high voltage rod. The inside gap between the chamber end-plate and the cathode must hold the arc voltage during striking and operation. The aperture in the end-plate allows cathode emitted electrons to pass out of this chamber along magnetic field lines, in the direction of the anode. Each electron gun has its own gas feed, so in principle each electron gun would strike independently and behave electrically like a normal arc discharge.

A substantial element in the preparation of this experiment was the completion of the upper ion source and the mechanisms that allow its insertion through a vacuum lock and into the cyclotron. The upper ion source is a mirror image of the lower source about the median plane. One feature of its installation is quite different--with the

lower source, we could check the central region alignment with the cyclotron cap up. This was not possible for the upper source, and a special fixture was constructed to set its alignment. After commissioning this source, the operators reported no difference in cyclotron tuning for lower or upper source operation.

A key feature of variable arc length source design is that the arc is defined via the intersection of the apertures of the electron gun end plates and the anode. This requires that the magnetic field curvature be small, and that accurate alignment of these apertures into both angle and radius be made. The former requirement is seen in Figure 6.2 to be reasonably satisfied--to the extent that the apertures are large and field curvature suggested by Figure 6.2 is not viewed as significant. The latter requirement was achieved by constructing fixtures to set the positions of the parts. The lower electron gun to anode alignment, set with these fixtures, was checked with the lower ion source installed in the center plug while it was out for installation of the anode. The upper source, installed in the upper center plug, could not be checked in this way, but since its position was set with the same fixtures as the lower source its alignment was reasonably assured.

The operational plan was as follows. The sources would be struck with the cathodes all the way in. In this configuration there are only small differences between this device and the normal source. The minimum cathode separation is 3.5 inches. The cyclotron could then be tuned and the beam current maximized on the main beam probe. The sources would then be retracted, and the beam current recorded as a function of cathode separation. The cathode motion is obtained from the drives that are used to insert and retract the ion sources from the cyclotron. At first the drives were operated manually from the cyclotron vault, and this meant turning off the cyclotron to move the sources. Measurement was slowed by this method, and we could see some effect on the vacuum coming from cycling the rf system. For later runs hydraulic check cylinders were added to allow provision for stopping the drives remotely. These check cylinders were affixed with helical follow potentiometers, that gave a voltage signal proportional to displacement, so that the position of the cathodes could be determined remotely as well.

The main goal was simply to measure the source length dependence of the ion source extracted current. Since we were interested in the development of multiply-charged ion sources, any such ion that could be obtained normally with a large current would be suitable, and we chose $^{14}N^{4+}$ to be the

primary study species. Additionally, we wanted to study whether there was any magnetic field dependence in this source output, and this could be accomplished by the acceleration of $^{14}N^{4+}$ at more than one energy. Finally one would like to know as well the charge state dependence of observed effects, and so a measurement of $^{14}N^{5+}$, at the same magnetic field as one of the N^{4+} cases, was also planned. The characteristics of the beams selected are summarized in Table 6.1.

Table 6.1. The beams that were selected for the variable arc length ion source experiment. The N^{4+} at 21.9 MeV/n and N^{5+} at 35 MeV/n had the same magnet settings.

ION	E_{final} (MeV/n)	FREQ (MHz)	B_o (kG)	V_{dee} (kV)
$^{14}N^{4+}$	21.9	15.19	34.6	52.
$^{14}N^{4+}$	30.0	17.67	40.3	70.5
$^{14}N^{5+}$	35.0	19.00	34.6	65.3

6.2 Measurement of N^{4+} and N^{5+} Currents versus Cathode Separation

The main results of this measurement are shown in Figure 6.4 and Figure 6.5. In Figure 6.4 we see the

dependence of the ion source extracted current on the change in cathode separation for N^{4+} and N^{5+} for the first and third beams in Table 6.1. After an initial rise in current, the curves show a sharp drop in beam current for a small displacement of 0.5 inches, to 70% of the peak value for N^{4+}, and about 50% for N^{5+}. The slope of the curve then changes to a more gradual decline in current out to 6 inches net change in in the position of a cathode separation (for a total separation of 15.5 inches when the initial separation of 3.5 inches is included). In Figure 6.5 the two N^{4+} cases are shown, and these results demonstrate good agreement at two different sets of cyclotron parameters.

Several investigations were made to study the nature of the these curves. First, moving the cathodes "out" versus "in" did not change the curve structure. Moving the cathodes "fast" versus "slow" also had no effect. Leaving the cathodes for some time at a fixed position, one could adjust the ion source and thereby change the beam current, but after moving the cathodes the shape of the curve was found to be the same. These data were so reproducable that it became clear that the cathode motion did not affect the ion source dynamics.

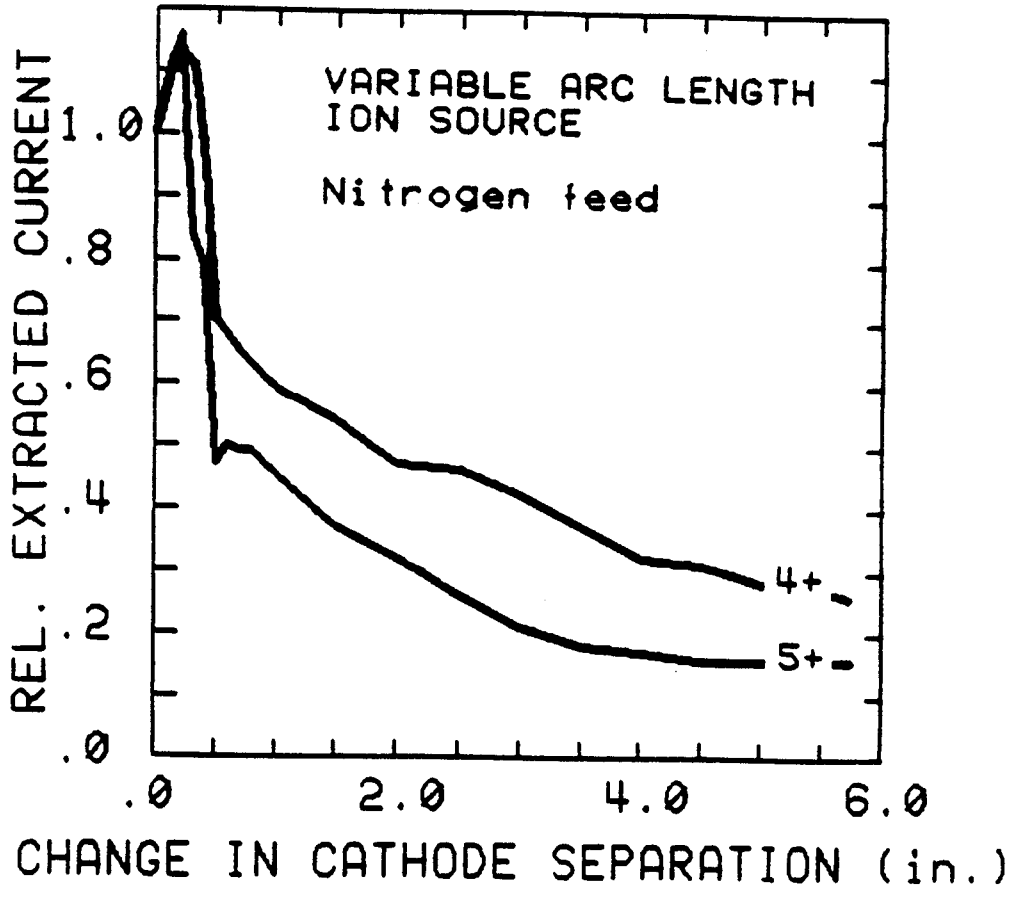

Figure 6.4. The dependence of ion source extracted current on an increase in cathode separation is shown for N^{4+} and N^{5+} ions in the same magnetic field. The initial cathode separation was 3.5 inches.

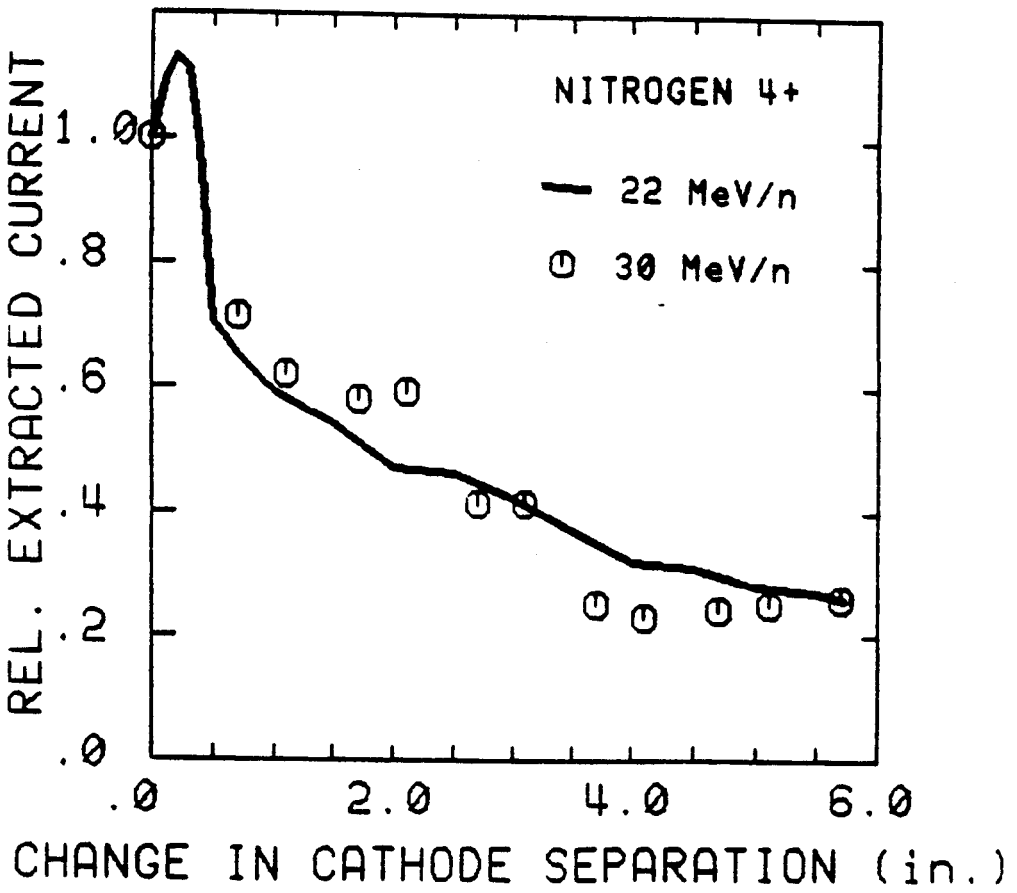

Figure 6.5. A comparison of N^{4+} production is made at two different cyclotron energies, corresponding to different magnetic fields and dee voltages (see Table 6.1).

6.3 Analysis and Conclusions

The electron gun sections of the variable arc length source produce an electron beam whose shape and direction are defined by the magnetic field. If the center of this electron beam shifts relative to the center of the anode apertures, then some of the electrons will spill onto the anode end-plates, reducing the electron current in the arc chamber. In Chapter 1 we showed that the rate of ion formation is directly proportional to the electron current, so that the loss of electrons above will reduce the ion density in the plasma, and also the extracted current. We will now propose an untested hypothesis based on these ideas, as the best explanation for the results shown in Figures 6.4 and 6.5.

The initial rise in beam current at small Δz is well correlated with the disengagement of an alignment collar in the ion source drive mechanisms as the sources retract. After disengagement a shift of .030 inches away from the cyclotron axis is possible, and in this case does result in a better arc alignment than obtained through the mechanical positioning process.

The decline of the beam current after this maximum is related to the effect that the actual curvature of the magnetic field in the center has on the arc alignment. In

the introduction to this chapter we argued that the magnetic field was very uniform-- and that therefore its possible effect on the arc alignment would be small, certainly smaller than the measured decline in the beam with cathode separation. The question that we would like to answer is, if it is larger than supposed, what would be the likely effect? The cathodes, after an initial shift, are moving axially, but at a fixed radius, into a region where the radial component of the magnetic field off the axis increases as z increases. This is shown in Figure 6.6, and we note also that in this cyclotron the cathodes do not lie on the axis, where the field would have no radial component. At higher z the field lines intercepted by the cathodes will not pass through the anode as they go through the median plane. Some of the electrons emitted by the cathodes at this elevated position will be stopped on the anode end-plates, and the percentage stopped will grow as the cathode separation grows, and would result in a reduction in the ion current. Since this loss process is entirely geometrical, it agrees with the characterics observed during the variable arc source operation.

During the last source run we changed the gun apertures to try to influence this effect, but did not have enough time to complete the measurements. After an extended cyclotron shutdown, our goals had shifted and unforetunately new measurements were not made.

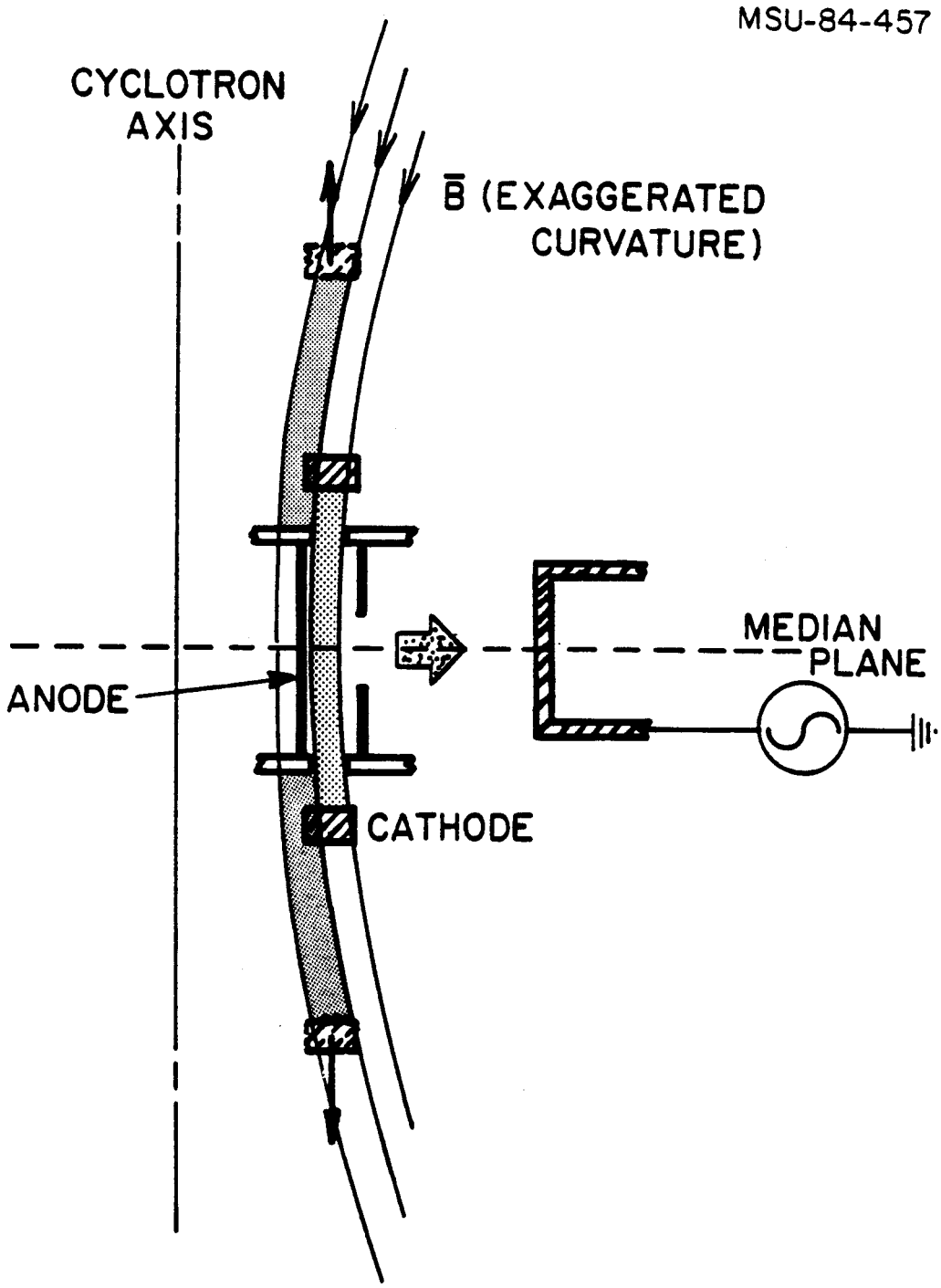

Figure 6.6. Raising the cathodes axially in a curving magnetic field causes a shift in the arc alignment relative to a fixed anode, as in the variable arc length ion source.

CHAPTER 7

FINAL PERSPECTIVE

The K500 Cyclotron PIG ion sources now fully exploit most of the techniques others have found useful for the production of multiply-charged ions. Some of those techniques were discussed in this dissertation. For nitrogen discharges, hafnium cathodes have produced the longest reported lifetimes for a PIG source operated with ions heavier than hydrogen or helium. Pulsed operation of the sources has given us a way to raise the intensity above dc operating levels for high charge state ions, and this has been found essential for Ne^{5+} or Ar^{6+} ion production. In addition, pulsed operation with hafnium cathodes has made N^{5+} a very successful beam. Solid sputter feed was accomplished through minimal changes in the source design, increasing the number of species that we are able to accelerate in the cyclotron. The variable cathode separation source showed that the ionization rate in the

region behind the source extraction slit is the most important, and that the cathodes must not cast a shadow in that region or the output of multiply-charged ions will decline. We have already seen our source design and operating procedures applied in a small heavy-ion source at Tohoku University in Japan [Ya 84].

Yet there is one outstanding problem which we have not solved -- the extracted beam currents from the K500 are smaller that those reported at other heavy-ion cyclotron laboratories for the same type of internal ion source. Figure 7.1 shows a comparison of K500 cyclotron extracted currents of carbon, nitrogen, oxygen and neon ions with those from the cyclotrons at Texas A&M University [Sa 79], Lawrence Berkeley Laboratory [Cl 81], and Oak Ridge National Laboratory [Hu 78]. As can be seen, the outputs of these three laboratories agree reasonably closely, and yet our performance is systematically about two orders of magnitude lower. The cyclotron extracted current depends on source ion production, source extraction, transmission during acceleration and cyclotron extraction efficiency, and differences in these factors would be expected from laboratory to laboratory. Yet the beam intensities obtained in those laboratories mentioned above are quite similar and differ by about 2 orders of magnitude from the beam intensities obtained from the K500.

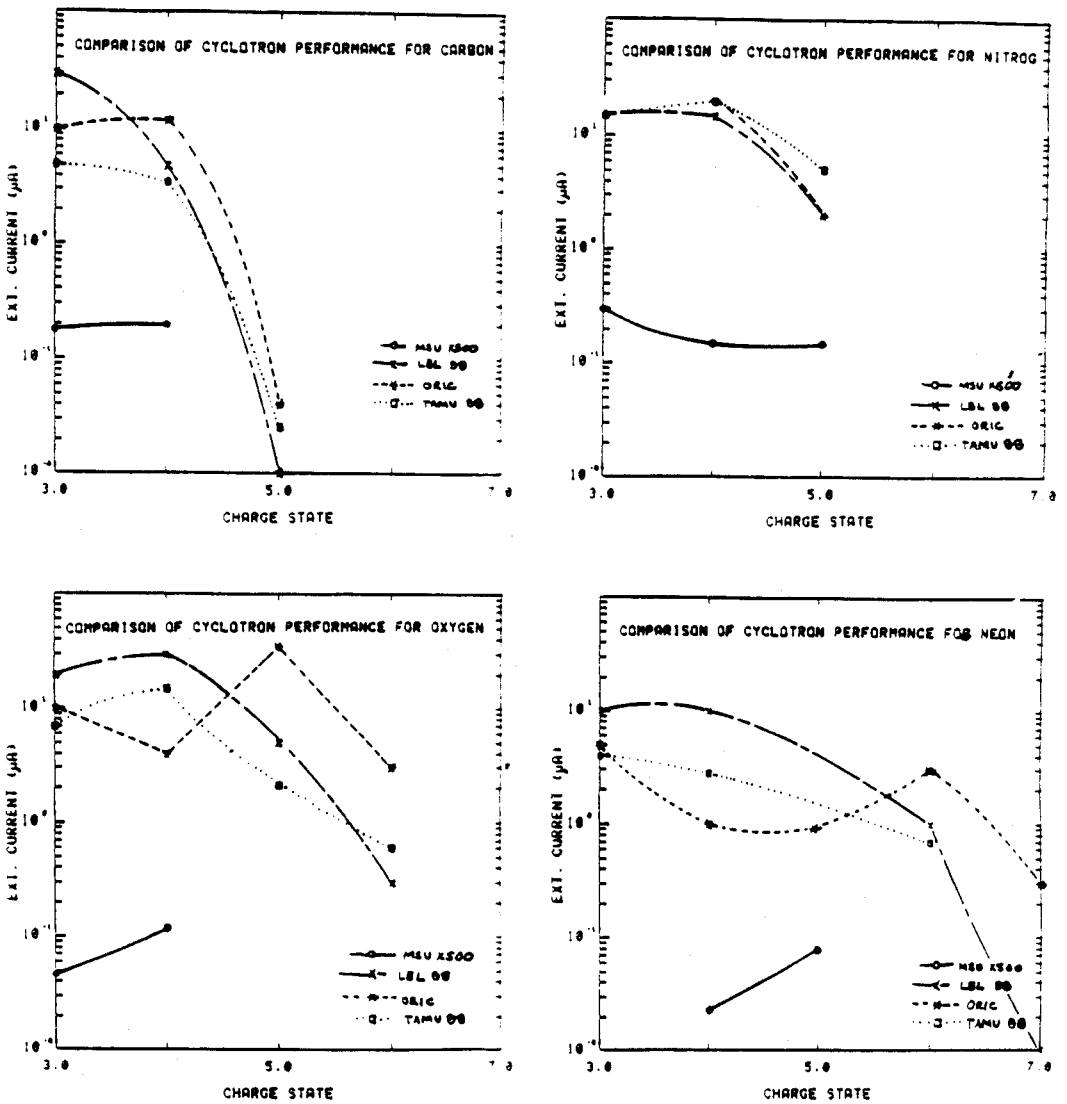

Figure 7.1. The extracted currents of carbon, nitrogen, oxygen and neon ions from heavy-ion cyclotrons at Texas A&M University [Sa 79], Lawrence Berkeley Laboratory [Cl 81], Oak Ridge National Laboratory [Hu 78] are compared to the K500 cyclotron at MSU [An 84]. Internal discharge heated PIG sources supplied the ions in each case.

In examining the reasons for this discrepancy, the four factors above need to be considered. The extraction efficiency of the K500 cyclotron is not the origin of the intensity problem since the measured internal beam before extraction is already low. In any case the extraction efficiency of the K500 cyclotron is quite comparable to those at Texas A&M, Berkeley, or Oak Ridge. In fact the problem is already apparent at a radius of 11 inches where the internal beam is first measured. Since we are unable to measure the current at a smaller radius, we can only speculate on possible difficulties in the first 11 inches.

The ion source output could be low. We have looked at the operating characteristics relative to sources at other laboratories, and find that the arc geometry and arc parameters of our source are quite comparable. For stable dc operation we require a gas flow of 1-2 sccm for arc currents of 2-4 A and arc powers of 1-2 kW; the gas flow decreases and the arc current increases as we go to pulsed operation. Furthermore, the K50 cyclotron at MSU operated the precursor to our K500 ion source; it had a similar geometry and the extracted beam currents were comparable to the above laboratories' experience, implying that the basic design is sound. In summary, we do not see any large deviation in source operation from that reported at other laboratories. We will, however, continue to seek improvements in source operation.

The extraction of ions from the source is another important area. This extraction depends on the arc alignment with the source extraction aperture, the size of the aperture, and the magnitude of the extraction electric field in the first gap. The extraction aperture and electric fields do not significantly differ from those at the above mentioned laboratories. With regard to the arc alignment, we recently did a series of measurements with tilted chimneys to alter the alignment, and found no alternate alignment more preferred than the normal case.

The final area of uncertainty is the transmission of the beam to 11 inches where it is first observed. We considered the possibility of large losses due to orbit errors in the cyclotron central region, but we see no unexpected erosion there -- evidence for large currents dumping on the metal surfaces in the cyclotron. Moreover, recent foil burn studies showed reasonably good axial and radial centering of the beam beyond the first turn. The cyclotron pressure at the center and its effect on the beam have not been explored. Large charge exchange losses of beam would occur if the pressure there is poor.

We have a situation where all of the component systems perform reasonably well, and where we have not found a large error in either the ion source design or the beam transmission process, but even so, the external comparisons

in Figure 7.1 nevertheless imply that we could do better. We can only conclude that further investigation is required.

LIST OF REFERENCES

A

[Ag 79] M.Agenda, K.Euler, B.Franczak, F.Hinterberger, H.D.Rosendaal, and H.V.Schmidt. IEEE Trans. Nucl. Sci., NS-22 (1979) 2156.

[An 83] T.A.Antaya, et.al. IEEE Trans. Nucl. Sci., NS-30 (1983) 2176.

[An 84] T.A.Antaya, et.al. Proceedings, 10th International Conference on Cyclotrons and Their Applications, East Lansing, Michigan (1984).

B

[Ba 72] E.Baron, et.al. AIP Conf. Proceedings, No.9, Cyclotrons-1972, AIP (1972) 243.

[Ba 79] A.Backouche, L.Bex, G.Cardin, B.Piquet and M.Voisin. 16th European Cyclotron Progress Meeting, SIN, Villigen Switzerland (1979).

[Be 69] J.R.J.Bennett. Fifth International Cyclotron Conference, Harwell, England (1969) 499.

[Be 72] J.R.J.Bennett. IEEE Trans. Nucl. Sci., NS-19 (1972) 48.

[Be 73] J.R.J.Bennett and Basil Gavin. Particle Accelerators, 3 (1973) 85.

[Bl 74] J.S.Blakemore. Solid State Physics, Philadelphia: W.B. Saunders Co., (1974) 188-192.

C

[CA 68] G.Carter and J.S.Colligon. Ion Bombardment of Solids, New York: American Elsevier Pub. Co. (1968).

[Ca 70] T.A.Carlson, et.al. Oak Ridge National Laboratory Report ORNL-4562, unpublished (1972).

[Cl 71] D.J.Clark, et.al.. IEEE Trans. Nucl. Sci., NS-18 (1971) 102.

[Cl 81] D.J.Clark, et.al. LBL Annual Report 1980-81, unpublished.

E

[Ev 82] R.D.Evans. The Atomic Nucleus, Malibar,Florida: Krieger (1982).

F

[Fu 72] G.Fuchs. IEEE Trans. Nucl. Sci., NS-19 (1972) 160.

G

[Ga 72] B.Gavin. 2nd International Conference on Ion Sources, Vienna, Austria (1972) 512.

[Ga 76] B.Gavin. IEEE Trans. Nucl. Sci., NS-23 (1976) 1008.

[Go 53] J.D.Gow and J.S.Foster jr., Rev. Sci. Instr., 24 (1953) 606.

[Go 79] R.A.Gough, D.J.Clark and L.R.Glasgow. IEEE Trans. Nucl. Sci., NS-26 (1979) 2164.

H

[Ha 67] C.A.Hampel. Rare Metals Handbook, New York: Reinhold Pub. Co., (1967) 205.

[Ha 74] Handbook of Chemistry and Physics, Cleveland: CRC Press (1974) B-16.

[Ha 84] L.Harwood, private comm.

[Ho 79] R.F.Holsinger. Poisson Group Programs, New England Nuclear (1979).

[Hu 73] E.D.Hudson, et.al. Physics Division Annual Progress Report, ORNL-4937 (1973) 403.

[Hu 75] E.D.Hudson, R.S.Lord, M.L.Mallory, J.E.Mann, J.A.Martin and W.R.Smith. IEEE Trans. Nucl. Sci., NS-22 (1975) 1544.

[Hu 78] E.D.Hudson, ORIC Beam List, Oak Ridge National Laboratory (1978) unpublished.

I

[It 82] T.Itahashi, et.al. RCNP Annual Report (1982) 167.

J

[Jo 72] E.J.Jones. IEEE Trans. Nucl. Sci., NS-19 (1972) 101.

K

[Ke 72] R.A.Kenefick, et.al. AIP Conf. Proceedings, No.9, Cyclotrons-1972, AIP (1972) 259.

L

[La 67] N.Laegreid and G.K.Wehner. Journ. Appl. Physics, 32 (1961) 365.

[Li 80] V.Littmark and J.F.Ziegler. Range Distribution for Energetic Ions in all Elements. Elmsford, NJ: Pergamon Press (1980).

M

[Ma 76] B.N.Makov, IEEE Trans. Nucl. Sci., NS-23 (1976) 1035.

[Ma 84] M.L.Mallory, T.Antaya, F.Marti and P.Miller. Nucl. Instr. and Meth., 222 (1984) 431.

[Ma 81] F.Marti, M.M.Gordon, M.B.Chen, C.Salgado, T.Antaya and E.Liukkonen. Ninth Int. Conf. on Cyclotrons and Their Applications, Caen, Fr (1981) 465.

[Mi 79] P.Miller, et.al. IEEE Trans. Nucl. Sci, NS-26 (1979) 3716.

P

[Pa 72] A.S.Pasyuk and Yu.D.Tretyakov. 2nd International Conference on Ion Siurces, Vienna, Austria (1972) 512.

[Pe 37] F.M.Penning. Physica, 4 (1937) 71.

[Pi 61a] Yu.D.Pigarov and P.M.Morozov. Soviet Physics-Technical Physics, 6 (1961) 336.

[Pi 61b] Yu.D.Pigarov and P.M.Morozov. Soviet Physics-Technical Physics, 6 (1961) 342.

R

[Ri 84] J.Riedel, private communication (1984).

[Ro 62] D.Rosenberg and G.K.Wehner. Journ. Appl. Physics, 33 (1962) 1842.

[Ro 63] R.W.Roberts and T.A.Vanderslice. Ultrahigh High Vacuum and its Applications, Englewood Cliffs, N.J.: Prentice-Hall (1963) 90.

S

[Sa 79] Y.Sakurada, et. al.. IEEE Trans. Nucl. Sci., NS-26 (1979) 2175.

[Sc 76a] H.Schulte, W.Jacoby, B.H.Wolf. IEEE Trans. Nucl. Sci., NS-23 (1976) 1042.

[Sc 76b] H.Schulte, B.H.Wolf, H.Winter. IEEE Trans. Nucl. Sci., NS-23 (1976) 1053.

[Sc 84] H.Schweickert, private comm.

[Sh 81] T.Shinozuka, et.al. Ninth Int. Conf. On Cyclotrons and their Applications, Caen (1981) 273.

V

[Va 69] P.I.Vasiliev, et.al.. Nuclear Instr. and Meth., 71 (1969) 201.

W

[Wa 84] W.Waltersheid, private comm.

[We 57] G.K.Wehner. Physical Review, 108 (1957) 35.

[Wi 78] H.Winter. "Production of Multiply Charged Ions", Lecture Notes in Physics, 83, Berlin: Springer-Verlag (1978) 1.

Y

[Ya 84] T.Yamada, et.al.. 5th Symposium on Accelerator Science and Technology, Ibaraki, Japan (1984).